Regional Landslide Susceptibility Assessment in Ambon Indonesia and Japan by Multivariate Quantitative Predictive Models and Slope Stability Analysis

アリル, アディティアン

出版情報：九州大学, 2016, 博士（農学）, 課程博士
バージョン：
権利関係：

Regional Landslide Susceptibility Assessment in Ambon Indonesia and Japan by Multivariate Quantitative Predictive Models and Slope Stability Analysis

ARIL ADITIAN

Regional Landslide Susceptibility Assessment in Ambon Indonesia and Japan by Multivariate Quantitative Predictive Models and Slope Stability Analysis

A dissertation submitted

by

Aril Aditian

In partial fulfillment of
the requirements for the degree of
Doctor of Agriculture at Department of
Forest and Forest Product Sciences, Graduate School of Bioresources and Bioenvironmental Sciences

Kyushu University

Fukuoka, Japan

2017

署　名

主　査

副　査

副　査

Table of Contents

List of Figures

List of Tables

"Are you sure you want to do this?" She said.

The voice still echoes in my mind

Chapter 1 Introduction

1.1 Background

Indonesia has been laid by a sequence of plate movements over time. There is a place of outstanding geological process related to the active plate tectonic movement (Figure 1.1). The Australian Plate is converging at an average rate of 70 mm/year in the 3° direction (Hutchinson, 2003) along the Java trench. It produces Sunda Arc which extends westward from Sumba passing through Java, Sumatera and Andaman Islands. Along the Timor trench, The Australian Plate is converging at an average 80 mm/year (Hamilton, 1979) which produces Sangihe and Halmahera arc and Sulawesi Arc. It is also the home of 127 active volcanoes located along Sumatra, Java, Bali, North Sulawesi, Sangihe and Halmahera islands as a part of the Pacific Ring of Fire. Those make Indonesian region, which is characterized by complicated seismological features causing several disasters, including the latest deadly disaster Aceh Tsunami in December 2004 affecting 173,741 deaths and Yogyakarta Earthquake affecting 5737 fatalities and 8904 injuries.

Indonesia is also prone to disaster due to climatic condition. The variation of rainfall is often linked with the monsoons because it lies between Asia in the northwest and Australia in the southeast. High pressure in the Asian continent during winter (December to February) forces the wind to blow to the southeast where there is low pressure during summer in Australia. This west monsoon causes rainy season in Indonesia during October to March because the wind crosses the South China Sea. In contrast, the monsoons reverse direction from Australia to Asia, called as east-monsoons, which causes dry season during April to September. Indonesia receives on average 1755 mm of precipitation annually or 146 mm each month. Drought usually occurs during the dry season; and sediment related disaster and flood usually occur during the rainy season.

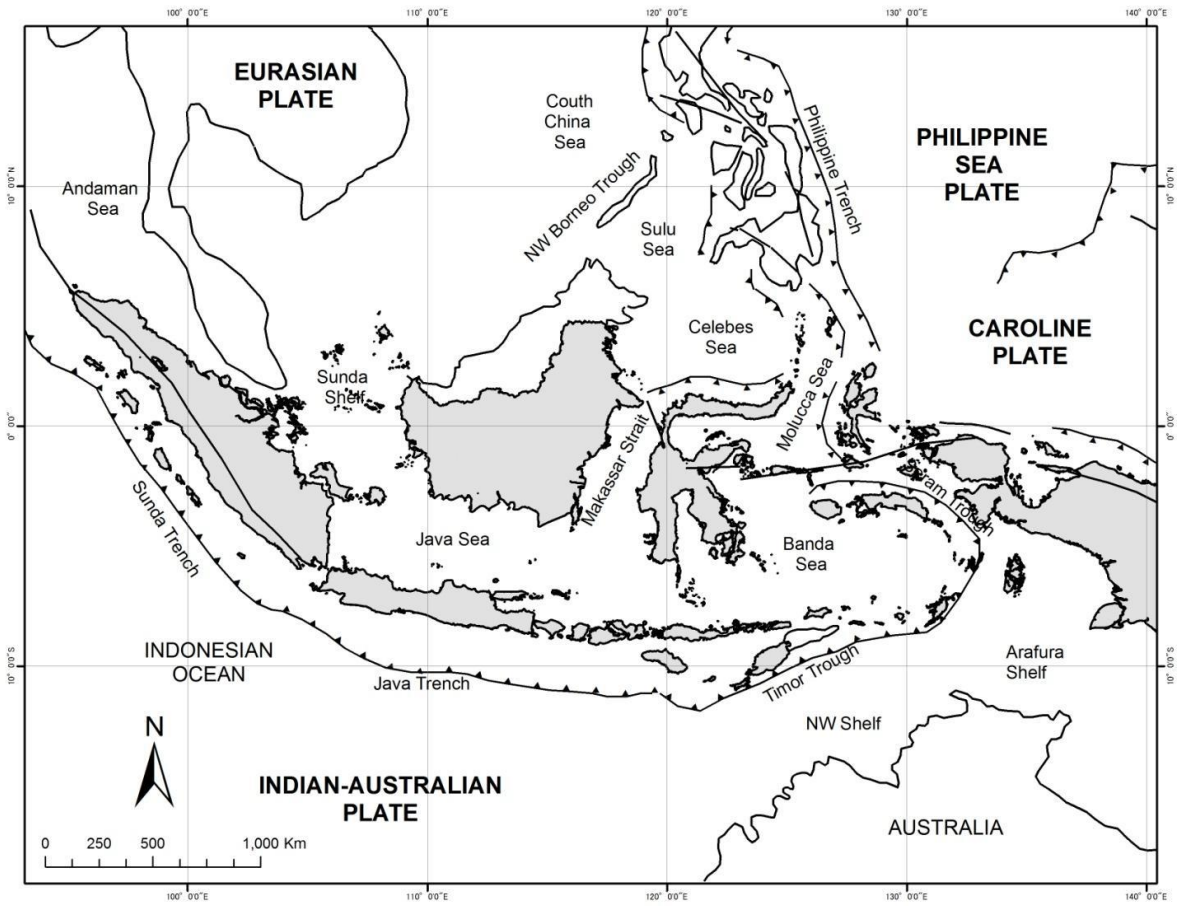

Figure 1.1 Indonesia regional tectonic setting

Indonesia's island arc and mountain range lying in the complex tectonic setting and high variation of rainfall are subjected to natural disasters, including geophysical disaster and hydro-meteorological disaster, killing 182.783 people during 1996-2014. Most of which are killed by geophysical disaster such as tsunami (92%), earthquake (5%) and volcanic eruption (0.2%). But, the high percentage of fatalities on geophysical disaster is due to Aceh Tsunami 2004 and Yogyakarta Earthquake 2006. Intense rainfall and weathering process may cause hydro-meteorological disaster such as landslide and flood which affect 1.9% and 1.2% fatalities respectively. Floods and landslides periodically occur in Indonesia. Landslide is ranked as the highest average annual occurrences and fatalities in Indonesia.

Even though not always as spectacular as earthquakes and tsunami, rainfall-induced landslides frequently occur in Indonesia during rainy season. The annual frequency, calculated from DIBI (Indonesian Disaster Database) 1998-2013, is 158 events/year (Figure 1.2). However, this data may be underestimated since landslides occurrences reported by DIBI are based on provincial and regency report. Smaller scale landslide without fatalities may not be reported in DIBI. Landslides caused 3432 loss lives with annual frequency fatalities 214 people/year (Table 1.1). Indonesia is also listed as the top three countries with the highest percentage of landslide fatalities in 2003, 2007 and 2008 (Kirschbaum, 2010).

Table 1.1Ranking of natural hazard and fatalities in Indonesia (DIBI, 2014)

Rank	Disaster Type	Fatalities	Injuries
1	Tsunami	167,780	18,860
2	Earthquake	8,950	58,993
3	Landslide	3,432	42,875
4	Flood	2,190	190,333
5	Volcanic Eruption	429	3,472
6	Drought	2	0
Total		314,533	533,416

Source: Indonesian Disaster Database (http://dibi.bnpb.go.id/DesInventar/dashboard.jsp)

Along with the increasing number of material and fatalities due to the landslide occurrence, there is increasing awareness toward the need of landslide prediction and risk reduction tools. Prevention and remediation as hard countermeasure are not always possible, especially in the rural area where settlement/housing is spread out. Hard measures installation in each single building will cost too much and not feasible. Practical considerations for the establishment of countermeasures is an important issue for administrators and stakeholders in the landslide prone area. It is feasible to map major instable areas and to take measures for avoidance, prevention or remediation of landslide occurrences based on observation, analysis and research. An integrated strategy for observation, research, assessment and management includes landslide hazard mitigation from a spatial zoning

point of view. The decision for avoidance, prevention and remediation is well approached by landslide risk analysis.

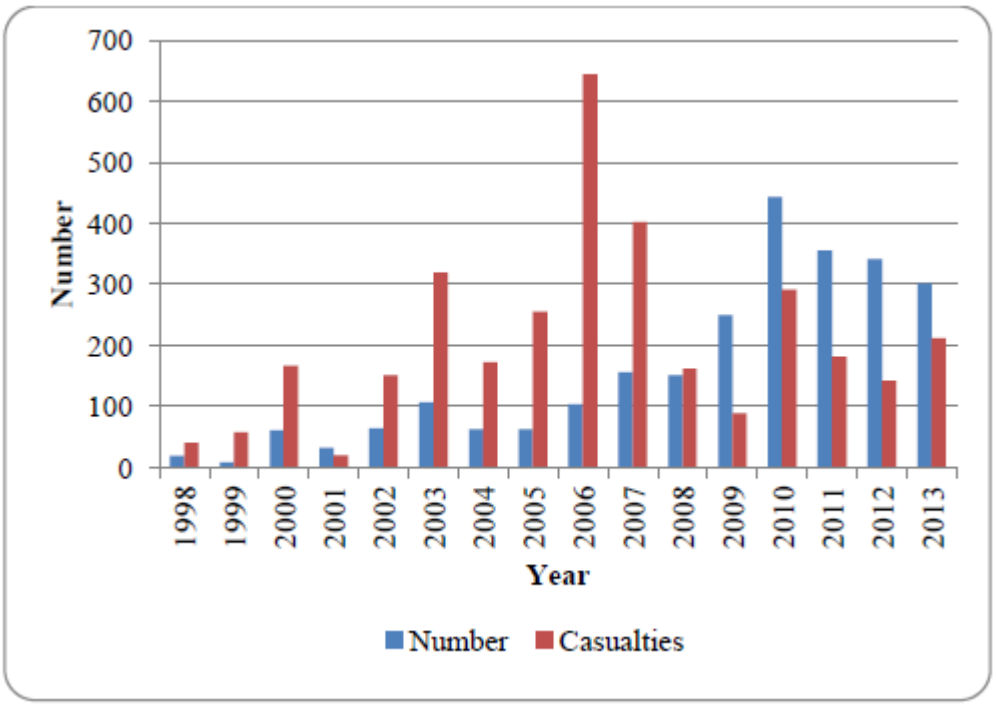

Figure 1.2 Landslide number and casualties in Indonesia (DIBI, 2014)

1.2 Disaster management in Indonesia

The shift in disaster management paradigm from focusing on disaster response to enhancing disaster risk reduction has been started in 2007 by enactment of Undang-Undang (Law) 24/2007. It was driven by scientific society and government awareness after post-tsunami emergency response and subsequent rehabilitation and reconstruction phase. The momentum was also appeared by the experiences of Nabire Earthquake 2004, Nias Earthquake 2005, and Yogyakarta Earthquake 2006 emergency response. However, the initiative to reform the Disaster Management Law has been started before the earthquake and tsunami of 26 December 2004. There were a discussion forum between BAKORNAS PB (National Disaster Management Coordination and Agency), NGO's and MPBI (Indonesian Society for Disaster Management) to promote national disaster management. Before the enactment Law 24/2007, the disaster management in Indonesia were focusing on crisis management and disaster response coordinated by BAKORNAS PB.

The Disaster Management Law 24/2007 enforces a systematic approach in disaster risk reduction that contains three phases of the disaster management cycle as follows:

1. pre-disaster planning and preparedness, including disaster risk reduction, mitigation, preparedness, risk assessment and contingency planning

2. emergency response, including evacuation, search and rescue, providing immediate assistance, assessing damage and disaster relief

3. post disaster management, including rehabilitation and reconstruction.

The law also mandates the creation of the "new BAKORNAS PB", later called as BNPB (National Disaster Management Agency), as a national coordinating agency for disaster management that is responsible for pre disaster planning, emergency response and post disaster management. BNPB must coordinate all contingencies, preparedness, mitigation, prevention, disaster management training, risk assessment and risk zoning. In the emergency response phase, BNPB has a responsibility to coordinate government, NGO's and international organization during the emergency response phase. BNPB must also coordinate damage and loss assessment and coordinate rehabilitation and reconstruction in the post disaster phase.

However, with the high responsibility for conducting disaster management, BNPB needs partners to provide all the technical support, to train technical personnel, and to create preventive disaster risk reduction culture in Indonesia. One of the representative partners to provide technical expertise in the full spectrum of disaster related fields is the university partner. It is expected to be an intellectual capital, which is able to provide technical assistance in disaster risk reduction including the research and technology development of early warning systems, damage assessment and risk analysis.

Risk analysis, as a basis for disaster risk reduction, is an important issue in the Law 24/2007. Disaster prevention planning should include disaster risk data documentation and risk analysis. Development activities which may have high risk must be equipped with risk analysis. The

implementation of risk analysis is closely related to spatial planning or landuse planning. Two other laws were also enacted in 2007 i.e. Law 26/2007 about spatial planning and Law 27/2007 about coastal zone management and small islands. Both have a strong attachment to disaster mitigation. Law 26/2007 dictates that spatial plan documents should be based on the consideration of disaster mitigation measures. Law 27/2007 states that disaster reduction strategy has to be included in the coastal zones and small islands spatial plan. Spatial planning at national, provincial and regency level is developed for 20 years and can be reviewed once in 5 years. If a disaster happens due to the development in a high risk area which is not equipped with disaster risk analysis, the responsible parties can be fined for up to US$ 26000 or jailed up to 3 years.

Thus, spatial planning based on disaster risk reduction is one of the primary issues of the Indonesia's national development agenda to promote sustainable development due to the increasing frequency of disasters and continuing environmental degradation. In terms of landslide disaster risk reduction, regional development and disaster mitigation are well approached by landslide susceptibility, hazard and risk zoning.

1.3 Landslide susceptibility analysis in developing country: lack of data availability

Landslide risk analysis involves several steps, i.e. scope definition, landslide hazard identification and risk estimation. Scope definition addresses several issues including delineating the study area, elements at risk identification, and methodology selection. Landslide hazard identification addresses several issues on understanding physical characteristic of study area regarding to landslide processes such as understanding geology, geomorphology, hydrogeology and climate. It also includes collecting landslide data, such as landslide classification, area, volume, travel distance, date occurrence, and elements at risk. Hazard identification activities are mostly related to landslide inventory. Risk estimation deals with consequence analysis and frequency analysis.

Landslide inventory is very important in the landslide risk analysis because it gives information related to frequency of occurrences, landslide typology, landslide extents and damage of elements at risk. Estimation of spatial probability, temporal, probability and magnitude probability is not possible without landslide inventory containing sufficient data of past landslide events. In Indonesia, especially where this research was undertaken, adequate landslide inventory is not available. It is a central problem of quantitative landslide risk analysis in Indonesia. Thus, producing landslide inventory maps and developing approaches of using those maps for landslide risk zoning in Indonesia are challenging task that this research focuses on.

1.4 Research Scope and Objectives

Landslide is defined, as general terminology, to describe the movement of rock, debris or soil down a slope due to gravitational process (Fell et al., 2008). However, the terminology of landslide, in this research, is used interchangeably to define shallow and deep seated slide. Landslide hazard and risk analysis, as a soft preventive countermeasure, is a vital tool for disaster risk reduction in Indonesia because of the shifting paradigm of its disaster management from focusing on disaster response to enhancing disaster risk reduction. However, the major drawback of generating landslide risk analysis is the unavailability of landslide inventory data, which makes difficulties in estimating spatial probability, temporal probability and magnitude probabilities.

This research will distinguish its analysis based on the availability of landslide causative factors. Thus, the objectives of this research are:

(1) To evaluate the importance of each causative factors in landslide susceptibility assessments and to compare landslide susceptibility models of using bivariate frequency ratio, multivariate logistic regression, and artificial neural network in the tertiary region of Ambon, Indonesia. For this, the occurrence of landslides was detected in the study area by field surveys and satellite imagery derived from Google Earth™.

(2) To comparatively evaluate the usage of artificial neural network (ANN) to optimize causative factors in landslide susceptibility assessment in Ambon, Indonesia

(3) To compare slope response under heavy rainfall with FEM (Finite Element Method) in Indonesia and Japan.

1.5 Thesis Organization

The thesis comprises of the following chapters.

Chapter 1 introduces (1) disaster in Indonesia, (2) the shifting disaster mitigation policy in Indonesia, (3) the problems in landslide risk zoning in Indonesia, (4) the scope and objectives of this study, and (5) the organization of the thesis.

Chapter 2 reviews terminologies used in landslide risk analysis and risk management. Although some terminologies are often used interchangeably, the terminology misconception can generate confusion for the decision maker, urban planner, stakeholders and even young engineer. Thus, this chapter attempts to overview the difference between susceptibility, hazard and risk in landslide studies.

Chapter 3 compares three different landslide susceptibility analysis using bivariate frequency ratio, multivariate logistic regression, and artificial neural network method. Data were separated into training data and validation data. The produced landslide susceptibility maps were compared to evaluate the accuracy of each map in the study area of Ambon, Indonesia.

Chapter 4 Optimized landslide causative factors (input data) to increase the accuracy of the landslide susceptibility map in Ambon, Indonesia by using artificial neural network approach. Two least influential causative factors derived from artificial neural network importance value were eliminated.

Chapter 5 utilizes Finite Element Method to evaluate the response of slope in similar volcanic region of Ambon, Indonesia and Aso, Japan. Heavy rainfall event from the year of 2012 were used in the seepage-coupled analysis.

Chapter 6 summarizes and concludes the results and achievements of the study. Problems are also highlighted for future studies.

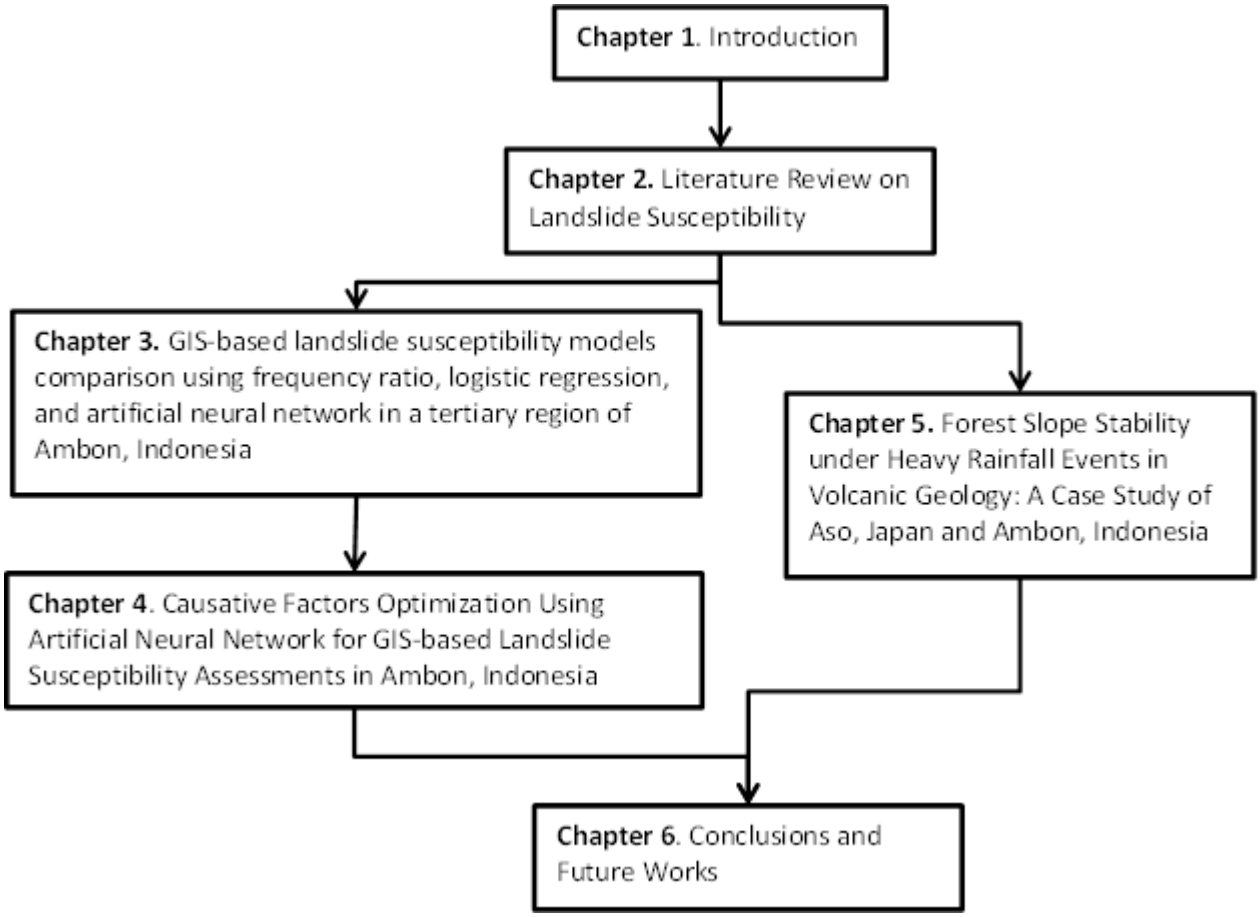

Figure 1.3 Flowchart of thesis organization

1.6 References

Anonym. 2007. Undang-Undang Nomor 24 Tahun 2007 tentang Penanggulangan Bencana, Lembaran Negara Republik Indonesia tahun 2007 nomor 66, Jakarta.

Anonym. 2007. Undang-Undang Nomor 26 Tahun 2007 tentang Penataan Ruang, Lembaran Negara Republik Indonesia tahun 2007 nomor 68, Jakarta.

Anonym. 2007. Undang-Undang Nomor 27 Tahun 2007 tentang Pengelolaan Wilayah Pesisir dan Pulau-pulau Kecil, Lembaran Negara Republik Indonesia tahun 2007 nomor 84, Jakarta.

DIBI. 2014. Indonesian Landslide Disaster Database 1998-2013. Accessed on March 2014 from http://dibi.bnpb.go.id/DesInventar/dashboard.jsp

Fell, R., Corominas, J., Bonnard, C., Cascini, L., Leroi, E., and Savage,W. Z. 2008. "Guidelines for landslide susceptibility, hazard and risk zoning for land use planning". Eng. Geol., 102, 85–98,.

Hamilton, W. 1979. Tectonics of the Indonesian Region. U.S. Geological Survey Profesiional Paper 1078. US Government Printing Office. Washington.

Hutchinson, C, S. 2003. in Gupta, A.(Ed.), 2003. The physical geography of Southeast Asia. Oxford Univercity. Press,

Kirschbaum, D.B., Adler, R., Hong, Y., Hill, S., dan Lerner-Lam, A. 2009. A Global Landslide Catalog for Hazard Application: Method, Result, and Limitations. Journal of Natural Hazard doi 10.1007/s11069-009-9401-4.

Chapter 2 Literature Review on Landslide Susceptibility

2.1 Introduction

Risk is defined, in the Oxford dictionary of English, as possibility of future harms viewed from the present (Soanes and Steventon, 2005). The concept of risk is also used by various disciplines resulting many definitions and paradigms on how it is calculated either qualitative, semi-quantitative or quantitative. For example, in Economics and finance, risk is defined as the probability of financial asset return or the probability that an actual return on a financial investment will be lower than the expected return (Andersen, et al., 2013). In natural hazard, risk is defined as the probability and severity of a future harm to health, property or the environment (IUGS, 1997; Fell et al., 2008). More specific to the effect of natural disaster, risk is defined as the expected number of lives lost, injured persons, damage to property, or disruption of economic activity due to a natural phenomenon (Varnes, 1984; Cardona, 2003). In application of risk analysis, they generally involve more mathematical term dealing with term "probability" which depend on hazard, vulnerability and elements at risk. Assuming their independency, it is described by the product of elements at risk (E), vulnerability (V) and hazard (H), expressed by the following formula (Varnes, 1984; Ebert *et al*., 2009):

$$Risk = f(hazard, vulnerability, element\ at\ risk) \quad (2.1)$$

Risk can be qualitative, semi-quantitative and quantitative. Qualitative risk uses a descriptive or word form to describe the degree of risk or the likelihood that potential consequences will occur. Semi-quantitative risk is rather similar with qualitative risk, but it uses a numeric rating scale.

Nowadays, geographical data related to disasters can be handled in a GIS (Geographic Information System) environment, even by users who are not experts in GIS or natural hazard field due to the advanced development and more user friendly GIS software. However, the terminology and methodology in landslide risk studies may be diverse significantly from country to country and

even within the same country such as Indonesia. The interchangeably terminology used of susceptibility and hazard in the scientific literature is one of the examples. Some literatures on landslide hazard zoning often discuss methods and techniques on landslide susceptibility zoning. Landslide susceptibility and landslide hazard are also often used as synonymous, even though those are rooted from different concept. The terminology misconception between susceptibility and hazard often generates confusion for the decision maker, urban planner, stakeholders and even young engineer.

Thus, this chapter attempts to overview the difference between landslide susceptibility, landslide hazard and landslide risk. The information on susceptibility involves mainly the spatial probability, whereas the information in hazard involves the spatial probability, temporal probability and landslide size (area or volume) probability. Some issues on landslide risk zoning are also highlighted.

2.2 Landslide risk

In landslides studies, quantitative risk assessment has been applied and developed since long time ago by geotechnical engineer on a site investigation scale, such as pipeline, road, dam, oil platform, and housing. The analysis will be more focused on the hazard analysis of a specific slope. It uses deterministic (factor of safety, numerical analyses) and/or probabilistic methods, e.g. first order, second-moment (FOSM), first order reliability method (FORM), point estimate methods, and Monte Carlo Simulation (MCS). However, quantitative risk zoning in large areas for landuse planning in which this research focuses on seems still need improvement.

Similar to equation 2.1, landslide risk also involves hazard, vulnerability and elements at risk. It should comprise probability of landslide, run out behavior, vulnerability of property and people to landslide (Dai *et al*., 2002). IUGS Working Group on Landslides (1997) also proposed the overall framework for quantitative risk analysis of landslide as follows: (1) hazard analysis – analysis of the probability and the characteristics of the potential landslide (2) identification of elements at risk (3)

analysis of the vulnerability of the elements at risk and (4) calculation of the risk from the hazard. Thus, landslide risk zoning assesses the loss of life or property or environmental features accounting for temporal probability, spatial probability, magnitude probability and vulnerability. In practice, it would not be simple to achieve and need detailed investigation on each risk element, i.e. hazard, vulnerability and element at risk.

2.3 Landslide hazard

Hazard can be defined as a potential condition as an effect of an occurrence to have an undesirable consequences or damage (IUGS, 1997). Furthermore, landslide hazard defined as the probability of occurrence within a specified period of time and within a given area of a potentially damaging phenomenon (Varnes, 1984) includes spatial, temporal and magnitude probability of landslide events. It is characterized by statements of 'what', 'where', 'when', 'how strong' and 'how often', demanding knowledge of variation in both spatial conditions, temporal and magnitude behavior (Glade et al., 2005). The information should include the location, size (area and or volume) classification and velocity of the potential landslides and any resultant detached material and the probability of their occurrence within a given period of time. It provides potential capability to describe landslide distribution spatially and temporally. The landslide hazard map is a tool used to portray the location of landslide, the predicted location of landslide, and can be used to divide the different level of risk areas (Guzzetti *et al*., 2000).

Landslide hazard is expected to answer temporal and magnitude probability which are not taken into account in landslide susceptibility zoning. Generating landslide hazard from landslide susceptibility requires estimation of spatial, temporal, and magnitude probabilities (Guzzetti et al., 1999; Glade et al., 2005; Fell et al., 2008; van Westen et al., 2008). Thus, landslide hazard analysis needs information about landslide susceptibility and landslide inventory containing the date of landslides events and area/volume of landslides. However, the date of the landslide events and area/volume of landslides are difficult to be included in most of landslide hazard maps because

several factors, i.e. 1) absence of multi-temporal data of landslide events, 2) heterogeneity of the subsurface conditions, 3) scarcity of input

data and 4) absence or insufficient length of historical records of triggering events (van Westen et al., 2006). Thus, generating landslide inventory is essential for landslide hazard analysis.

2.4 Landslide inventory

A landslide inventory, called also as landslide map or just "inventory" (Guzetti et al. 2012), is the simplest form of landslide map (Hansen, 1984; Wieczorek, 1984; Guzetti et al., 1999). It is a data set that represents single or multiple events as well as shows the locations and outlines of landslides (Chacon 2006). Location, type of landslide, the volume, activity, date of occurrence and other characteristic of landslides in the area (Fell et al., 2008) as well as information on triggering factors (Godt et al., 2008) should be available in landslide inventory.

Landslide inventory is the basis for landslide susceptibility, hazard and risk zoning (Carrara and Merenda, 1976; Guzzetti et al., 2000; Brardinoni et al., 2003). It provides spatial distribution of landslide which is useful for landslide susceptibility; date of occurrences for generating landslide temporal probability and information of area or volume for generating magnitude probabilities. Without complete temporal archives, it is difficult to generate temporal probability by relative times. But some historical inventories obtained from well archived data will give information related to date of occurrences. There are several methods for preparing a landslide inventory such as traditional methods (field survey, interpretation of aerial photograph) and modern techniques (interpretation of very detailed DTMs and interpretation and analysis of satellite imagery) (Guzetti, 2006; van Westen et al., 2008). Many attempts have been made to prepare landslide hazard maps based on traditional inventory method (Guzzetti et al., 2005; Pradhan, 2010; van Westen et al., 2003). Traditional method based landslide inventory is produced by interpretation of aerial photographs coupled with field surveys. It can be defined as geomorphological inventories and can also be combined with collecting historical information on individual landslide events called as

archive inventory (Guzetti et al., 2000; Malamud et al., 2004). According to the availability of temporal database, traditional method can be classified further as historical, event, seasonal or multi-temporal inventories. Temporal information is usually given in relative terms, i.e., recent, old or very old.

An event inventory informs landslide occurrences that caused by a single trigger, such as earthquake, a rainfall or snowmelt event showing the date of the landslides which corresponds to the date (or period) of the trigger event. Seasonal and multi-temporal inventories are obtained by interpretation multiple sets of aerial or satellite images of different dates. The main difference both of those inventories is the period (short/season or long period) of the triggering event. A seasonal inventory shows landslide triggered by single or multiple events during a single season or a few seasons, while multi-temporal inventory indicates landslide occurrences triggered by multiple events over longer periods. Similar to the event inventory, the seasonal and multi-temporal inventories inform the date of the landslides which corresponds to the period of the trigger event. Preparation of landslide inventories by traditional methods is a substantial challenge because it requires time and a team of experienced people. Galli et al. (2008) estimated that preparation of an inventory took an average one month per interpreter to cover 100 km^2 area in the Umbria region of Italy.

In some cases, it is difficult to obtain all the landslides by field survey and interpretation of aerial photograph, especially in a vastly inaccessible mountainous area. It is also often subjective, prone to error (Malamud et al., 2004), time consuming and difficult to carry out in forested terrain (Brardinoni et al., 2003; Van den Eeckhaut et al., 2005). Recent techniques of landslide inventory are comparatively fast, unbiased and data driven, and the outputs are also visually consistent. It involves interpretation of very detailed DTMs (Digital Terrain Models) and interpretation and analysis of satellite imagery which have been widely used to resolve this problem (Nichol and Wong, 2005; Mondini et al., 2011, Barlow et al., 2006; Martha et al., 2010b; Moine et al., 2009).

Automatic identification was also applied to identify landslides using satellite imagery data (Barlow et al., 2006; Borghuis et al., 2007; Martha et al., 2010b; Nichol and Wong, 2005b; Rosin and Hervas, 2005). However, it is data driven, cloud problem image in tropical country and still expensive in developing countries.

2.5 Landslide susceptibility

Landslide susceptibility is an estimate of spatial distribution in which landslide potentially may occur in an area. It shows the likelihood of occurrence of landslide in a given location (Corominas and Moya, 2008) and takes the output of the landslide inventory mapping or by computing probability of failure of the slopes. Susceptibility poses the spatial probability in which the landslide may occur or an estimation "where" landslides are likely to occur. Landslide susceptibility does not consider "when", "how frequent" and "how large" landslides are likely to occur.

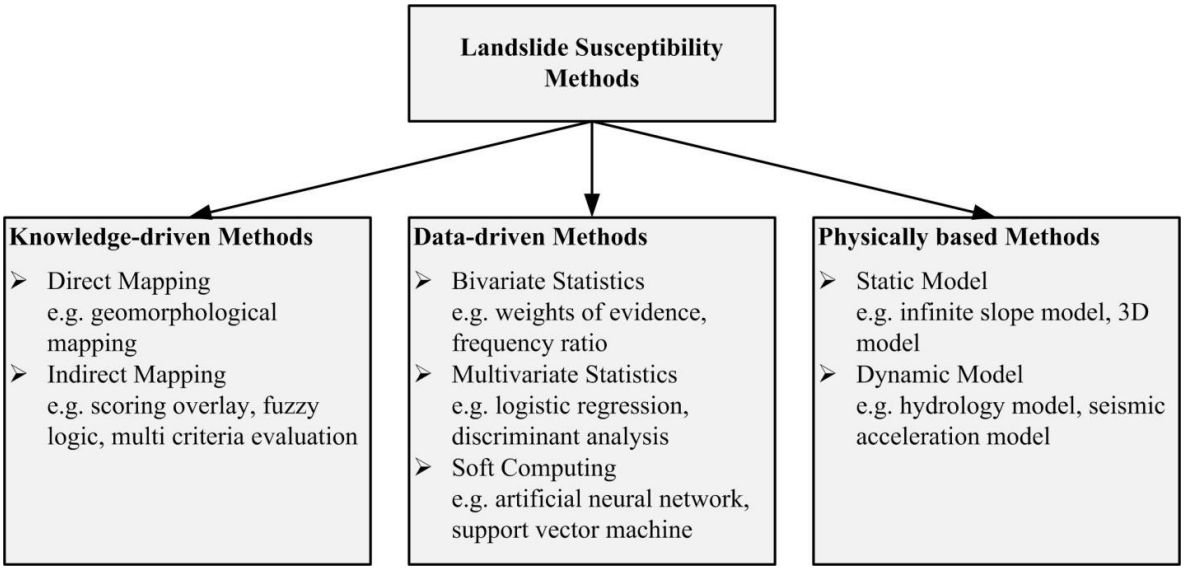

Figure 2.1 Landslide susceptibility assessments methods

Landslide susceptibility zoning is usually carried out in GIS-based system. GIS (Geographic Information Systems) and remote sensing technology offer more effective and efficient data handling for modeling of the real world. It can support efficient and effective data capture, storage, management, retrieval, analysis, integration and display, and have shown great advantages to the

study and mapping of landslide distributions and potential (Carrara *et al*., 1995). Recently, GIS technology has influenced the development of landslide susceptibility zoning and given more benefits to model it (Atkinson and Massari, 1998; Westen *et al*., 2003; Huabin *et al*., 2005). Several methods of landslide susceptibility include knowledge driven, data driven, and physically based methods (Figure 2.1).

Knowledge-driven method is classified into qualitative, whereas data driven and physically based methods are classified as quantitative. The assessment of landslide susceptibility can also be classified based on the area extents i.e. in site-specific location and in wide areas. In the site-specific location, landslide susceptibility zoning is usually emphasized on the safety factor of the slope. In the other hand, the assessment of the wide area is usually represented by landslide susceptibility zoning either in qualitative, semi-quantitative or quantitative.

Knowledge-driven or heuristic method can be direct (i.e. geomorphology-landslide mapping) and indirect (i.e. index based, AHP, fuzzy logic and spatial multi criteria evaluation). Direct Geomorphological susceptibility zoning is a traditional method in landslide susceptibility zoning. It includes the identification of landforms related to landslide. Long experiments, fieldwork and laboratory analysis were done in order to provide a landslide hazard assessment. Some geomorphology features were analyzed, including soil properties related to the landslide. This work was especially done in specific geomorphology features presumed as the main factor of landslide such as in micrograben (Moeyersons *et al*., 2003). In Indonesia, direct geomorphological hazard zoning is usually combined with heuristic or index-based method (Priyono *et al*., 2006; Kumajas, 2006; Mardiatno, 2001; Sutikno *et al*., 2002).

Geomorphology features were analyzed through terrain mapping unit. Soil properties were analyzed based on terrain mapping unit in order to index the potential landslide hazard. This method usually did not analyze the past landslide occurrences or without landslide inventory mapping. It is very subjective and depends on the experience and the judgment of the researcher (Atkinson and

Massari, 1998; Nagarajan *et al*., 2000; Huabin *et al*., 2005). However, it sometimes can be used to control mathematic or statistic procedure used in landslide susceptibility zoning or modeling (Westen *et al*., 2003; Guzzetti, 2005).

The more objective methods and quantitatively sound are geotechnical or physically based models and statistically based models. Geotechnical or physically based models are usually based on the slope analysis, determining safety factor in the slope. It is usually applied in site-specific location (large scale mapping) and detail measurement of slope failure. The limitation of geotechnical models are that the model can only be applied in the homogeneous geological region (Dahal, *et al*., 2007), similar landslide mechanism, and cannot be analyzed easily (Huabin *et al*., 2005). It is not possible to be applied in the wide area because of the mechanical parameter of the slope cannot be extrapolated in the regional scale (Ruff and Czurda, 2007)

The statistical (data-driven) based model was widely used due to the development of GIS technology. The model is usually applied either based on bivariate, multivariate or soft computing. Bivariate involves weight of evidence (van Westen, 1993; Bonham-Carter, 1994; Suzen and Doyuran, 2004), likelihood ratio model (Lee, 2005), and favourability functions (Chung and Fabbri, 1993; Luzi, 1995). Multivariate model involves discriminant analysis (Carrara, 1983; Gorsevski et al., 2000) and logistic regression (Ohlmacher and Davis, 2003; Gorsevski et al., 2006).

Soft computing involves ANN (Lee et al., 2004; Ermini et al., 2005; Kanungo et al., 2006) and SVM (Yao et al., 2008) Landslide susceptibility is an initial step towards landslide hazard and risk, but it can also be an an end product that can be used in land use planning (Corominas et al., 2013). In Indonesia, geomorphological mapping combined with heuristic weighting is one of the most common methods of landslide susceptibility zoning due to unavailability of spatial past landslide inventory data. Geomorphology approach, focusing on landform, material, and geomorphic processes were used in order to construct a landslide susceptibility map (Sutikno, 1994). Either data driven method and physically based method are rarely applied in Indonesia. Comparison of

quantitative method is essential to generate the most suitable method in landslide susceptibility zoning.

2.6 Temporal probability

It is difficult, up to now, to predict exactly when landslide will occur due to the limitations to human knowledge of nature. Temporal probability is used as an approach to estimate the occurrence of landslides during a specified time in a particular area (Crovelli, 2000). It can be expressed in terms of frequency, return period or exceedance probability. Frequency, as annual frequency, represents the number of landslide event in a year in an area (i.e. number/km2/year). The return period represents the average time interval of a landslide event expected to occur. It is an inverse of the annual probability. The exceedance probability expresses the probability that one or more events will occur in a certain period. Exceedance probability usually includes the magnitude of landslides which means the probability of landslides with magnitude equal or larger than a certain value in a certain period.

Temporal probability estimation is mainly based on the availability of past landslide data. Temporal probability or cumulative occurrence of landslide is estimated based on known intervals (Hungr et al., 1999; Guthrie and Evans, 2004; Jaiswal and Westen, 2009). Temporal probability can also be derived by establishing an empirical relation between landslides event and its triggering factor, i.e. intensity of rainfall or or earthquake, which later called as magnitude-frequency analysis (Crozier, 1999; van Westen, et al., 2006). Ghosh (2011) estimated temporal probability, by using landslide event-days and associated daily and antecedent rainfall to model the temporal relationship between landslide events and the amount of triggering rainfall. Keefer (2002) estimated landslide occurrences by using the intensity of the landslide and earthquake.

2.7 Magnitude probability

In natural hazard studies, the magnitude-frequency relationship has been observed based on complete past events data i.e. earthquake and floods. It describes the specific relationship between the frequency of events falling in different magnitude classes. The well-known magnitude-frequency relationship is a relation between earthquake magnitude and cumulative frequency expressed by Gutenberg equation as follows:

$$logN(m) = a - bM \quad (2.2)$$

where *N(m)* is the cumulative number of earthquake events with magnitudes equal or greater than M, a and b are constant.

The magnitude of landslides refers to the volume of material which may fail, the velocity of movement during failure, and the land area which may be affected (Fell, 1994; Crozier, 1995 and Hutchinson, 1995). It is usually represented by the statistics of landslide sizes (area or volume) either using the cumulative or the non-cumulative distribution. Both indicate landslides area or landslides volume, above threshold, is generally well approximated by negative power law (Brunetti, 2009). It is formally equivalent to the Gutenberg-Richter equation. The cumulative number of landslide is described by the equation as follows:

$$NL = rV_L^{-\alpha} \quad (2.3)$$

where N_L is the cumulative number of landslides, V_L is the landslide volume, α is the cumulative power-law scaling exponent, and *r* is a constant. In the other hand, non-cumulative number-volume distribution also follows a power law:

$$N_L' = \frac{dN_L}{dV_L} = -\alpha r V_L^{-(\alpha+1)} = sV_L^{-\beta} \quad (2.4)$$

Where *dNL* is the number of landslides in the volume interval [*VL; VL+dVL*] (i.e. in a "bin" size *dVL*), *β* is the non-cumulative scaling exponent and s is a constant. Non-cumulative power law distribution with exponent β>1 has exponent α= β-1 (Guzzetti et al., 2002). Without the estimation

of the expected annual frequency of landslide events of a given magnitude or exceeding magnitude threshold, quantitative hazard assessment is not feasible.

2.8 Landslide vulnerability

The ability to measuring vulnerability has been increasing significantly through the increasing frequency of disasters and environmental degradation (Arakida, 2006; Wisner, 2006; Villagran de Leon, 2006). It has been increasing due to the undesirable for defining landslide primarily as a physical process. For example, factor safety is not always being able to perform the capabilities on inhibiting undesirable behavior (Morgenstern, 1997). It is traditionally that landslide was viewed as an isolated physical event and few linkages were made to link the landslide event with the people affected by the disaster (Bollin and Hidajat, 2006). As a kind of disaster, landslide is better viewed as a result of complex interaction among physical processes and social process. Vulnerability is an important thing to formulate social aspect as a result of interaction between landslide occurrence and potentially damaging event.

The vulnerability in rural area more tends to have such a tendency rather randomly. Since the nature of people, social structure and culture were less influenced by the development of technology and modernization, the natural feature and condition would more dominantly influence the way of life. It is related to the preference of the people to build settlements in the hilly and rural area. According to Whynne-Hammond (1979) the growing of settlement (village) is based on the combination of four factors i.e. topographical, economic, historical, and cultural. The conceptual framework of vulnerability has been proposed by several authors in order to systematize the definition and to make relevant indicators to measure it. (Birkmann, 2006) explains several conceptual framework of vulnerability, i.e. the double structure of vulnerability as defined by Bohle, vulnerability within the framework of hazard and risk, and vulnerability based on the UN/ISDR framework for disaster risk reduction.

The double structure of vulnerability indicates two major sides of vulnerability, i.e. internal and external side. Internal side relates to the capacity to anticipate, cope with, resist and recover from the impact of hazards; whereas external side relates to the exposure to risks as an impact of hazards. It seems that exposure, coping capacity, and response capacity should be analyzed simultaneously. In contrast, vulnerability within the framework of hazard and risk defines that vulnerability is defined separately with coping capacity and exposure. It results in the formulation of risk as the sum of hazard, exposure, vulnerability, and capacity measures. Therefore, vulnerability is defined as one component of disaster risk. Moreover, (UN/ISDR, 2004) defines vulnerability as a key factor, a tool, and a preconditioning to determine risk. It is divided into physical, environmental, social, and economic components.

Vulnerability can be defined as the condition increased the susceptibility of the community as the impact of hazard, which is determined by physical, social, economic and environmental factors or process (UN/ISDR, 2004). Similar with UN/ISDR, ADPC (2004) divides the factors of vulnerability into four types:

1. Physical vulnerability (building age, construction, material, infrastructures, lifeline facilities)

2. Social vulnerability (risk perception and way of life related to culture, religion, ethnicity, social interaction, age, gender, attitude of population property)

3. Economic vulnerability (income, investments, potential loss of stock)

4. Environmental vulnerability (water, air, land, flora and fauna)

Varnes, (1984) defines a vulnerability definition subjected to landslide as the degree of loss to a given element at risk resulted from the impact of the natural phenomenon of a given magnitude. The vulnerability degree is expressed on a scale from 0 (no damage) to 1 (total loss). Elements at risk of landslides can be settlement building, properties, population, and public services in a given area. Thus, landslide vulnerability can be viewed as intrinsic feature that determines the degree of

loss to a given element at risk as an impact of landslide which can be measured through the proxies of physical, social, economic, and environmental dimension.

The landslide hazard map will be more valuable with the analysis of landslide vulnerability in order to develop landslide risk. Vulnerability is related to the consequences of the impact of disaster which is generally measured by damage or loss (Glade, 2003). Therefore, it is important to define the degree of vulnerability in each type of landslide. The degree of vulnerability will also be different related to the ability of individual, community, or society to cope and to anticipate the impact of disaster. When the disaster happens, more complex systems are usually involved to tackle down the problem (Bell and Glade, 2004). It includes the physical, social, economic, and environmental dimension. Both landslide vulnerability and landslide risk assessment will be more informative to be represented as a map processed by GIS.

2.9 Current issues in landslide risk analysis

Several issues in quantitative landslide risk analysis include developing technique in inventory mapping, particularly in a data scarce environment, selecting methods for landslide susceptibility assessment, and developing approaches for landslide risk analysis. It varies depending on the availability of secondary data, geomorphological characteristic, and landslide typology. The availability of data input is very important prior to landslide risk analysis. It can affect the overall methodology or approaches applied in the landslide risk analysis.

Despite the availability of landslide inventory, geomorphological characteristic of the study area should also be considered prior to selecting suitable landslide susceptibility and risk analysis. Some approaches in landslide susceptibility and risk analysis can also not be applied in rockfall susceptibility and risk analysis. For example, landslide susceptibility assessment based on GIS and statistics uses landslide area represented by polygon to estimate susceptibility.

2.9.1 Insufficient landslide inventory mapping

Generating landslide analysis is difficult in some areas because the unavailability of the landslide inventory map. However, the recent technology developments such as the availability of the modern field instrument, high resolution DTMs, high resolution satellite imagery, recent development on GIS and remote sensing technology have made generating landslide map easier. But, the selection of this technique should be carefully reviewed based on the purpose, the extent of the study area, the scale of base maps and analysis, resolution and characteristics of the available imagery, and the skill and experience of the interpreter (Guzetti et al., 2000; van Westen et al., 2006).

Mapping landslide through field survey is the oldest technique for landslide inventory mapping and considered as the most accurate technique for mapping fresh landslide events. But it is difficult, by using field survey, to recognize old landslides in the field where the natural process (e.g. erosion, vegetation) and the anthropogenic activities (e.g. urbanization, road construction, ploughing) are exist. The use of aerial photograph interpretation is also difficult in Indonesia due to unavailability of multiple sets of aerial photograph in the same area and different time. In the other hand the use of recent technology such as very high resolution of DTMs and remote sensing imagery faces problems related to budget limitation and cloud problem in remote sensing images. Thus, combination techniques are needed to map landslide events either old or recent landslide events.

2.9.2 Landslide susceptibility selection method

Quantitative statistical analysis has been widely applied as a standard method for landslide susceptibility zoning in wide areas (regional scale mapping). It includes bivariate statistic, multivariate statistic and soft computing. Bivariate analysis assumes that the presumed controlling factors of landslide are not interrelated each other (Suzen and Doyuran, 2004). It is a robust and flexible method, but has several limitations, including over simplification of input thematic data related to landslides and loss of data sensitivity of controlling factors (Thiery et al., 2007). Bivariate

statistical methods can also be used to determine which factors or combination of factors play a role in the initiation of landslides.

In the other hand, multivariate analysis assumes that the presumed controlling factors of landslide are interrelated each other. It determines the relative contribution of each landslide causal factor in the presence or absence of past landslide events (Dai et al., 2001; Süzen and Doyuran, 2004; Ayalewand Yamagishi, 2005; Nandi and Shakoor, 2009). Multivariate statistical analysis can be used to predict a result measured by a binary variable such as the absence or presence of landslides based on a set of one or more landslide causal factors as independent variables. The independent variables can be nonlinear, continuous, categorical or a combination of both continuous and categorical; and does not to be normally distributed.

Soft computing techniques were used in the assessment of the landslide susceptibility because of a limitation such as insufficient knowledge about the area of interest. Its computing procedure has the ability to handle imprecise and fuzzy data with continuous, categorical and binary data without violating assumptions and also independent of the statistical distribution of the data. The purpose of soft computing technique, i.e. ANN, is to build a model of the data-generating process so that the network can generalize and predict outputs from inputs that it has not previously seen (Lee et al., 2001).

One of the main advantages of data driven landslide susceptibility is the easily updating of the landslide susceptibility assessment procedure and also relatively easy to apply for land-use planning. However, it can be affected by shortcomings such as the assumption that landslides occur due to the same combination of factors throughout a study area, spatial factors can vary widely in areas with complex geomorphological settings, and the lack of suitable expert opinion on landslide processes and causal factors (Corominas et al., 2013). Selecting method, i.e. either bivariate, multivariate or soft computing is essential to apply for landuse planning based on complete landslide inventory.

2.10 Conclusions

Landslide risk analysis comprises several terminologies which are used interchangeably and often generates confusion. It includes risk, hazard, inventory, susceptibility, temporal probability, magnitude probability and vulnerability. Understanding terminologies in the landslide risk analysis is important in which allows scientists and engineer quantify landslide risk in an objective way, reproducible and the result can be compared from one region to another region. The confusion may also arise when there are available methodologies applied for different landslide mechanism and typology. Generating landslide inventory, distinguishing landslide typology for different method on risk analysis, and selecting an appropriate method for susceptibility are among the current issues which should be taken into account in the quantitative landslide risk analysis.

2.11 References

ADPC. 2004. A Framework for Reducing Risk, in CBDRM Field Practitioners Handbook. Bangkok, Thailand. Accessed on September 2009 from http://www.adpc.net/PDR SEA/publications/12Handbk.pdf

Agliardi, F. and Crosta, G. 2003. High resolution three-dimensional numerical modelling of rockfalls. *Int. J. Rock Mech. Min., Sci.,* 40, 455–471.

Andersen, T., G., Bollerslev, T., Christoffersen, P. F., and Diebold, F. X. 2013. *Financial Risk Measurement and Management* in Constantinides, G. M.,

Harris, M., and Stulz, R. M (Eds.). Handbook of the Economics and Finances. Elsevier.

Anonym. 2007. Undang-Undang Nomor 24 Tahun 2007 tentang Penanggulangan Bencana, Lembaran Negara Republik Indonesia tahun 2007 nomor 66, Jakarta.

Arakida, M. 2006. Measuring Vulnerability: The ADRC Perspective for the Theoretical Basis and Principles of Indicator Development, edited by Birkmann, J. *Measuring Vulnerability to Natural Hazard: Towards Disaster Resilient Societies*. United Nation University Press. USA.

Atkinson, P. M. and Massari, R. 1998. Generalized Linear Modelling of Susceptibility to Landsliding in The Central Apennines, Italy. *Computers & Geosciences* vol. 24, no. 4:373-385.

Ayalew, L. and Yamagishi, H. 2005. The application of GIS-based logistic regression for landslide susceptibility zoning in the Kakuda-Yahiko Mountains, Central Japan. Geomorphology, 65, 15-31.

Barlow, J., Franklin, S., Martin, Y. (2006). "High spatial resolution satellite imagery, DEM derivatives, and image segmentation for the detection of mass wasting processes". Photogrammetric Engineering and Remote Sensing, 72, pp. 687-692.

Bell, R and Glade, T. 2004. Quantitative Risk Analysis for Landslides-Examples from Bildudalur, NW-Iceland. *Natural Hazards and Earth System Sciences (2004) 4*: *117–131*. European Geoscience Union, 2004.

Birkmann, Jorn. 2006. Measuring Vulnerability to Promote Disaster-Resilient Societies: Conceptual Framework and Definitions, edited by Birkmann, J. *Measuring Vulnerability to Natural Hazard: Towards Disaster Resilient Societies*. United Nation University Press. USA.

Bollin, C. and Hidajat, R. 2006. Community Based Disaster Risk Index: Pilot Implementation in Indonesia, edited by Birkmann, J. *Measuring Vulnerability to Natural Hazard: Towards Disaster Resilient Societies*. United Nation University Press. USA.

Bonham-Carter, G. F. 1994. Geographic Information Systems for Geoscientists: Modelling with GIS. Computer Methods in the Geosciences, 13: pp 267-302.

Pergamon. Borghuis, A. M., Chang, K., Lee, H. Y. 2007. Comparison between automated and manual mapping of typhoon-triggered landslides from SPOT-5 imagery". International Journal of Remote Sensing, 28, pp. 1843-1856.

Brardinoni, F., Slaymaker, O., Hassan, M. A. 2003. Landslide inventory in a rugged forested watershed: a comparison between air-photo and field survey data. *Geomorphology* 54:179–196.

Cardona, O. D. 2003. *The Notion of Disaster Risk: Conceptual Framework for Integrated Risk Management,* IADB/IDEA Program on Indocators for Disaster Risk Management, Universidad Nacionalde Colombia, Manizales accessed from http://idea.manizales.unal.edu.co/ProyectosEspeciales/adminIDEA/centroDocumentacion/DocDigitales/documentos/01%20Conceptual%20Framework%20IADB-IDEA%20Phase%20I.pdf

Carrara, A. and Merenda, L. 1976. Landslide inventory in northern Calabria, southern Italy. Geol Soc Am Bull. 87: 1153−1162.

Carrara, A., Cardinali, M., Guzzetti, F., and Reichenbach, P. 1995. GIS Technology in Mapping Landslide Hazard. In: Carrara, A. and Guzzetti, F. (eds.), *Geographical Information Systems in Assessing Natural Hazards* page: 135–175. Kluwer Academic Publisher, Dordrecht, the Netherlands.

Carrara A., *1983*. *Multivariate models* for landslide hazard evaluation. Mathematical Geol., v. 15, n. 3, p. 403-426.

Chacon, J., Irigaray, C., Fernandez, T., and El Hamdouni, R. 2006. Engineering geology maps: landslides and Geographical Information Systems (GIS), *Bull. Eng. Geol. Environ*., 65, 341–411.

Chen. G. 2003. Numerical Modelling of Rockfall using Extended DDA. *Chinese Journal of Rock Mechanics and Engineering*, 22 (6):926-931.

Chung, C. F. and Fabbri, A. G. 1993. The representation of geosciences information for data integration. *Nonrenewable Resources*, 2(2), PP.122-139.

Corominas J and Moya J. 2008. A review of assessing landslide frequency for hazard zoning purposes. Engineering Geology 102:193–213. doi:b10.1016/j.enggeo.2008.03.018.

Corominas, J., van Westen, C., Frattini, P., Cascini, L., Malet, J. P., Fotopoulou, S., Catani, F., Van Den Eeckhaut, Mavrouli, O., Agliardi, F., Pitilakis, K., Winter, M. G., Pastor, M., Ferlisi, S., Tofani, V., Hervas, J., Smith, J. T. 2014. Recommendations for the quantitative analysis of landslide risk. *Bulletin Engineering Geology and the Environment*. Vol. 73, Issue 2, pp 209-263.

Crovelli, R. A. 2000. *Probability models for estimation of number and costs of landslides*. USGS Denver, Colorado.

Crozier, M. J. 1995. Landslide hazard assessment: a review of papers submitted to theme G4. Bell, D. H. (Ed.) Proceedings of the sixth International Symposium, 10-14 February 1992. Christchurch, New Zealand, A.A. Balkema, Rotterdam:1843-8.

Crozier MJ (1999) Prediction of rainfall-triggered landslides: A test of the antecedent water status model. *Earth Surface Processes and Landforms* 24:825-33.

Dahal, R.K., Hasegawa, S., Nonomura, A., Yamanaka, M., Masuda, T., Nishino, K. 2007. GIS Based Weights-of-Evidence Modeling of Rainfall Induced Landslides in Small Catchments for Landslide Susceptibility Mapping. *Environ Geol,* doi: 10.1007/s00254-007-0818-3

Dai, F.C., Lee, C.F., Li, J. and Xu, Z.W. 2001. Assessment of landslide susceptibility on the natural terrain of Lantau Island, Hong Kong. *Environmental Geology*, Vol. 40, 381- 391

Dai FC, Lee CF (2002) Landslide characteristics and slope instability modeling using GIS, Lantau Island Hongkong. *Geomorphology* 42:213-228.

Ebert, A., Kerle, N., & Stein, A. 2009. Urban Social Vulnerability Assessment with Physical Proxies and Spatial Metrics derived from Air- and Spaceborne Imagery and GIS Data. *Nat Hazards 48:275–294*.

Ermini, L., Catani, F., Casagli, N. 2005. Artificial neural networks applied to landslide susceptibility. *Geomorphology* 66:327-343.

Fell R, Corominas J, Bonnard C, Cascini L, Leroi E, Savage W.Z (2008) Guidelines for landslide susceptibility, hazard, risk zoning for land-use planning. *Engineering Geology* 102:99-111.

Fell, R. 1994. Landslide risk assessment and acceptable risk. *Canadian Geotechnica*

Journal , 31: 261-272.

Galli M, Ardizzone F, Cardinali M, Guzzetti F, Reichenbach P (2008) Experimental acute renal failure. Dissertation, University of California. Comparing landslide inventory maps. *Geomorphology* 94:268–289.

Ghosh, S. 2011. Knowledge Guided Empirical Prediction of Landslide Hazard. *PhD Thesis*. University of Twente, Netherland.

Glade, T., Anderson, M., Crozier M.J. 2005. *Landslide hazard and Risk*. John Wiley & Sons Ltd.

Glade, T. 2003. Vulnerability assessment in landslide risk analysis, *Die Erde*, 134, 2, 121–138, 2004b. Accessed February 2007 from homepage.univie.ac.at/thomas.glade/Publications/Glade2003b.pdf

Godt J.W., Baum R.L., Savage W.Z., Salciarini D, Schulz W.H., Harp E.L. 2008. Transient deterministic shallow landslide modeling: Requirements for susceptibility and hazard assessments in a GIS framework. *Engineering Geology* 102:214–226.

Gorsevski, P. V., Gessler, P., Foltz, R. B. 2000. Spatial prediction of landslide hazard using discriminant analysis and GIS. GIS in the Rockies 2000 Conference. Available online at http://www.fs.fed.us/rm/pubs_other/rmrs_2000_foltz_r001.pdf

Gorsevski, P.V., Gessler, P.E., Foltz, R.B.and Elliot, W.J. 2006. Spatial prediction of landslide hazard using logistic regression and ROC analysis. *Transactions in GIS* 10 (3), 395-415.

Guhtrie RH, Evans SG (2004) Analysis of landslide frequencies and characteristics in a natural system, coastal British Columbia. *Earth Surf. Process. Landforms* 29:1321–1339.

Guzetti, F., Carrara, A., Cardinali, M., Reinchenbach, P. 1999. Landslide hazard evaluation: a review of current techniques and their application in a

multi-scale study, Central Italy. *Geomorphology* 31:181-216.

Guzzetti F., Cardinali M., Reichenbach P., Carrara A. 2000. Comparing landslide maps: a case study in the upper Tiber River Basin, Central Italy. *Environmental Management* 25 (3):247–363.

Guzzetti, F., Malamud, B., Turcotte, D. L., Reichenbach, P. 2002. Power–law correlations of landslide areas in central Italy. *Earth and Planetary Science Letters* 195:169–183.

Guzzetti, F., Reichenbach, P., Cardinali, M., Galli, M., Ardizzone, F. 2005. Probabilistic landslide hazard assessment at the basin scale. *Geomorphology* 72:272–299.

Guzzetti, F., Galli, M., Reichenbach, P., Ardizzone, F., Cardinali, M. 2006. Landslide hazard assessment in the Collazzone area, Umbria, central Italy. *Natural Hazards and Earth System Sciences* 6:115–131.

Guzzetti F, Mondini A.C., Cardinali M, Fiorucci F, Santangelo M, Chang K.-T. 2012. Landslide inventory maps: New tools for an old problem. *Earth-Science Reviews* 112:42–66.

Hansen, A. (1984). "Strategies for classification of landslides". In: Brunsden, D., Prior, D.B. (Eds.), Slope Instability. Wiley, New York, pp. 523-602.

Hoek, E. 2007. Practical Rock Engineering. available online at : http://www.rocscience.com/hoek/pdf/Practical_Rock_Engineering.pdf

Huabin, W., Gangjun, W., Weiya, X., and Gonghui, W. 2005. GIS-based Landslide Hazard Assessment: an Overview. *Progress in Physical Geography* 29, 4 page 548-567

Hungr, O., Evans, S. G., and Hazzard, J. (1999). "Magnitude and frequency of rockfalls and rock slides along the main transportation corridors of south-western British Columbia". *Can. Geotech. J.*, 36, 224–238,. Hutchinson, J. N.: Keynote paper: landslide hazard assessment, In: Landslides, (Ed.) Bell, Balkema, Rotterdam, 1805–1841, 1995

IUGS Working Group on Landslides. 1997. Quantitative Risk Assessment for Slopes and Landslides – The State of The Art in Cruden, D and Fell, R. (Eds). *Landslide Risk Assessment*. Balkema, Rotterdam. The Netherlands

Jaiswal, P. and van Westen, C.J. 2009. Estimating temporal probability for landslide initiation along transportation routes based on rainfall thresholds. *Geomorphology* 12, 1-2 pp. 96-105.

Kanungo, D. P., Arora, M. K., Sarkar, S., Gupta, R.P. 2006. Comparative study of conventional, ANN black box, fuzzy and combined neural and fuzzy weighting procedures for landslide susceptibility zonation in Darjeeling Himalayas. *Engineering Geology*, 85, pp. 347-366.

Keefer, D. K. 2000. Statistical analysis of an earthquake-induced landslide distribution of the 1989 Loma Prieta, California event. *Engineering Geology*, 58, pp. 231-249.

Kumajas, M. 2006. Inventarisasi dan Pemetaan rawan Longsor Kota Manado – Sulawesi Utara. *Forum Geografi*, vol. 20, no. 2, December 2006: 190-197.

Lan, H., Martin, C. D., and Lim, C. H. 2007. RockFall analyst: a GIS extension for three-dimensional and spatially distributed rockfall hazard modeling. *Computer and Geoscience*., 33, 262–279.

Lee, S., Ryu, J., Min, K., Won, J. 2001. Development of two artificial neural network methods for landslide susceptibility analysis. Proceeding of Geoscience and Remote Sensing Symposium, IGARSS `01. IEEE 2001 International 5:2364-2366.

Lee, S., Ryu, J., Won, J., Park, H. (2004). Determination and application of weights for landslide susceptibility mapping using an artificial neural network. *Engineering Geology*, 71, pp. 289-302.

Lee, S. 2004. Application of likelihood ratio and logistic regression models to landslide susceptibility mapping using GIS. *Environmental Management* 34 (2), 223-232

Luzi, L., 1995, GIS for Slope Stability Zonaton in the Fabriano Area, Central Italy. ITC, Enschede, The Netherlands.

Malamud B.D., Turcotte D.L., Guzetti F, Reichernbach P (2004) Landslide inventories and their statistical properties. *Earth Surf. Process. Landforms* 29:687–711. 10.1002/esp.1064.

Mardiatno, D. 2001. Resiko Longsor di Kecamatan Girimulyo. *Thesis*. Fakultas Geografi UGM, Yogyakarta.

Martha T.R., Kerle N, Jetten V, van Westen C.J., Kumar K.V (2010) Characterising spectral, spatial and morphometric properties of landslides for semi-automatic detection using object-oriented methods. *Geomorphology* 116:24–36. doi: 10.1016/j.geomorph.2009.10.004.

Moeyersons, J., Trefois, Ph., Lavreau ,J., Alimasi, D., Badriyo, I., Mitima, B.,Munadala, M., Munganga, D. O., Nahimana, L. 2004. A Geomorphological Assessment of Landslide Origin at Bukavu, Democratic Republic of the Congo. *Engineering Geology* 72, page 73-87.

Moine, M., Puissant, A., Malet, J. P. (2009). "Detection of landslides from aerial and satellite images with a semi-automatic method. Application to the Barcelonnette basin (Alpes-de-Haute-Provence, France)". In: Malet, J.-P., Remaitre, A., Bogaard, T. (Eds.), Landslide Processes: From Geomorphological Mapping to Dynamic Modelling. CERG, Strasbourg, France, pp. 63-68.

Mondini, A. C., Guzzetti, F., Reichenbach, P., Rossi, M., Cardinali, M., Ardizzone, F. (2011). Semi-automatic recognition and mapping of rainfall induced shallow landslides using satellite optical images. *Remote Sensing of Environment*,

115, pp. 1743-1757.

Morgenstern, N. R. 1997. Toward Landslide Risk Assessment in Practice in Cruden, D. M and Fell, R. (eds). *Landslide Risk Assessment*, Balkema: Rotterdam. The Netherlands.

Nagarajan, R., Roy, A., Vinod Kumar, R., Mukherjee, A., Khire, M. V. 2000. Landslide Hazard Susceptibility Mapping Based on Terrain and Climatic Factors for Tropical Monsoon Regions. *Bull Eng Geol Env* 58: 275-287. Springer-Verlaag

Nandi A, Shakoor A (2009) A GIS-based landslide susceptibility evaluation using bivariate and multivariate statistical analyses. *Engineering Geology* 110:11-20.

Nichol, J., Wong, M. S. (2005). Satellite remote sensing for detailed landslide inventories using change detection and image fusion. *International Journal of Remote Sensing*, 26, pp. 1913-1926.

Ohlmacher, C.G., Davis, C.J., 2003. Using multiple regression and GIS technology to

predict landslide hazard in northeast Kansas, USA. *Engineering Geology* 69,

331–343

Pierson, L.A., Davis, S.A., Van Vickle, R. 1990. Rockfall Hazard Rating System Implementation Manual, Federal Highway Administration (FHWA) Report FHWA-OREG- 90-01, FHWA, United States Department of Transportation.

Pradhan B (2010) Remote sensing and GIS-based landslide hazard analysis and cross-validation using multivariate logistic regression model on three test areas in Malaysia. *Advance in Space Research* 45:1244-1256.

Priyono, D.K., Priyana, Y., Priyono. 2006. *Analisis Tingkat Bahaya Longsor Tanah di Kecamatan Banjarmangu Kabupaten Banjarnegara*. *Forum Geografi*, Vol. 20, No. 2, hal: 175 – 189.

Romana, M. 1993. A geomechanical classification for slopes: slope mass rating, *Comprehensive Rock Engineering*, Oxford, Pergamon.

Rosin, P.L., Hervás, J., 2005. Remote sensing image thresholding methods for determining landslide activity. *International Journal of Remote Sensing* (6), 1075–1092.

Ruff, M. and Czurda, K. 2007. Landslide susceptibility Analysis with a Heuristic Approach at The Eastern Alps (Voralberg, Austria). *Geomorphology*, doi: 10.1016/j.geomorph.2006.10.032.

Sasaki, Y. Dobrev, N., Wakizaka, Y. 2002. The detailed Hazard Map of road Slopes in Japan, in Instability-Planning and Management, London, Thomas Telford, p.381-388. Eds: McInnes, R. G and Jakeways Jenny

Shirzadi, A., Saro, L., Joo, O. H., and Chapi, K. 2012. A GIS-based logistic regression model in rockfall susceptibility mapping along a mountainous road: Salavat Abad case study, Kurdistan, Iran. *Nat. Hazards*, 64, 1639–1656.

Soanes C, Stevenson A (eds) (2005) Oxford dictionary of English, (revised) 2nd edn. Oxford University Press, Oxford

Sutikno. 1994. Pendekatan Geomorfologi untuk Mitigasi Bencana Alam Akibat Gerakan Massa Tanah Batuan. *Makalah Simposium Nasional Mitigasi Bencana Alam*. Fakultas Geografi. Universitas Gadjah Mada, Yogyakarta.

Sutikno, Huda, M., Sarwondo, Triyono. 2002. Sistem Informasi Penanggulangan

Bencana Alam Tanah Longsor Kabupaten Kulon Progo. *Simposium Nasional Pencegahan Bencana Alam*. ISDM Project. Yogyakarta.

Suzen, M. L. and Doyuran, V. 2004. Data Driven Bivariate Landslide Susceptibility Assessment Using GIS: a Method and Application to Asarsuyu Catchment, Turkey. *Engineering Geology* 71, pp 303-321.

Thierry, Y., Malet, J.P., Sterlacchini, S. Puisant, A., Maquaire, O. 2007. Landslide susceptibility assessment by bivariate methods at large scale: application to a complex mountainous environment. *Geomorphology, 92, 38-59.*

UN/ISDR (International Strategy for Disaster Reduction). 2004. *Living with Risk: A Global Review of Disaster Reduction Initiatives*. Geneva: UN Publications.

Van Den Eeckhaut M, Poesen J, Verstraeten G, Vanacker V, Moeyersons J, Nyssen J,

Van Beek LPH (2005) The effectiveness of hillshade maps and expert knowledge in mapping old deep-seated landslides. *Geomorphology* 67: 351–363.

van Westen, C. J., Rengers. N., Soeters. R. 2003. Use of Geomorphological Information in Indirect Landslide Susceptibility Assessment. *Natural Hazard* 30: 399-419. Kluwer Academic Publishers. Netherlands.

van Westen CJ, Asch TWJ, Soeters R (2006) Landslide hazard and risk zonation-why is it still so difficult? *Bull Eng Geol Env* 65: 67-184

van Westen C.J., Castellanos E, Kuriakose S.L. 2008. Spatial Data For Landslide Susceptibility, Hazard, and Vulnerability Assessment: An Overview. *Engineering Geology* 102:112-131.

van Westen, C. J. 1993. Application of geographic information systems to landslide hazard zonation. *PhD dissertation*, Technical University Delft. ITC-publication number 15, ITC,

Varnes, D.J. (1984). *Landslide Hazard Zonation*: *a Review of Principles and Practice*. United Nations Educational, Scientific and Cultural Organization (UNESCO). Paris

Villagran de Leon, J. C. 2006. Vulnerability Assessment: The Sectoral Approach, in Birkmann, J. (eds). *Measuring Vulnerability to Natural Hazard*: *Towards Disaster Resilient Societies*. United Nation University Press. USA.

van Westen, C. J., Rengers. N., Soeters. R. 2003. Use of Geomorphology Information in Indirect Landslide Susceptibility Assessment. *Natural Hazard* 30: 399-419. Kluwer Academic Publishers. Netherlands.

Whynne-Hammond, C. 1979. *Elements of Human Geography*. George Allen and Unwin. London.

Wieczorek, G.F., 1984, Preparing a detailed landslide-inventory map for hazard evaluation and reduction: *Association of Engineering Geologists Bulletin*, v. 21, no. 3, p. 337–342

Wisner, B. 2006. Self-Assessment of coping capacity: Participatory, Proactive, and Qualitative Engagement of Communities in Their Own Risk Management, in Birkmann, J (eds). *Measuring Vulnerability to Natural Hazard*: *Towards Disaster Resilient Societies*. United Nation University Press. USA.

Yao, X., Tham, L. G., and Dai, F. C.: Landslide susceptibility mapping based on Support Vector Machine: A case study on natural slopes of Hong Kong, China, Geomorphology, 101, 572–582, 2008.

Chapter 3 GIS-based landslide susceptibility models comparison using frequency ratio, logistic regression, and artificial neural network in a tertiary region of Ambon, Indonesia

3.1 Introduction

Landslide is a major geological hazard worldwide, accounts for a high number of human casualties and an enormous amount of property loss, and causes severe damage to natural ecosystems and human-built infrastructures (Dai et al., 2002; Guzzetti et al., 2012). It is necessary to understand the potential exposure to landslide hazard in the areas of mountainous and hilly terrain. The elucidation of the triggering mechanism, characteristics of movement, soil mechanical properties, and the associated geology of landslides can translate to sufficient geologic investigations, geotechnical engineering practices, and ultimately effective enforcement of land management regulation to reduce landslide hazards.

Both environmental and triggering factors control landslide events (van Westen et al., 2008). The environmental factors comprised of elevation (e.g. slope, aspect, curvature, relief amplitude, and drainage density), geological settings (e.g. rock types, faults, and structural aspects), soil (e.g. soil types, soil depth, and geotechnical properties), hydrological regimes (e.g. proximity to stream and soil moisture), geomorphological situation (i.e. physiographic unit, terrain mapping units and geomorphological units) and land-use in the area (e.g. roads, buildings and vegetation characteristics). The triggering factors comprised of parameters that are often temporally relevant rather than spatially such as precipitation, earthquake, and volcano, except when dealing with large areas on a small mapping scale.

Over the last two decades, many models for landslide susceptibility mapping have been proposed with the assumptions that landslide susceptibility is related to causative factors and can be evaluated

as long as the causal relationship is known (Zhu et al., 2014). Even though the methods for landslide susceptibility mapping can be qualitative and quantitative, it is important to implement (Clerici et al., 2002; Süzen and Doyuran, 2004): 1) mapping of previous landslide inventory in the target region, 2) creation of geological and geomorphological factors that are directly or indirectly correlated with landslides, 3) estimation of the causative factors with the landslides, and 4) classification of the target region into categorical landslide susceptibility (hazard zoning).

Qualitative methods are based on the opinions of an individual or a group of experts (Neaupane and Piantanakulchai, 2006). Based on landslide inventory and historical information, experts evaluate landslides, determine the main factors inducing them, and identify sites that have similar geological and geomorphological properties and are susceptible to failure. Some qualitative approaches include ranking and weighting, hence become semi-quantitative (Ayalew and Yamagishi, 2005). Such examples are the Analytic Hierarchy Process (AHP) (Barredo et al., 2000; Kamp et al., 2008; Yalcin, 2008) and the weighted linear combination (WLC) (Jiang and Eastman, 2000; Ayalew and Yamagishi, 2005; Akgun et al., 2008). The disadvantages of these qualitative or semi-quantitative approaches are the involvement of subjective judgments and the failure to quantify of the weight of each contributing factor. The results for these approaches are somehow subjective and are highly dependent on knowledge of the experts. Based on landslide inventory and heuristic analysis, qualitative or semi-quantitative methods define the hazard zones in descriptive terms and are often useful for regional studies at small scales (< 1:125,000) (Soeters and Van Westen, 1996; Guzzetti et al., 1999; Bălteanu et al., 2010).

Quantitative methods employ mathematical models to estimate the probability of landslide occurrence in a region and thus define hazard zones on a continuous scale (Guzzetti et al., 1999). To achieve an accurate estimation of the probability of slope failure, a recent landslide inventory map, and complete information on the past mass movements are necessary. Quantitative methods include bivariate statistical models such as frequency ratio (Süzen and Doyuran, 2004; Thiery et al., 2007),

multivariate statistical techniques such as discriminant analysis (Carrara et al., 2003), and linear and logistic regression (Dai et al., 2002; Ayalew and Yamagishi, 2005; Yesilnacar and Topal, 2005; Greco et al., 2007), as well as non-linear methods such as artificial neural networks (Lee et al., 2004; Yesilnacar and Topal, 2005; Kanungo et al., 2006). They are less subjective than qualitative approaches (Ermini et al., 2005; Thiery et al., 2007), but have a high demand for data quality and quantity.

Although a large number of models and methods have been proposed to produce LS maps using geographic information systems (GIS), a consensus has not been established regarding which methods are most suitable (Vahidnia et al., 2010) because qualitative techniques can be limited by unconsidered phenomena or incomplete knowledge that the expert decisions are based upon, on the other hand quantitative methods suffer from inaccurate or low-precision data.

This study aims to evaluate the importance of each causative factors in landslide susceptibility assessments and to compare landslide susceptibility models of using bivariate frequency ratio, multivariate logistic regression, and artificial neural network in the tertiary region of Ambon, Indonesia. For this, the occurrence of landslides was detected in the study area by field surveys and satellite imagery derived from Google Earth™.

During May to August 2012, high-intensity rainfall in Ambon city triggered 89 landslides, most of these landslides happened in municipality area. The damage was severe in the city and at several sites along the transportation network. The landslides resulted in 167 houses destroyed, including 32 deaths, injured numerous people and 305 people evacuated (Fig. 3.1). Economic losses caused by the landslide events are estimated to be around 25 million U.S. dollars. Therefore, it is necessary to assess and manage areas that are susceptible to landslides and to mitigate any damage associated with them.

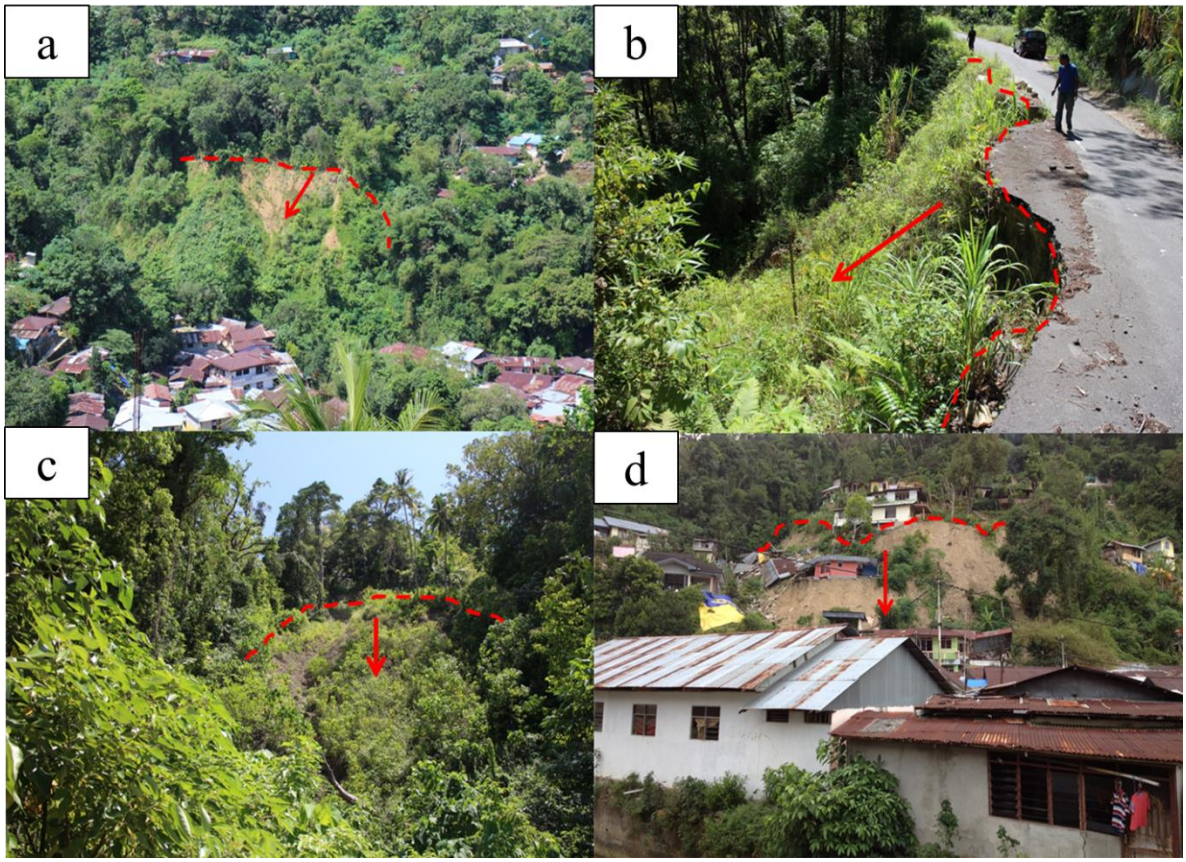

Figure 3.1 a) landslides near settlement area; b) landslide along the road network; c) landslide case in the Ambon volcanic rocks geology, d) houses affected by landslides.

3.1.1 Regional Setting

The study area was located in the Ambon Island at the 3°–4°S and 128°–129°E extending to an area of 377 km^2 (Fig. 2). The study was conducted in all area of Ambon City which includes five subdistricts: Nusaniwe subdistrict, Sirimau subdistrict, South Leitimur subdistrict, Baguala subdistrict, and Ambon Bay subdistrict totaling to 50 villages.

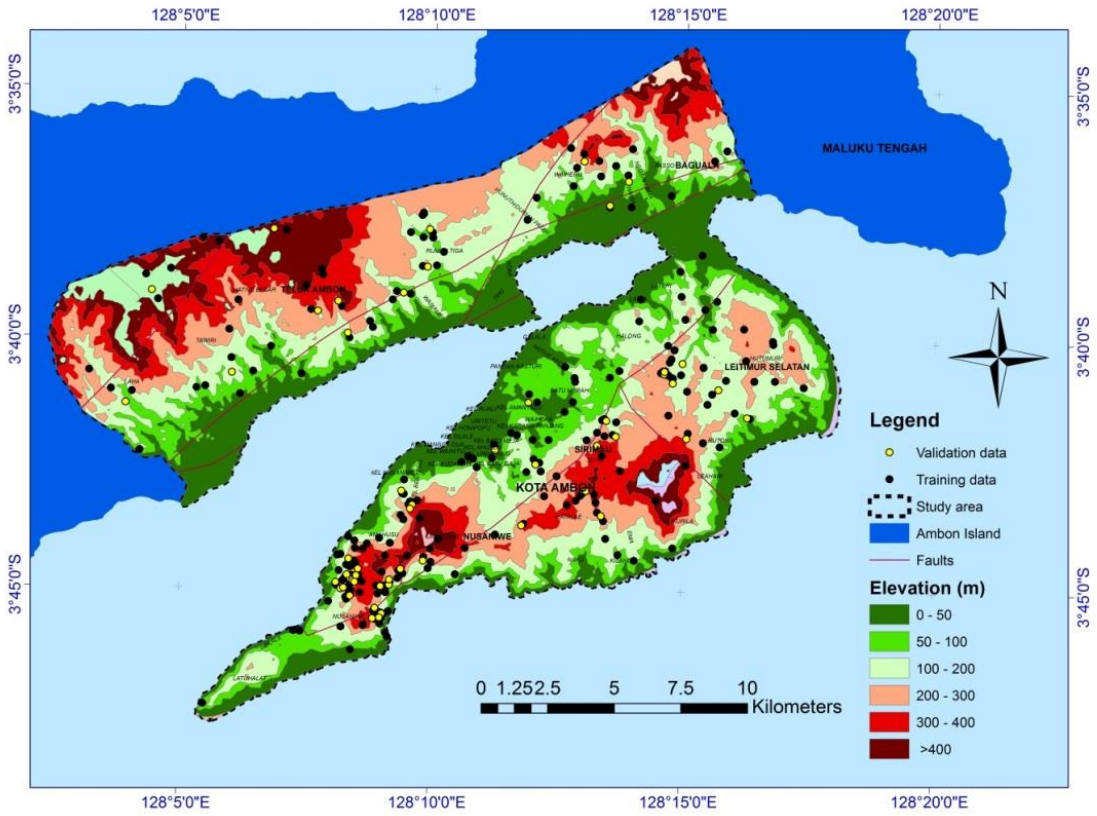

Figure 3.2 Simplified map of the study area

Ambon island lies south of the large island of Seram which belongs to the outer ridge of the Banda Arc. The outer ridge consists mostly of Tertiary subduction melange and imbricated complexes including slices of old continental crust. Active volcanoes only occur along the inner ridge of the Banda Arc (Marini and Susangkyono, 1999). Ambon has tropical monsoon climate when dry season occurs during December–March, while rainy season occurs during May–October. During the last decade, June has the highest average monthly rainfall counting up to 674.7 mm. When floods occurred in July and August 2013, rain fell every day during the month of July with total monthly rainfall in July 2013 was 1928 mm and maximum daily rainfall was 432 mm.

Varied topography characterizes Ambon; this is shown with elevation variation of 0 m on coastline area and > 900 m for the inner mountainous area. This topographical factor affects the slope distribution throughout Ambon. Slope class of 0 to > 40^{o} is distributed in the entire area of Ambon.

The geology of Ambon is represented by many rock conglomerates, such as alluvial, Kanikeh formation, ultrabasic, Ambon volcanic ash, and Ambon granites (Table 3.1). The fault lines direction is mainly from northwest to southwest and northeast to southeast. The structural element that was made by the tectonic process is the fault lines, reverse fault lines, and strike-slip fault. Earthquake occurs at the depth 0–99 km with the magnitude up to 7 Richter scale.

Table 3.1 Ambon regional geology description.

Geological formation	**Geological composition**	**Geological deposition**	**Starting age**	**Ending Age**
Ambon volcanic rocks	Extrusive: intermediate: lava	Volcanism: subaerial	Pliocene	Pliocene
Coral limestone	Sediment: chemical: limestone	Sedimentation: neritic: shallow	Holocene	Holocene
Alluvial	Sediment: clastic: alluvium	Sedimentation: terrestrial: alluvial	Holocene	Holocene
Kanikeh formation	Sediment: clastic: sandstone	Sedimentation: neritic: offshore	Jurassic	Triassic Late
Ambon granite	Intrusive: felsic: granitoid	Plutonism: batholith	Pliocene Late	Pliocene Middle
Ultrabasic rocks	Tectonite: ophiolite	Sedimentation:terrestrial	Cretaceous	Jurassic

3.2 Datasets

Independent variables were generated from datasets using ArcGIS® 10.1 SP1 for desktop. The databases containing the landslides causative factors were prepared in raster format using identical spatial projection and cell size (30 x 30 meter).

Eight landslide causative factors, slope angle, slope aspect, elevation, geology, density of geological boundaries, proximity to fault lines, proximity to river, and proximity to road networks were taken into consideration in this study (Fig. 3.3)

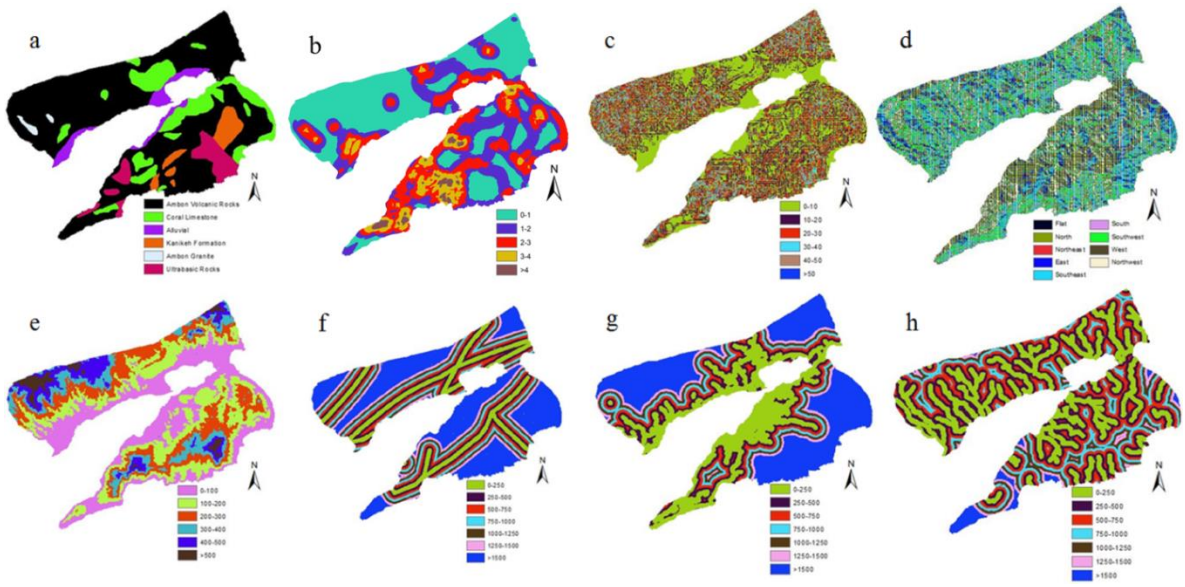

Figure 3.3 Distribution of the eight causative factors used as independent variables in this study. a) lithology; b) density of geological boundaries; c) slope; d) slope aspect; e) elevation; f) proximity to faults; g) proximity to road networks; h) proximity to river

The geomorphological factors were derived from ASTER GDEM including, elevation, slope angle, slope aspect. The geological factors were obtained from the Geological Research and Development Center. The anthropological factors have been collected from Indonesia Geospatial Information Agency. The landslide inventory was produced from the combination of an intensive field survey conducted in January 2015 and satellite imageries derived from Google Earth™. Known landslides were mapped in the field using GPS based on the information obtained from the Ambon Board for Disaster Management. The datasets sources are shown in Table 3.2.

Table 3.2 Datasets sources.

Dataset	**Primary format**	**Scale/Resolution**	**Data source**
DEM	Grid	30 x 30 m	ASTER GDEM
Geology	Shapefile (polygon)	1:250000	Geological Research and Development Center
Rivers	Shapefile (line)	1:10000	Indonesia Geospatial Information Agency
Road	Shapefile (line)	1:10000	Indonesia Geospatial Information Agency
Landslide Inventory	Shapefile (point)	1:50000	Field survey and Google Earth™ Imageries

The total landslide number in the study area is 282 cases which translated to 841 pixels of landslide. The landslide inventories were divided into training data (80% of total landslide cases, 741 pixels) and validation data (20% of total landslide cases, 100 pixels).

3.2.1 Geomorphological factors

Elevation is often associated with landslides occurrence (Bălteanu et al., 2010; Kamp et al., 2008; Süzen and Doyuran, 2004). The Digital Elevation Model (DEM) of the study area is provided by the Ministry of Economy, Trade, and Industry (METI) of Japan and the United States National Aeronautics and Space Administration (NASA), i.e. ASTER Global Digital Elevation Model (GDEM)V002, which is a GeoTIFF format, 1 arc-second (30 m) grid of elevation postings with geographic latitude/longitude coordinates. This global DEM product has an accuracy of 20 m in vertical dimension and 30 m in horizontal dimension, both at a confidence of 95% (Hirano et al., 2003). Elevation of the study area ranged from 0 to 1207 m and was divided into six classes: 0–100 m, 100–200 m, 200–300 m, 300–400 m, 400-500 m, and >500 m.

Slope angle is one of the most important factors in mass wasting, and is frequently used in mapping landslide susceptibility (Clerici et al., 2002; Ercanoglu and Gokceoglu, 2002; Süzen and Doyuran, 2004; Conoscenti et al., 2008; Poiraud, 2014). Slope angle is a derivate parameter from DEM by ArcGIS® Spatial Analyst Tools. The slope in the study area was divided into six classes: 0–10°, 10–20°, 20–30°, 30–40°, 40–50°, and >50°.

Some studies found no significant influence regarding slope aspect and slope stability (Ayalew and Yamagishi, 2005), and others found the effect it has on landslide initiation (Dai and Lee, 2002) and relates slope aspect with temperature and vegetation which prompts the formation of dongas in the susceptible material. In the southern hemisphere, south-facing slopes are shadowed resulting in sparser vegetation (Goudie, 2013). These settings of south-facing slopes are thus expected to be associated with a greater amount of landslide events as compared to those facing the north.

Proximity to river may adversely affect slope stability by erosion or by saturating the lower part of material and resulting in a water level increase (Gökceoglu and Aksoy, 1996; Kamp et al., 2008; Yalcin, 2008; Song et al., 2012; Meinhardt et al., 2015). Seven classes were created to evaluate proximity to river influence to landslide occurrences: 0–250 m, 250–500 m, 500–750 m, 750–1000 m, 1000–1250 m, 1250–1500 m, and >1500 m .

3.2.2 Geological factors

Lithology is an important causative factor in landslide susceptibility assessment (Kamp et al., 2008; Yalcin, 2008; Vahidnia et al., 2010; Song et al., 2012; Meinhardt et al., 2015) because different lithological units show significant differences in slope instability. The lithology map in this study was characterized in six different units based on the formation such as Ambon volcanic rocks, alluvial, coral limestone, Ambon granite, and ultrabasic rocks.

Proximity to faults plays a role in slope failures and landslide susceptibility, contributing not only in the surface structures but also the permeability of terrain (Vahidnia et al., 2010). The proximity to faults was created by creating buffer zone for each fault line with GIS. The buffers were set to be 0–250 m, 250–500 m, 500–750 m, 750–1000 m, 1000–1250 m, 1250–1500 m, and >1500 m.

In this study, density of geological boundaries is considered as one of the independent variables. Density of geological boundaries is expressed as the length of geological boundaries per an area. According to (Kawabata and Bandibas, 2009), the density of geological boundaries plays a significant role in slope instabilities. The parameter were set to be 0–1 km/km^2, 1–2 km/km^2, 2–3 km/km^2, 3–4 km/km^2, and >4 km/km^2. The layer was produced using Spatial Analyst tools of ArcGIS®.

3.2.3 Anthropological factors

Proximity to road networks was taken as the anthropological factors in this study. (Richards et al., 2006; Regmi et al., 2014) stated that slope failures in the study area is most often a byproduct of excavation activities for road construction, trenches, and cut and fill terracing. In general, road construction exposes slope to natural degrading elements which may introduce seepage conditions that may lead to further breakdown of the slope. This causative factor was set into seven classes: 0–250 m, 250–500 m, 500–750 m, 750–1000 m, 1000–1250 m, 1250–1500 m, and >1500 m.

3.3 Methodology

3.3.1 Bivariate frequency ratio Analysis

The Frequency Ratio (FR) is used to derive the correlation between landslide occurrences distribution and landslide causative factors (Lee and Talib, 2005; Ferentinou and Chalkias, 2013; Shahabi et al., 2014). The ratio is defined by the area where landslide occurrences are found to the total study area. Average value of 1 is produced so that it can be inferred area exceeding 1 has higher correlation to landslide occurrences and area that has value below 1 has lower correlation to landslide occurrences (Pradhan and Lee, 2009).

The FR per causative factors class is defined as follows (He and Beighley, 2008):

$$FR = \left(\frac{Nij}{Aij} / \frac{Nr}{Ar} \right) \quad (3.1)$$

where *Nij* is the area of landslides in the spatial extent associated with the *j*th class of *i*th parameter. *Aij* is the land area associated by the *j*th class of *i*th parameter. *Nr* and *Ar* are the total areas of landslides and the total area of the study area. Hence, it is evident that the $\frac{Nij}{Aij}$ represents the landslide class density and the $\frac{Nr}{Ar}$ represents the landslide causative parameter density.

3.3.2 Multivariate logistic regression analysis

Multivariate Logistic Regression (LR) is the most common method used for landslide susceptibility study (Budimir et al., 2015). LR is expressed as a linear equation:

$$\log(y) = \beta_0 + \beta_1 x_1 + \ldots + \beta_i x_i + e \quad (3.2)$$

where y is the dependent variable, β_0 is a constant, β_i is the ith regression coefficient, x_i is the ith explanatory variable, and e is the error.

Probability occurrence (p) of y is:

$$p = \frac{exp^{\beta_0 + \beta_1 x_1 + \ldots + \beta_i x_i + e}}{1 + exp^{\beta_0 + \beta_1 x_1 + \ldots + \beta_i x_i + e}} \quad (3.3)$$

Lithology causative factor was reclassified and treated as categorical data. LR is useful for predicting the absence or presence of a characteristic or outcome based on values of a set of predictor values. Coding was conducted to converse the parameters from nominal to numeric and ranking of the various classes was based on the FR value of FR approach. We then calculated the coefficient of each landslide causative factor. All the factors (slope angle, slope aspect, elevation, lithology, density of geological boundaries, proximity to faults proximity to river, and proximity to road networks), were treated as ordinal variables in the SPSS 22.0 software.

3.3.3 Artificial neural networks

Artificial neural networks (ANN) are computational information processing units inspired by the structure and behavior of real biological neurons whose architecture mimics the knowledge acquisition and organizational skills of human brain cells. According to (Cilliers, 1998), the importance of ANN can be summarized in the following features. They conserve the complexity of the systems they model because they have complex structures themselves. They encode information

about their environment in a distributed form. The advantages include that they recognize different sets of data within a whole data set, do not require pre-existing knowledge or experience, do not need a statistical pre-existing model in order to train data and finally, they give reasonable results even when data are inaccurate and incomplete (Jing and Hudson, 2002; Jing, 2003).

In this study, multi-layer perceptron (MLP) was applied. MLP is the most popular and most widely used ANN architecture which consists of input layer, output layer, and hidden layers in between. Each layer in a network contains a sufficient number of neurons. The output layer produces the neural network's results. Thus, the number of neurons in the input and output layers typically depends on the problem which the network was designed for. Each hidden and output layer neuron processes its inputs by multiplying each input (x_i) by a corresponding weight (w_i), summing the product (Eq. 3.4), and then processing the sum (if that exceeds the neuron threshold, the neuron is then activated) using a non-linear activation function (Eq. 3.5) to produce a result (y_i), which is the output node.

$$net = \sum_{i=0}^{n} w_i x_i \tag{3.4}$$

$$y_i = f\left(net\right) \tag{3.5}$$

A three layer feed-forward ANN was built. Optimum network architecture was selected following trial and error and considering the minimum mean square error. Initial weights were randomly initiated in a small range. The parameter of learning rate was set to 0.01. In this study, the network training activation transfer function for all layers was hyperbolic tangent.

3.4 Results

3.4.1 Bivariate frequency ratio

FR values of each class of the eight causative factors are summarized in Table 3. FR value increases with increasing density of geological boundaries. FR values for 0–1 km/km^2, 1–2 km/km^2, 2–3 km/km^2, 3–4 km/km^2, and >4 km/km^2 of density of geological boundaries were 0.78, 1.00, 1.26, 1.38, and 1.46, respectively. Landslide relative densities, the ratio of the subclass landslide area pixel area to the subclass area pixel, were 0.17%, 0.22%, 0.28%, 0.30%, and 0.32%, respectively.

For the lithology, the Ambon granite (lava, andesite, breccia, tuff, and conglomerate) and the ultrabasic rocks (harzburgite, dunite, serpentinite, and gabbro) had the highest FR values (2.56 and 2.45, respectively) and landslide relative density (0.56% and 0.54%, respectively). The proximity to fault class shows high FR value of 1.28 (landslide relative density: 0.28%) in the subclass of 0-250 m.

For slope angle, class showed highest FR value in the subclass of 30–40^o had the highest FR value of 1.86 and landslide relative density of 0.41%). For slope aspect, high FR value was observed in the western-facing slope (FR value: 1.25, landslide relative density: 0.28). Elevation class generated high FR value in the 200–300 m subclass (FR value: 1.41, landslide relative density: 0.31%). The proximity to river class showed the highest FR value in the subclass of 1000 – 1250 m (FR value: 2.06, landslide relative density: 0.45).

The proximity to road networks class showed the highest FR value of 1.85 in the subclass of 500–750 m with landslide relative density of 0.41%.

The landslide susceptibility maps were reclassified using natural break classification system. The outcome was an interpretable map showing increasing spatial possibility of future landslide incidence ranging from very low to very high susceptibility to landslide (Fig. 3.4a). The resulting

map shows that the area in the south of the study area, Nusaniwe and Leitimur Selatan, are potential landslide prone area due to their high landslide susceptibility.

Table 3.3 The total and landslide areas and frequency ratio (FR) value of each subclass for the eight causative factors.

Causative Factors	Subclass	Pixel of land area	Pixel of landslide area	FR Value
Slope (^{o})	0-10	157611	268	0.77
	10-20	91921	182	0.90
	20-30	56264	179	1.45
	30-40	23263	95	1.86
	40-50	5414	16	1.34
	>50	2700	1	0.17
Slope aspect	Flat	74229	167	1.02
	North	27409	59	0.98
	Northeast	4975	8	0.73
	East	10905	16	0.67
	Southeast	61265	120	0.89
	South	24858	50	0.92
	Southwest	64838	143	1.00
	West	18858	52	1.25
	Northwest	49836	126	1.15
Elevation (m.a.s.l)	0-100	102174	135	0.60
	100-200	92528	248	1.22
	200-300	68992	214	1.41
	300-400	35803	71	0.90
	400-500	25512	63	1.12
	>500	12164	10	0.37
Lithology	Ambon Volcanic Rock	232726	524	1.02
	Coral Limestone	50099	57	0.52
	Alluvial	15527	0	0.00
	Kanikeh Formation	14924	31	0.95
	Ambon Granite	2131	12	2.56
	Ultrabasic Rock	21766	117	2.45
Density of geological boundaries (km/km^2)	0-1	138242	236	0.78
	1-2	96509	213	1.00
	2-3	71703	198	1.26
	3-4	24793	75	1.38
	>4	5926	19	1.46
Proximity to fault (m)	0-250	45981	129	1.28
	250-500	42199	112	1.21
	500-750	37491	88	1.07
	750-1000	33150	79	1.08

	1000-1250	30315	64	0.96
	1250-1500	26536	63	1.08
	>1500	121501	206	0.77
Proximity to river (m)	0-250	107763	199	0.84
	250-500	90429	204	1.03
	500-750	61185	115	0.86
	750-1000	38903	71	0.83
	1000-1250	19675	89	2.06
	1250-1500	9279	37	1.81
	>1500	9939	26	1.19
Proximity to road (m)	0-250	92364	109	0.54
	250-500	39842	140	1.60
	500-750	25275	103	1.85
	750-1000	21171	49	1.05
	1000-1250	18996	41	0.98
	1250-1500	16533	42	1.16
	>1500	122992	257	0.95

3.4.2 Multivariate logistic regression

The LR coefficient for each landslide causative factor is shown in Table 3.5. The higher the LR coefficient, the higher the expected importance of the factor on landslide occurrence.

The Hosmer–Lemeshow test revealed that the fitting goodness of the equation can be accepted due to the significance of Chi-square is larger than 0.05. The value of Cox and Snell (R^2) and Nagelkerke (R^2) showed that the independent variables can explain the dependent variables (Table 3.4).

The obtained logistic regression equation is as follows:

$$\begin{aligned} &-11.646+\left(0.557\times FR_{slope}\right)+\left(0.625\times FR_{road}\right)+\left(0.535\times FR_{lithology}\right)\\ &+\left(0.678\times FR_{geodens}\right)+\left(0.799\times FR_{elevation}\right)+\left(0.981\times FR_{slopeaspect}\right)\\ &+\left(0.631\times FR_{river}\right)+\left(0.497\times FR_{faults}\right) \end{aligned} \quad (6)$$

Where, FR_{slope} is the frequency ratio value of slope angle class, FR_{road} is the frequency ratio value of proximity to road class, $FR_{lithology}$ is the frequency ratio value of lithology class, $FR_{geodens}$ is the frequency ratio value of density of geological boundaries class, $FR_{elevation}$ is the frequency ratio value of elevation class, $FR_{slopeaspect}$ is the frequency ratio value of slope aspect class, FR_{river} is the frequency ratio value of proximity to river class, and FR_{faults} is the frequency ratio value of proximity to faults class.

Table 3.4 Logistic regression model summary.

-2 Log likelihood	Cox & Snell R Square	Nagelkerke R Square	Overall Percentage
10146.880[a]	.001	.037	99.8

a. Estimation terminated at iteration number 10 because parameter estimates changed by less than .001.

The produced LS map is shown in Fig. 3.4b, similar to the LS map produced by FR technique both Nusaniwe and Leitimur Selatan show high susceptibility to landslides events.

3.4.3 Artificial neural networks

The normalized importance of each landslide causative factor is presented in Table 5. The ANN analysis was performed with a mean square error of 0.02 in the training set. The final landslide susceptibility map was produced by multiplying each causative factor with the independent variable importance calculated through the ANN analysis and then an overlay of these layers was performed.

$$LS\ ANN = \sum_{I=1}^{n} fw_i \times w_{ij} \tag{3.7}$$

where LS ANN is the final landslide susceptibility map calculated for each pixel, fw_i is the weight of each causative factor and $w_{i,j}$ is the normalized weight for the category j of the factor i. The produced landslide susceptibility map is shown in Fig. 3.4c.

Table 3.5 The coefficients of logistic regression (LR) and importance and normalized importance value derived from artificial neural network (ANN).

Number	Causative factors	LR	ANN Importance	ANN Normalized Importance
1	Proximity to road	0.62	0.23	100.00%
2	Density of geological boundaries	0.68	0.19	82.80%
3	Slope	0.56	0.12	51.70%
4	Proximity to fault	0.49	0.11	47.40%
5	Elevation	0.80	0.11	46.20%
6	Lithology	0.54	0.10	41.30%
7	Aspect	0.98	0.09	38.10%
8	Proximity to river	0.63	0.06	26.80%

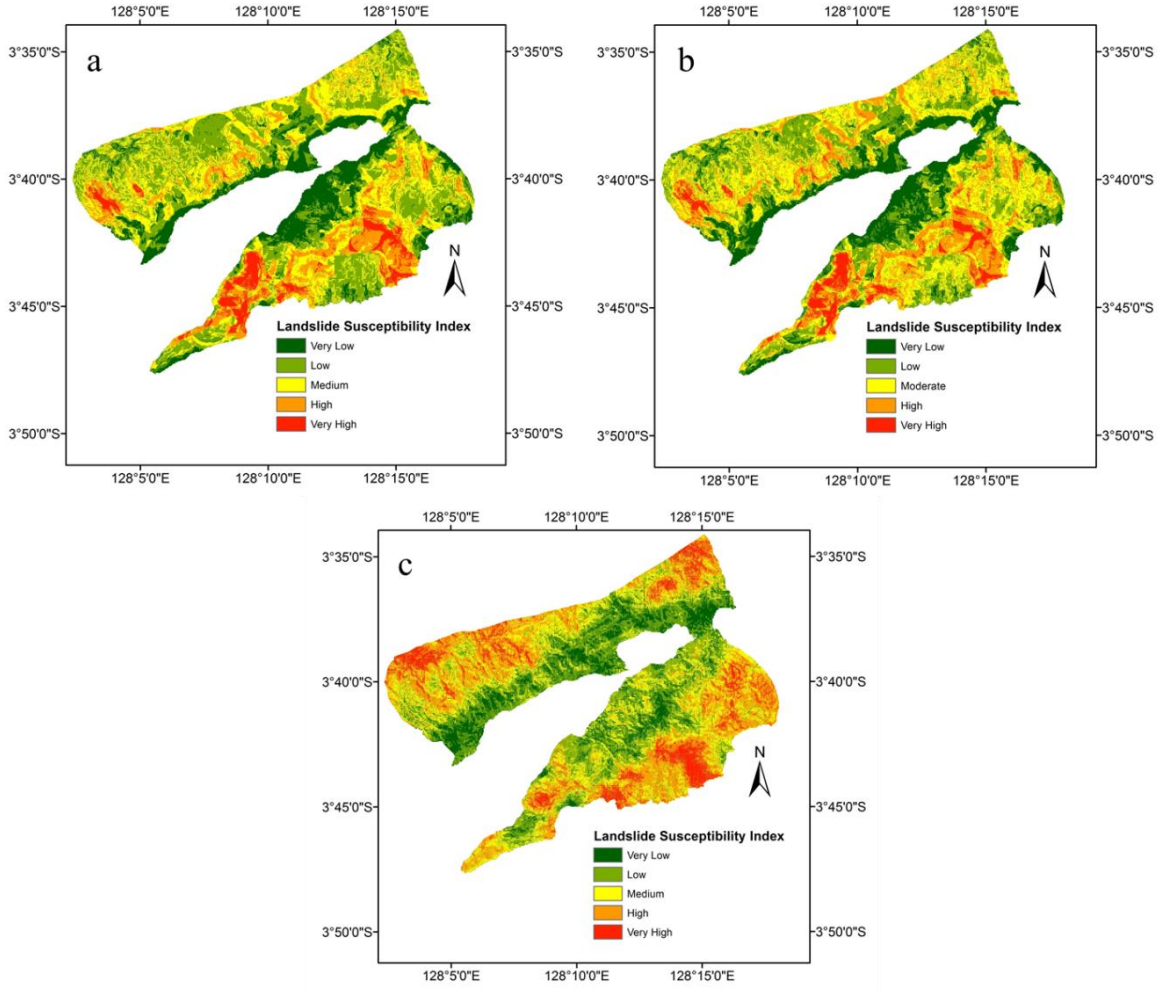

Figure 3.4 Landslide susceptibility maps by the bivariate frequency ratio (FR), multivariate logistic regression (LR), and artificial neural network (ANN) models.

.

3.4.4 Models validation

3.4.4.1 Relationship between susceptibility maps and training/validation data

Susceptibility maps were validated by comparing landslide areas to susceptibility classes, the likelihood of landslide occurrences in a particular region. It was observed that the smaller degree of fit was distributed in the low and very low susceptibility classes. The higher values of the degree of fit were found to be in the high and very high susceptibility classes for the landslide susceptibility maps produced by the three models.

The preliminary analysis stemming from the bivariate statistical frequency ratio model gave the following results. The training set also showed a close connection where 67% of landslide pixels occurred in the very high susceptibility class and only 1% in the very low susceptibility class. The low, moderate and high susceptibility classes hold 7%, 8% and 17% of landslide pixels (Fig. 3.5a). The validation set for the FR model generated a good correlation with the occurrence of landslides. It is evident from the presence of a large percentage of landslides being 55% in the very high susceptibility class and only 1% occurring in the very low susceptibility class. A total of 3%, 14% and 27% of the remaining landslide pixels occurred within the low, moderate and high susceptibility classes respectively. A good degree of fit is obtained for the overlay analysis of the validation and training set for the FR-derived maps, which shows a constant increase from the very low to very high susceptibility classes.

The comparison between the validation and training set of the LR-derived susceptibility map shows similar results across all susceptibility categories (Fig. 3.5b). The overlay of the LR-derived susceptibility map and the training set data indicates that 65% and 3% of the landslide pixels occur in the very high and very low susceptibility classes respectively and 4%, 13% and 15% in the high, moderate and low susceptibility classes respectively. The validation set for the LR-derived map

shows a total of 53% and 2% of pixels occurring in the very high and very low susceptibility classes respectively and a total of 45% of landslide pixels occurring in the high, moderate and low susceptibility classes. It is evident that there is a variation between results produced by the training and validation set. The very high susceptibility class shows a difference of 12% whereas a total of 4% represents the difference in the moderate susceptibility class.

The comparison between the validation and training set overlay analysis of the ANN-derived susceptibility map shows similar results across all susceptibility categories (Fig. 3.5c). The training set data indicates that 79% and 0% of the landslide pixels occur in the very high and very low susceptibility classes respectively and that 18%, 3% and 0% in the high and moderate susceptibility classes respectively. The validation set shows a total of 63% and 0% of pixels occurring in the very high and very low susceptibility classes and 47% occur in the high, moderate, and low susceptibility classes respectively. It is evident that there is a variation between results produced by the validation and training set for the very high susceptibility class, which shows a difference of 13% whereas a total of 10% represents the difference in landslide pixels in the moderate susceptibility class.

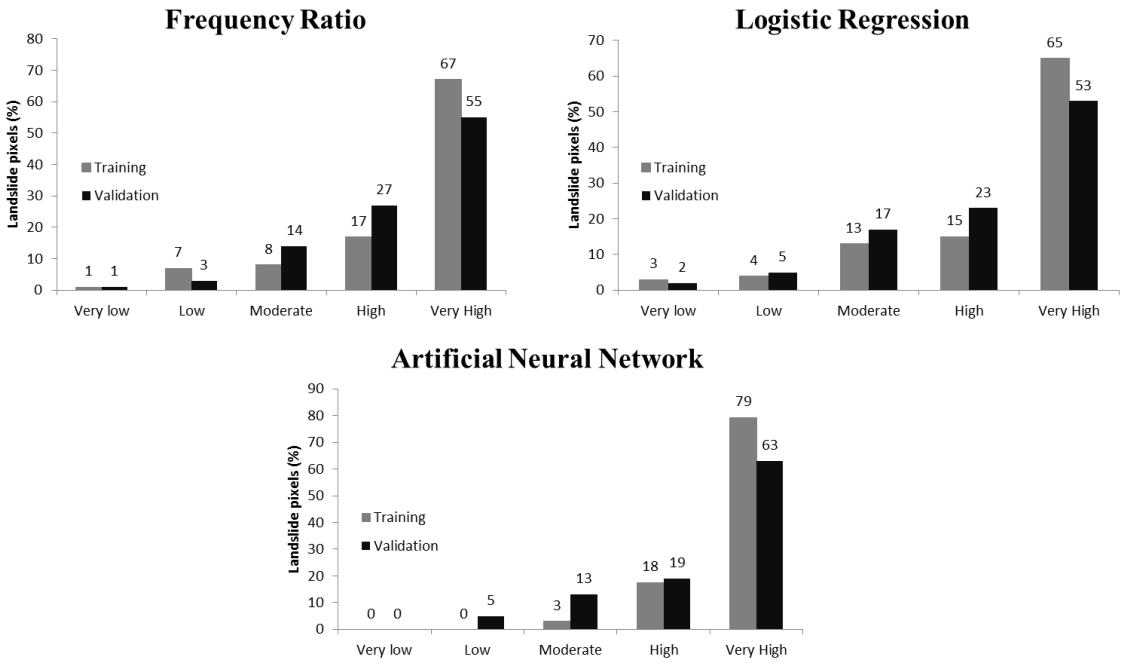

Figure 3.5 The ratio (%) of landslide pixels for each susceptibility class to the total landslide pixels for landslide sustainability maps based on training and validation data. Figure 3.5a, 3.5b, 3.5c were derived using frequency ratio, logistic regression, artificial neural network

3.4.4.2 Receiver Operating Curves

A standard validation analysis to compare prediction performance of various classifiers is the Receiver Operating Curve (ROC) and the calculation of Area Under Curve (AUC) (Akgun et al., 2012; Tien Bui et al., 2012). The ROC is a useful method for representing the quality of deterministic or probabilistic landslide susceptibility model classifiers. In the ROC graph, the sensitivity of the model which is determined as the percentage of the correctly predicted landslide pixels by the model is plotted against specificity, which is the proportion of predicted landslide pixels over the total study area. The AUC represents the quality of the models to reliably predict the occurrence or the non-occurrence of landslides.

A good fit model has an AUC value from 0.5 to 1. The ideal model performs an AUC value close to 1.0 (perfect fit), whereas a value close to 0.5 indicate inaccuracy in the model (random fit), (Carvalho et al., 2014). Fig. 3.6 and Table 3.6 show the ROC of FR, LR and ANN models for the training and validation sets. The measurement of how well the model performs is represented in the

success rate curve (training data) while the capability of the model to predict is represented in the prediction rate curve (validation data). It is observed that all the models have good success rate with the highest one being the ANN model (AUC: 0.734). The FR has AUC of 0.688, and the LR has an AUC of 0.687. In the case of the prediction rate curve, ANN shows the highest value (AUC: 0.717) whereas the LR and FR are 0.668 and 0.667 respectively.

Table 3.6 Area under curve (AUC) values of the three landslide models for the training and validation dataset.

Number	Landslide Susceptibility Model	AUC
Training dataset		
1	Frequency ratio	0.688
2	Logistic regression	0.687
3	Artificial neural network	0.734
Validation dataset		
1	Frequency ratio	0.668
2	Logistic regression	0.667
3	Artificial neural network	0.717

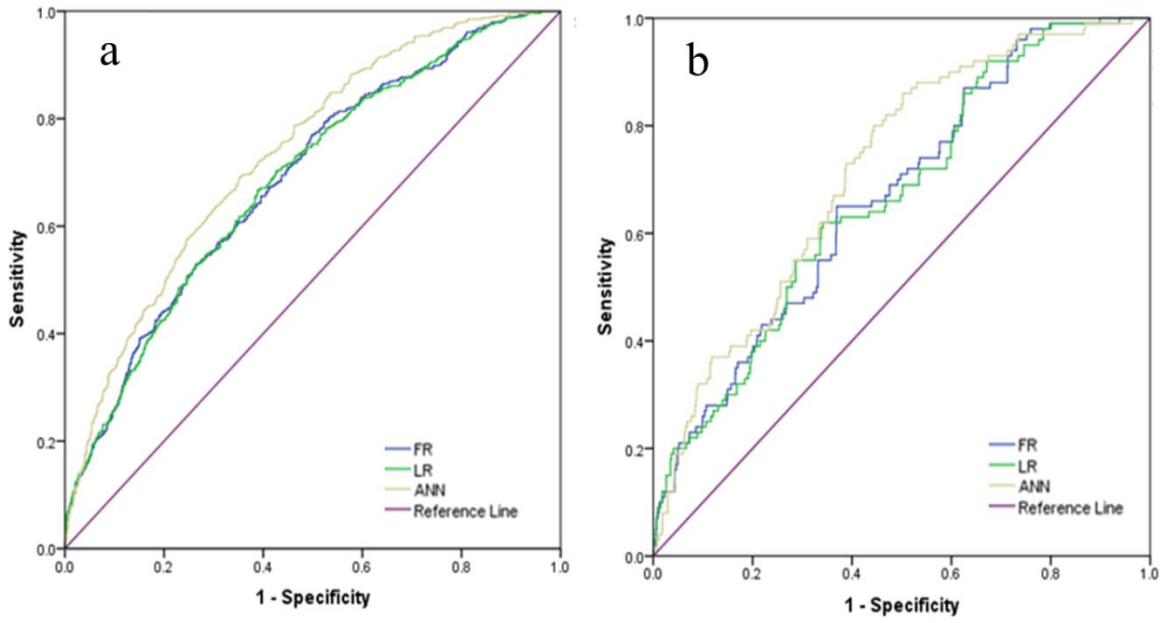

Figure 3.6 Receiver operating curves (ROC) for frequency ratio (FR), logistic regression (LR), and artificial neural network methods. Figure 3.6a indicates success rate curves and Figure 3.6b indicates prediction rate curves.

3.5 Discussions

Landslide susceptibility refers to the likelihood of a landslide occurring in a particular area and is a function of previous landslide locations and the possible influences that led to their occurrence. Numerous different methods can be utilized to model this relationship where geographic information systems represent an essential component.

The aim of this study was to evaluate each causative factors in landslide susceptibility assessments in Ambon and to compare three models of the spatial probability of landslide occurrence using FR, LR and ANN methods. We finally presented landslide susceptibility maps, which categorize the area into individual homogeneous zones with varying degrees of landslide susceptibility. Three models were based on the integration of eight identical and individually weighted causative factors and a landslide inventory.

Bivariate statistical analysis works by combining causative factor maps of weighted classes with a landslide distribution map. It has the advantage of measuring susceptibility in a quantitative and objective manner by determining which causative factors has the strongest influence on landslide initiation (Corominas et al., 2014), and being a straightforward and easy to reproduce approach.

The three susceptibility models training data goodness of fit are good. However, there are small differences between the models with the ANN model showing the highest degree of fit with AUC values of the ROC being 0.734. The selection of the landslide causative factors is one of the most important required steps that affects the quality of a landslide susceptibility analysis, several authors (Chacón et al., 2006; Irigaray et al., 2007) have discussed on the selection of the causative factors as a linear correlation. In general topography, geology, hydrology, and geomorphology use are widely used and accepted causative factors in landslide susceptibility modeling.

In this study, three methods were applied to rate the importance of the causative factors and the findings through the three applied models identified differences. The general trends, however,

dictate that the geological factors and topography be amongst the most significant (Sakellariou and Ferentinou, 2005). The geomorphology and slope morphology has a definite influence on slope stability and is considered as the most important causative factors related to mass movement activity. Parameter class relationships are evident through the assessment of landslide densities with the occurrence of observed landslides.

Lithology varies regarding chemical and physical properties, which give rise to different levels of susceptibility to landslide occurrence. In this study area, the highest landslide occurrence is found in the Ambon granite formation which comprises of biotite granite and biotite cordierite granite. Ultrabasic formation which comprises of harzburgite, dunite, serpentinite and gabbro follows as the second highest density in the lithology parameters.

In term of density of geological boundaries, the parameter class >4 km/km^2 showed the highest landslide occurrence which suggests the interlayers of geological structures affects slope stability in a negative way. A consistent increase of landslide density is observed in density of geological boundaries parameter suggesting that density of geological boundaries showed high correlation with landslide occurrences. Based on the normalized importance value obtained from ANN (Table 3.5), density of geological boundaries is the second most important parameter after proximity to road network (normalized importance value: 0.19). A previous study (Kawabata and Bandibas, 2009) suggested that landslide occurrences increase as the density of geological boundaries increases due to unstable relationship between geological substrata. Higher density of geological boundaries correlates with weaker slope stability which corresponds to landslide occurrences. This phenomenon is evident in the southern part of the study area which has the highest density of geological boundaries where most of the identified landslides are located.

The highest landslide occurrence is associated with elevation ranging from 200–300 m which occurs mostly along the northeastern and southwestern part of the study area. Steeper slope angles

indicate larger driving forces relative to resisting forces which result in a greater potential to fail. In the studied area, most landslides are associated with slope angles ranging from 30°–40° where some municipalities area are located. The western-facing slope shows the highest landslide density compared to other class in the slope aspect classes. Past study in the area showed similar findings that most of the landslide occurrence happened in the west slope due to soil resistivity contrast between adjacent rocks (Souisa et al., 2015).

Drainage networks impact negatively on landslide susceptibility due to their abrasion processes along the base of slopes, which also result in the saturation of associated material thereby reducing the stability of the slope (Demir et al., 2013). It is thus expected that more landslides should occur within a limited distance from the stream network. However, this study findings show that the greatest landslide occurrence is associated with the class representing 1000–1250 m from the river network. This might be because of underreported landslide cases found in natural slopes.

The class of > 1500 m of proximity to faults shows the highest landslide occurrences. Even though realistically not associated with the occurrence of landslides, but statistically show high values of occurrence. Closer distances to faults do not show high landslide densities, which may be attributed to that fact that most observed and mapped landslides occur far from the fault lines suggesting that the statistical relationship is based solely on landslide events recorded around a single fault in the interior only.

The highest occurrence of landslides occurs within 250–500m from the road network. This pattern is expected since the excavation of road cuts reduce the lateral support of material and may trigger landslides. Moreover, this process alters the natural terrain and drainage system. Proximity to road network is regarded as the most important parameter in this study by the ANN model (normalized importance value: 0.23)

The three produced LS maps shows good accuracy >66%. It is evident from the obtained results that ANN shows higher accuracy (AUC = 0.734) when compared with the FR and LR models (AUC = 0.688 and 0.687, respectively). These results agree with past studies (Lee, 2007; Lee and Pradhan, 2007) showing that the soft-computing performance of ANN better suits LS mapping in the study area when compared to FR and LR models. The relationship between training data and validation data to landslide occurrences also shows acceptable data goodness of fit demonstrated by the consistent increases of landslide pixels per susceptibility classes. Most of the landslide pixels are identified in very high and high susceptibility class across three models.

3.6 Concluding remarks

In conclusion, the current paper provides an evaluation the causative factors in landslide susceptibility assessments in Ambon and contributes to a systematic comparison and evaluation of three landslide susceptibility models. The landslide locations mapped in the studied Ambon city were substantial to the spatial prediction of future landslides. Their relationship with various causative factors has proven to be that of a critical combination. The identification of areas susceptible to the occurrence of landslides is important as it could serve as a preliminary tool in future development planning and for identifying priority areas for early warning systems against potential damage.

Geological factors proved to be critical for all models where they are represented differently being lithological type, proximity to faults, and density of geological boundaries. In detail, Ambon granite and ultrabasic rocks are exposed to high degree on the susceptibility maps. Proximity to road network was found to be amongst the most influential causative factor with the center portion of the region exhibiting higher densities. In all three maps, the highest susceptibility to landslides was seen in the southwestern part of the city and on the outskirts of the eastern side. These areas are defined by subdistricts such as Nusaniwe and Leitimur Selatan. The resulting susceptibility maps were classified into five classes (very low to very high susceptibility).

Model performance was tested using an independent validation set comprising 20% of all mapped landslides. For verification of the model performance, receiver operating curves (ROCs) were calculated and the areas under the curve (AUC) for success rate curve were 0.688, 0.687, and 0.734 for FR, LR, and ANN respectively. The prediction rate curves AUC were 0.668, 0.667, and 0.717 for FR, LR, and ANN respectively. The results revealed that models showed promising results for shallow landslide susceptibility modeling since they all give accuracies greater than 66%, but ANN model proved to be superior in representing landslide susceptibility throughout the study area. Since the ANN method produced more reliable results. The map derived from this approach is best suited to aid in land-use planning and landslide mitigation. Furthermore, this information can be employed to validate and verify any results acquired at regional and national scale. However, it must be noted that all results obtained are a function of the accuracy of the original database including input causative factors and the inventory.

The increasing development in Ambon region will increase pressure to the population and economic which will bring the finding of this study to the utmost relevance. The produced landslide susceptibility map is expected to be useful for government officials and urban planner in planning the development of the region. It is also worthy to be mentioned that landslide susceptibility study is still limited in the study area as a result of many unreported landslide cases.

3.7 References

Akgun, A., Dag, S., Bulut, F., 2008. Landslide susceptibility mapping for a landslide-prone area (Findikli, NE of Turkey) by likelihood-frequency ratio and weighted linear combination models. Environ. Geol. 54, 1127–1143. doi:10.1007/s00254-007-0882-8

Akgun, A., Kincal, C., Pradhan, B., 2012. Application of remote sensing data and GIS for landslide risk assessment as an environmental threat to Izmir city (west Turkey). Environ. Monit. Assess. 184, 5453–5470. doi:10.1007/s10661-011-2352-8

Ayalew, L., Yamagishi, H., 2005. The application of GIS-based logistic regression for landslide susceptibility mapping in the Kakuda-Yahiko Mountains, Central Japan. Geomorphology 65, 15–31. doi:10.1016/j.geomorph.2004.06.010

Bălteanu, D., Chendeş, V., Sima, M., Enciu, P., 2010. A country-wide spatial assessment of landslide susceptibility in Romania. Geomorphology 124, 102–112. doi:10.1016/j.geomorph.2010.03.005

Barredo, J., Benavides, A., Hervás, J., van Westen, C.J., 2000. Comparing heuristic landslide hazard assessment techniques using GIS in the Tirajana basin, Gran Canaria Island, Spain, in: International Journal of Applied Earth Observation and Geoinformation. pp. 9–23. doi:10.1016/S0303-2434(00)85022-9

Budimir, M.E.A., Atkinson, P.M., Lewis, H.G., 2015. A systematic review of landslide probability mapping using logistic regression. Landslides 12, 419–436. doi:10.1007/s10346-014-0550-5

Carrara, A., Crosta, G., Frattini, P., 2003. Geomorphological and historical data in assessing landslide hazard. Earth Surf. Process. Landforms 28, 1125–1142. doi:10.1002/esp.545

Carvalho, L.F., Fernandes, G., De Assis, M.V.O., Rodrigues, J.J.P.C., Lemes Proença, M., 2014. Digital signature of network segment for healthcare environments support. IRBM 35, 299–309. doi:10.1016/j.patrec.2005.10.010

Chacón, J., Irigaray, C., Fernández, T., El Hamdouni, R., 2006. Engineering geology maps: Landslides and geographical information systems. Bull. Eng. Geol. Environ. 65, 341–411. doi:10.1007/s10064-006-0064-z

Cilliers, P., 1998. Complexity and postmodernism: Understanding complex systems. South African J. Philosopy. doi:10.4324/9780203012253

Clerici, A., Perego, S., Tellini, C., Vescovi, P., 2002. A procedure for landslide susceptibility zonation by the conditional analysis method. Geomorphology 48, 349–364. doi:10.1016/S0169-555X(02)00079-X

Conoscenti, C., Di Maggio, C., Rotigliano, E., 2008. GIS analysis to assess landslide susceptibility in a fluvial basin of NW Sicily (Italy). Geomorphology 94, 325–339. doi:10.1016/j.geomorph.2006.10.039

Corominas, J., van Westen, C., Frattini, P., Cascini, L., Malet, J.P., Fotopoulou, S., Catani, F., Van Den Eeckhaut, M., Mavrouli, O., Agliardi, F., Pitilakis, K., Winter, M.G., Pastor, M., Ferlisi, S., Tofani, V., Herv??s, J., Smith, J.T., 2014. Recommendations for the quantitative analysis of landslide risk. Bull. Eng. Geol. Environ. 73, 209–263. doi:10.1007/s10064-013-0538-8

Dai, F.C., Lee, C.F., 2002. Landslide characteristics and slope instability modeling using GIS, Lantau Island, Hong Kong. Geomorphology 42, 213–228. doi:10.1016/S0169-555X(01)00087-3

Dai, F.C., Lee, C.F., Ngai, Y.Y., 2002. Landslide risk assessment and management: An overview. Eng. Geol. 64, 65–87. doi:10.1016/S0013-7952(01)00093-X

Demir, G., Aytekin, M., Akgün, A., Ikizler, S.B., Tatar, O., 2013. A comparison of landslide susceptibility mapping of the eastern part of the North Anatolian Fault Zone (Turkey) by likelihood-frequency ratio and analytic hierarchy process methods. Nat. Hazards 65, 1481–1506. doi:10.1007/s11069-012-0418-8

Ercanoglu, M., Gokceoglu, C., 2002. Assessment of landslide susceptibility for a landslide-prone area (north of Yenice, NW Turkey) by fuzzy approach. Environ. Geol. 41, 720–730. doi:10.1007/s00254-001-0454-2

Ermini, L., Catani, F., Casagli, N., 2005. Artificial Neural Networks applied to landslide

susceptibility assessment. Geomorphology 66, 327–343. doi:10.1016/j.geomorph.2004.09.025

Ferentinou, M., Chalkias, C., 2013. Mapping mass movement susceptibility across greece with gis, ann and statistical methods, in: Landslide Science and Practice: Landslide Inventory and Susceptibility and Hazard Zoning. pp. 321–327. doi:10.1007/978-3-642-31325-7-42

Gökceoglu, C., Aksoy, H., 1996. Landslide susceptibility mapping of the slopes in the residual soils of the Mengen region (Turkey) by deterministic stability analyses and image processing techniques. Eng. Geol. 44, 147–161. doi:10.1016/S0013-7952(97)81260-4

Goudie, A., 2004. Encyclopedia of geomorphology. Volume 1. Zhurnal Eksp. i Teor. Fiz.

Greco, R., Sorriso-Valvo, M., Catalano, E., 2007. Logistic Regression analysis in the evaluation of mass movements susceptibility: The Aspromonte case study, Calabria, Italy. Eng. Geol. 89, 47–66. doi:10.1016/j.enggeo.2006.09.006

Guzzetti, F., Carrara, A., Cardinali, M., Reichenbach, P., 1999. Landslide hazard evaluation: A review of current techniques and their application in a multi-scale study, Central Italy. Geomorphology 31, 181–216. doi:10.1016/S0169-555X(99)00078-1

Guzzetti, F., Mondini, A.C., Cardinali, M., Fiorucci, F., Santangelo, M., Chang, K.T., 2012. Landslide inventory maps: New tools for an old problem. Earth-Science Rev. doi:10.1016/j.earscirev.2012.02.001

He, Y., Beighley, R.E., 2008. GIS-based regional landslide susceptibility mapping: A case study in southern California. Earth Surf. Process. Landforms 33, 380–393. doi:10.1002/esp.1562

Hirano, A., Welch, R., Lang, H., 2003. Mapping from ASTER stereo image data: DEM validation and accuracy assessment. ISPRS J. Photogramm. Remote Sens. 57, 356–370. doi:10.1016/S0924-2716(02)00164-8

Irigaray, C., Fernández, T., El Hamdouni, R., Chacón, J., 2007. Evaluation and validation of landslide-susceptibility maps obtained by a GIS matrix method: Examples from the Betic Cordillera (southern Spain). Nat. Hazards 41, 61–79. doi:10.1007/s11069-006-9027-8

Jiang, H., Eastman, J.R., 2000. Application of fuzzy measures in multi-criteria evaluation in GIS. Int. J. Geogr. Inf. Sci. 14, 173–184. doi:10.1080/136588100240903

Jing, L., 2003. A review of techniques, advances and outstanding issues in numerical modelling for rock mechanics and rock engineering. Int. J. Rock Mech. Min. Sci. 40, 283–353. doi:10.1016/S1365-1609(03)00013-3

Jing, L., Hudson, J.A., 2002. Numerical methods in rock mechanics. Int. J. Rock Mech. Min. Sci. 39, 409–427. doi:10.1016/S1365-1609(02)00065-5

Kamp, U., Growley, B.J., Khattak, G.A., Owen, L.A., 2008. GIS-based landslide susceptibility mapping for the 2005 Kashmir earthquake region. Geomorphology 101, 631–642. doi:10.1016/j.geomorph.2008.03.003

Kanungo, D.P., Arora, M.K., Sarkar, S., Gupta, R.P., 2006. A comparative study of conventional, ANN black box, fuzzy and combined neural and fuzzy weighting procedures for landslide susceptibility zonation in Darjeeling Himalayas. Eng. Geol. 85, 347–366. doi:10.1016/j.enggeo.2006.03.004

Kawabata, D., Bandibas, J., 2009. Landslide susceptibility mapping using geological data, a DEM from ASTER images and an Artificial Neural Network (ANN). Geomorphology 113, 97–109. doi:10.1016/j.geomorph.2009.06.006

Lee, S., 2007. Comparison of landslide susceptibility maps generated through multiple logistic regression for three test areas in Korea. Earth Surf. Process. Landforms 32, 2133–2148. doi:10.1002/esp.1517

Lee, S., Choi, J., Min, K., 2004. Probabilistic landslide hazard mapping using GIS and remote sensing data at Boun, Korea. Int. J. Remote Sens. 25, 2037–2052. doi:10.1080/01431160310001618734

Lee, S., Pradhan, B., 2007. Landslide hazard mapping at Selangor, Malaysia using frequency ratio and logistic regression models. Landslides 4, 33–41. doi:10.1007/s10346-006-0047-y

Lee, S., Talib, J.A., 2005. Probabilistic landslide susceptibility and factor effect analysis. Environ. Geol. 47, 982–990. doi:10.1007/s00254-005-1228-z

Marini, L., Susangkyono, A.E., 1999. Fluid geochemistry of Ambon Island (Indonesia). Geothermics 28, 189–204. doi:10.1016/S0375-6505(99)00003-6

Meinhardt, M., Fink, M., Tünschel, H., 2015. Landslide susceptibility analysis in central Vietnam based on an incomplete landslide inventory: Comparison of a new method to calculate weighting factors by means of bivariate statistics. Geomorphology 234, 80–97. doi:10.1016/j.geomorph.2014.12.042

Neaupane, K.M., Piantanakulchai, M., 2006. Analytic network process model for landslide hazard zonation. Eng. Geol. 85, 281–294. doi:10.1016/j.enggeo.2006.02.003

Poiraud, A., 2014. Landslide susceptibility–certainty mapping by a multi-method approach: A case study in the Tertiary basin of Puy-en-Velay (Massif central, France). Geomorphology 216, 208–224. doi:10.1016/j.geomorph.2014.04.001

Pradhan, B., Lee, S., 2009. Delineation of landslide hazard areas on Penang Island, Malaysia, by using frequency ratio, logistic regression, and artificial neural network models. Environ. Earth Sci. 60, 1037–1054. doi:10.1007/s12665-009-0245-8

Regmi, A.D., Devkota, K.C., Yoshida, K., Pradhan, B., Pourghasemi, H.R., Kumamoto, T., Akgun,

A., 2014. Application of frequency ratio, statistical index, and weights-of-evidence models and their comparison in landslide susceptibility mapping in Central Nepal Himalaya. Arab. J. Geosci. 7, 725–742. doi:10.1007/s12517-012-0807-z

Richards, N.P., Botha, G. a, Schoeman, P., Clarke, B.M., Kota, M.W., Ngcobo, F.N., 2006. Engineering geological mapping in Pietermaritzburg , South Africa : Constraints on development. 10th IAEG Int. Congr. Nottingham, United Kingdom, 6-10 Sept. 2006, Pap. 407.

Sakellariou, M.G., Ferentinou, M.D., 2005. A study of slope stability prediction using neural networks. Geotech. Geol. Eng. 23, 419–445. doi:10.1007/s10706-004-8680-5

Shahabi, H., Khezri, S., Ahmad, B. Bin, Hashim, M., 2014. Landslide susceptibility mapping at central Zab basin, Iran: A comparison between analytical hierarchy process, frequency ratio and logistic regression models. CATENA 115, 55–70. doi:10.1016/j.catena.2013.11.014

Soeters, R., Van Westen, C.J., 1996. Slope instability recognition, analysis, and zonation. Spec. Rep. - Natl. Res. Counc. Transp. Res. Board 247, 129–177.

Song, Y., Gong, J., Gao, S., Wang, D., Cui, T., Li, Y., Wei, B., 2012. Susceptibility assessment of earthquake-induced landslides using Bayesian network: A case study in Beichuan, China. Comput. Geosci. 42, 189–199. doi:10.1016/j.cageo.2011.09.011

Souisa, M., Hendrajaya, L., Handayani, G., 2015. Determination of Landslide Slip Surface Using Geoelectrical Resistivity Method at Ambon City Moluccas-Indonesia. Int. J. Emerg. Technol. Adv. Eng. 5, 42–47.

Süzen, M.L., Doyuran, V., 2004. Data driven bivariate landslide susceptibility assessment using geographical information systems: a method and application to Asarsuyu catchment, Turkey. Eng. Geol. 71, 303–321. doi:10.1016/S0013-7952(03)00143-1

Thiery, Y., Malet, J.-P., Sterlacchini, S., Puissant, A., Maquaire, O., 2007. Landslide susceptibility assessment by bivariate methods at large scales: Application to a complex mountainous environment. Geomorphology 92, 38–59. doi:10.1016/j.geomorph.2007.02.020

Tien Bui, D., Pradhan, B., Lofman, O., Revhaug, I., Dick, O.B., 2012. Spatial prediction of landslide hazards in Hoa Binh province (Vietnam): A comparative assessment of the efficacy of evidential belief functions and fuzzy logic models. CATENA 96, 28–40. doi:10.1016/j.catena.2012.04.001

Vahidnia, M.H., Alesheikh, A.A., Alimohammadi, A., Hosseinali, F., 2010. A GIS-based neuro-fuzzy procedure for integrating knowledge and data in landslide susceptibility mapping. Comput. Geosci. 36, 1101–1114. doi:10.1016/j.cageo.2010.04.004

van Westen, C.J., Castellanos, E., Kuriakose, S.L., 2008. Spatial data for landslide susceptibility, hazard, and vulnerability assessment: An overview. Eng. Geol. 102, 112–131. doi:10.1016/j.enggeo.2008.03.010

Yalcin, A., 2008. GIS-based landslide susceptibility mapping using analytical hierarchy process and bivariate statistics in Ardesen (Turkey): Comparisons of results and confirmations. CATENA 72, 1–12. doi:10.1016/j.catena.2007.01.003

Yesilnacar, E., Topal, T., 2005. Landslide susceptibility mapping: A comparison of logistic regression and neural networks methods in a medium scale study, Hendek region (Turkey). Eng. Geol. 79, 251–266. doi:10.1016/j.enggeo.2005.02.002

Zhu, A.-X., Wang, R., Qiao, J., Qin, C.-Z., Chen, Y., Liu, J., Du, F., Lin, Y., Zhu, T., 2014. An expert knowledge-based approach to landslide susceptibility mapping using GIS and fuzzy logic. Geomorphology 214, 128–138. doi:10.1016/j.geomorph.2014.02.003

Chapter 4 Causative Factors Optimization Using Artificial Neural Network for GIS-based Landslide Susceptibility Assessments in Ambon, Indonesia

4.1 Introduction

Landslide is a major geological hazard worldwide, accounts for a high number of human casualties and an enormous amount of property loss, and causes severe damage to natural ecosystems and human-built infrastructures [*Dai et al.* 2002; *Guzzetti et al*. 2012]. It is necessary to understand the potential exposure to landslide hazard in the areas of mountainous and hilly terrain. The elucidation of the triggering mechanism, characteristics of movement, soil mechanical properties, and the associated geology of landslides can translate to sufficient geologic investigations, geotechnical engineering practices, and ultimately effective enforcement of land management regulation to reduce landslide hazards.

Over the last two decades, many models for landslide susceptibility mapping have been proposed with the assumptions that landslide susceptibility is related to causative factors and can be evaluated as long as the causal relationship is known [*Zhu et al*. 2014]. Even though the methods for landslide susceptibility mapping can be qualitative and quantitative, it is important to implement [*Clerici et al.* 2002; *Süzen & Doyuran* 2004]: 1) mapping of previous landslide inventory in the target region, 2) creation of geological and geomorphological factors that are directly or indirectly correlated with landslides, 3) estimation of the causative factors with the landslides, and 4) classification of the target region into categorical landslide susceptibility (hazard zoning).

During May to August 2012, high-intensity rainfall in Ambon city triggered 89 landslides, most of these landslides happened in municipality area. The damage was severe in the city and at several

sites along the transportation network. The landslides resulted in 167 houses destroyed, including 32 deaths, injured numerous people and 305 people evacuated (**Fig. 4.1**).

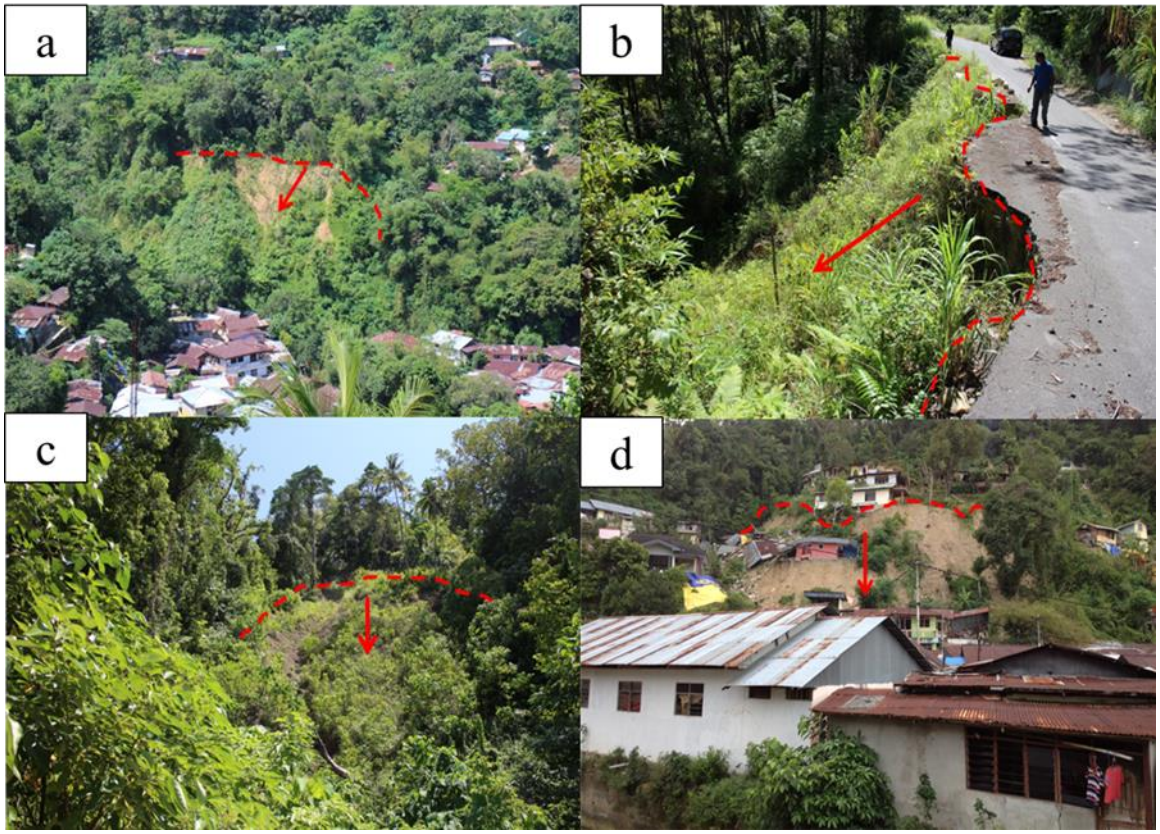

Figure 4.1 Landslide cases found during field investigation in 2015 a) landslides near settlement area; b) landslide along the road network; c) landslide case in the Ambon volcanic rocks geology, d) houses affected by landslides..

Economic losses caused by the landslide events are estimated to be around 25 million U.S. dollars. Therefore, it is necessary to assess and manage areas that are susceptible to landslides and to mitigate any damage associated with them.

This study aims to comparatively evaluate the usage of artificial neural network (ANN) to optimize causative factors in landslide susceptibility assessment in Ambon, Indonesia. In this regard, the occurrences of landslides were identified in the study area by field surveys and satellite imagery.

4.2 Study area

The study area was located in the Ambon Island at the 3°–4°S and 128°–129°E extending to an area of 377 km^2 (**Fig. 4.2**). The study was conducted in all area of Ambon City which includes five subdistricts: Nusaniwe subdistrict, Sirimau subdistrict, South Leitimur subdistrict, Baguala subdistrict, and Ambon Bay subdistrict totaling to 50 villages.

Ambon has tropical monsoon climate when dry season occurs during December–March, while rainy season occurs during May–October. During the last decade, June has the highest average monthly rainfall counting up to 674.7 mm. When floods occurred in July and August 2013, rain fell every day during the month of July with total monthly rainfall in July 2013 was 1928 mm and maximum daily rainfall was 432 mm.

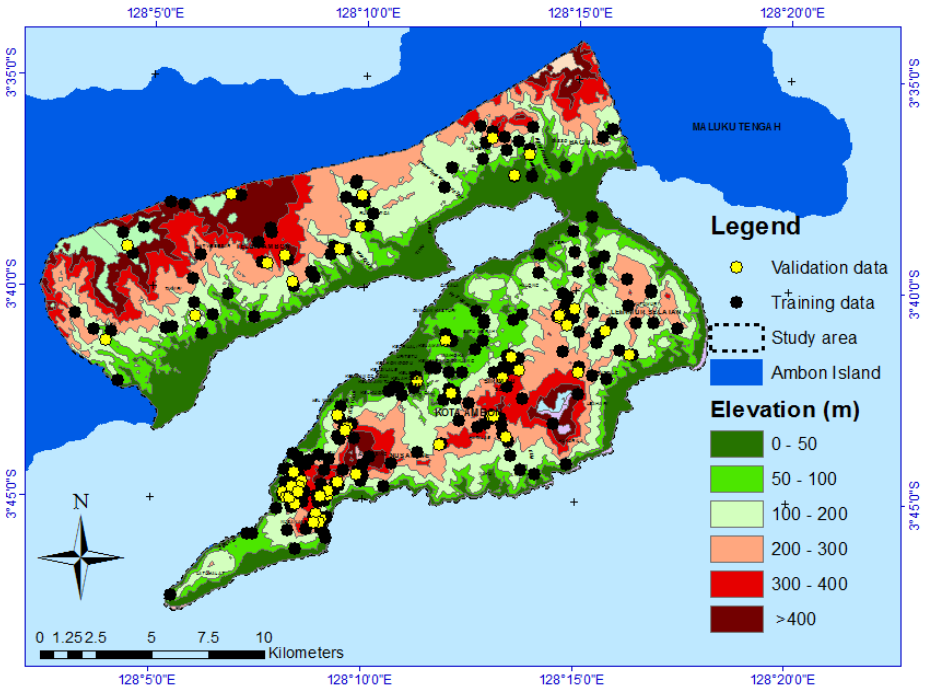

Figure 4.2 Landslide training and validation data in the study area.

Varied topography characterizes Ambon; this is shown with elevation variation of 0 m.a.s.l on coastline area and > 900 m.a.s.l for the inner mountainous area. This topographical factor affects the slope distribution throughout Ambon. Slope class of 0 to > 40^{o} is distributed in the entire area of Ambon.

The geology of Ambon is represented by many rock conglomerates, such as alluvial, Kanikeh formation, ultrabasic, Ambon volcanic ash, and Ambon granites (**Table 4.1**). The fault lines direction is mainly from northwest to southwest and northeast to southeast. The structural element that was made by the tectonic process is the fault lines, reverse fault lines, and strike-slip fault. Earthquake occurs at the depth 0–99 km with the magnitude up to 7 Richter scale.

Table 4.1Regional geological description of the study area

Formation	**Composition**	**Deposition**	**Age**
Ambon	Extrusive;	Volcanism;	Pliocene

volcanic rocks	intermediate; lava	subaerial	
Coral limestone	Sediment; chemical; limestone	Sedimentation; neritic; shallow	Holocene
Alluvial	Sediment; clastic; alluvium	Sedimentation; terrestrial; alluvial	Holocene
Kanikeh formation	Sediment; clastic; sandstone	Sedimentation; neritic; offshore	Triassic Late
Ambon granite	Intrusive; felsic; granitoid	Plutonism; batholith	Pliocene Middle
Ultrabasic rocks	Tectonite; ophiolite	Sedimentation; terrestrial	Jurassic

4.3 Methodology

4.3.1 Datasets

Independent variables were generated from datasets using ArcGIS® 10.1 SP1 for desktop. The databases containing the landslides causative factors were prepared in raster format using identical spatial projection and cell size (30 x 30 meter).

Based on the availability of data in the study area, eight landslide causative factors, slope angle (in degree), slope aspect, elevation (meter above sea level), geology, geological density (km/km^2),

proximity to fault lines (meter), proximity to river (meter), and proximity to road networks (meter) were taken into consideration in this study (**Fig. 4.3**).

The geomorphological factors were derived from ASTER GDEM including, elevation, slope angle, slope aspect. The geological factors were obtained from the Geological Research and Development Center. The anthropological factors have been collected from Indonesia Geospatial Information Agency. The landslide inventory was produced from the combination of an intensive field survey conducted in January 2015 and analyses from high-resolution satellite imagery

The total landslide number in the study area is 282 cases which translated to 841 pixels of landslide area. The landslide inventories were divided into training data (80% of total landslide cases, 741 pixels of landslide area) and validation data (20% of total landslide cases, 100 pixels of landslide area).

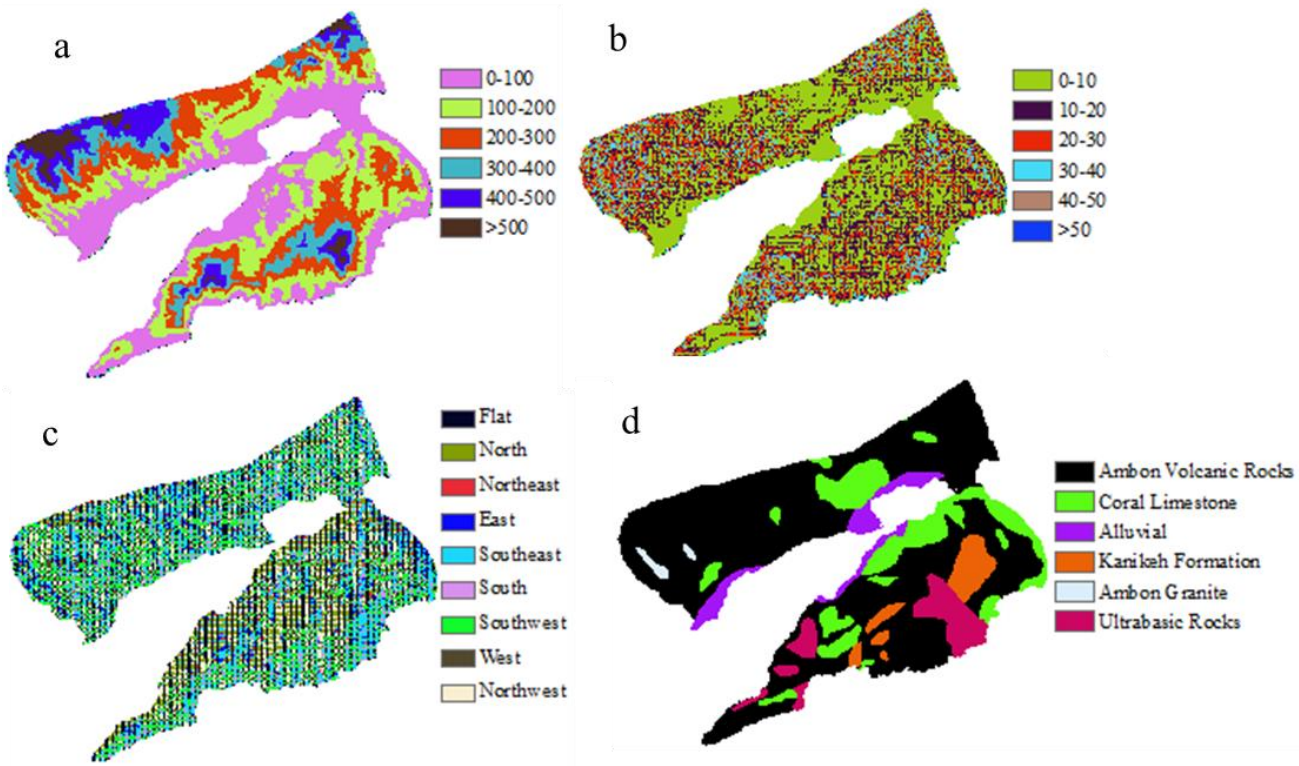

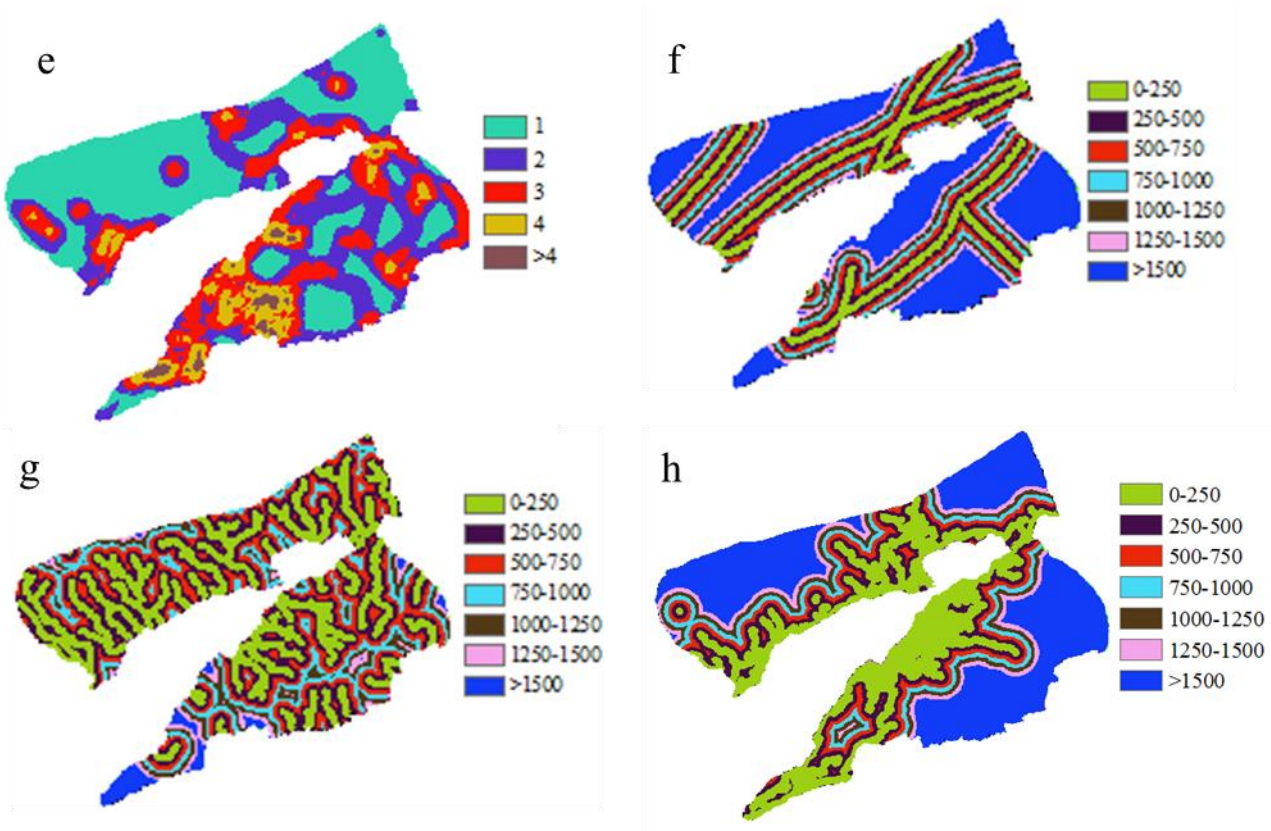

Figure 4.3Distribution of the eight causative factors used as independent variables in this study. a) elevation; b) slope; c) slope aspect; d) lithology; e) geological density; f) proximity to faults; g) proximity to river; h) proximity to road networks.

4.3.2Artificial neural networks

Artificial neural networks (ANN) are computational information processing units inspired by the structure and behavior of real biological neurons whose architecture mimics the knowledge acquisition and organizational skills of human brain cells. According to Cilliers [1998], the importance of ANN can be summarized in the following features. They conserve the complexity of the systems they model because they have complex structures themselves. The advantages include that they recognize different sets of data within a whole data set, do not require pre-existing knowledge or experience, do not need a statistical pre-existing model in order to train data and finally, they give reasonable results even when data are inaccurate and incomplete [*Jing & Hudson*. 2002; *Jing* 2003].

In this study, multi-layer perceptron (MLP) was applied. MLP is the most popular and most widely used ANN architecture which consists of input layer, output layer, and hidden layers in between. Each layer in a network contains a sufficient number of neurons. The output layer produces the neural network's results. Thus, the number of neurons in the input and output layers typically depends on the problem which the network was designed for **Fig. 4.4**. Each hidden and output layer neuron processes its inputs by multiplying each input (x_i) by a corresponding weight (w_i), summing the product (**Eq. 4.1**), and then processing the sum (if that exceeds the neuron threshold, the neuron is then activated) using a non-linear activation function (**Eq. 2**) to produce a result (y_i), which is the output node.

$$net = \sum_{i=0}^{n} w_i x_i \tag{4.1}$$

$$y_i = G(b^{(2)} + W^{(2)}(s(b^{(1)} + W^{(1)} i))) \tag{4.2}$$

with bias vectors $b^{(1)}$, $b^{(2)}$; weight matrices $W^{(1)}$, $W^{(2)}$ and activation functions G and s. A three layer feed-forward ANN was built. Optimum network architecture (8 inputs x 17 hidden neurons x

2 outputs) was selected following trial and error and considering the minimum mean square error. Initial weights were randomly initiated in a small range. The parameter of learning rate was set to 0.01. In this study, the network training activation transfer function for all layers was hyperbolic tangent.

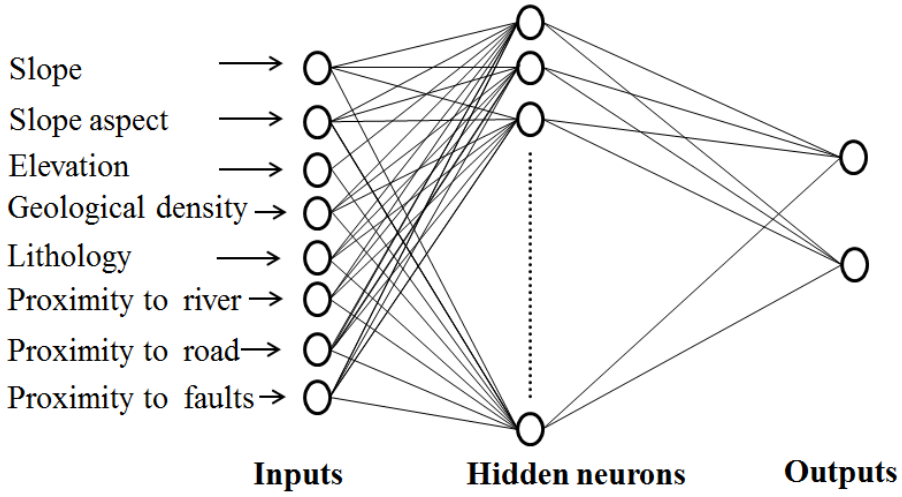

Figure 4.4 Architecture of artificial neural network in this study

Causative factors optimization was conducted by eliminating two factors with the least influential effects by the normalized importance value obtained from the ANN analysis.

4.4 Results and Discussions

4.4.1 Artificial neural networks

The normalized importance of each landslide causative factor is presented in **Table 4.2**. The ANN analysis was performed with a mean square error of 0.02 in the training set. The final landslide susceptibility map was produced by multiplying each causative factor with the independent variable importance calculated through the ANN analysis (**Eq. 4.3**) and then an overlay of these layers was performed.

$$LSANN = \sum_{j=1}^{n} fw_i \times wi_j \quad (3)$$

where *LSANN* is the final landslide susceptibility map calculated for each pixel, fw_i is the weight of each causative factor and $w_{i,j}$ is the normalized weight for the category *j* of the factor *i*.

Based on the normalized importance value obtained from the ANN analysis, the slope aspect and proximity to river were eliminated for the optimized six causative factors landslide susceptibility analysis. Previous study by Pradhan & Lee [2010] showed that ANN techniques is suitable for optimizing causative factors in landslide susceptibility assessment by eliminating the least influential factors.

Table 4.2 The importance and normalized importance value derived from artificial neural network (ANN).

Causative factors	**ANN importance**	**ANN normalized importance**
Proximity to road	0.23	100.0%
Geological density	0.19	82.8%
Slope	0.12	51.7%
Proximity to fault	0.11	47.4%
Elevation	0.11	46.2%
Lithology	0.10	41.3%
Aspect	0.09	38.1%
Proximity to river	0.06	26.8%

The produced landslide susceptibility maps were categorized using Jenk's natural break method into five classes (very low to very high). The produced landslide susceptibility maps are shown in **Fig. 4.5**

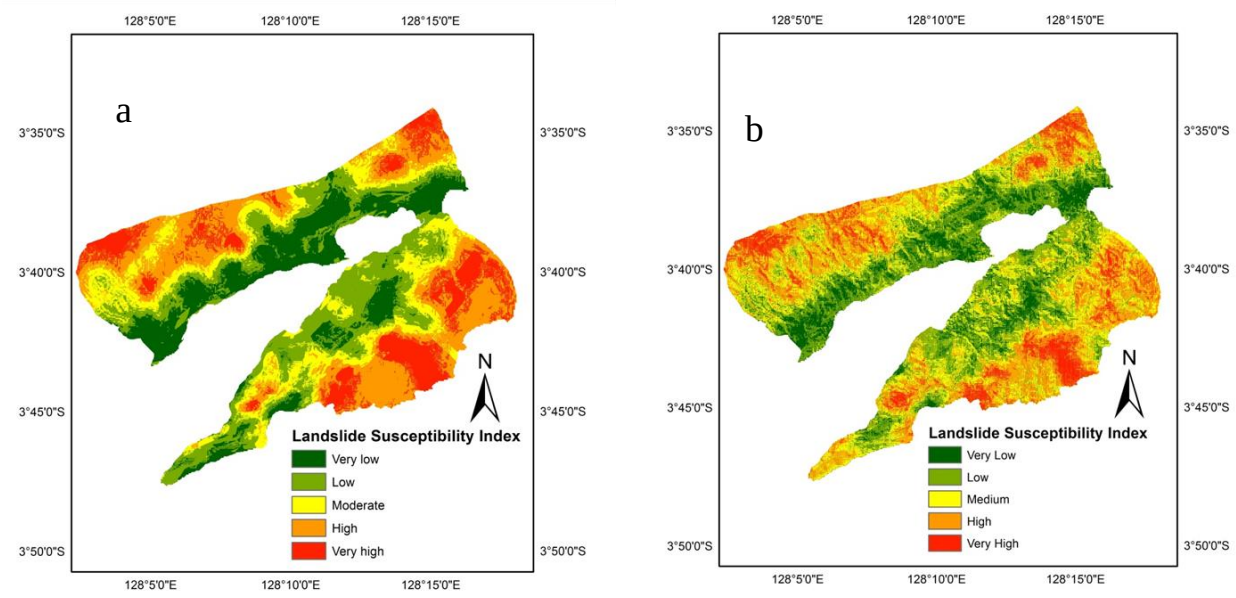

Figure 4.5 Landslide susceptibility maps derived from 6 factors (a) and 8 factors (b) using artificial neural network (ANN) models.

4.4.2 Models Validation

Susceptibility maps were validated by comparing landslide areas to susceptibility classes, the likelihood of landslide occurrences in a particular region. It was observed that the smaller degree of fit was distributed in the low and very low susceptibility classes. The higher values of the degree of fit were found to be in the high and very high susceptibility classes for the landslide susceptibility maps produced by the three models.

The comparison between the validation and training set overlay analysis of the ANN-derived susceptibility maps show similar results across all susceptibility categories (**Fig. 4.6**).

For the 8 factors LS models, the training set data indicates that 79% and 0% of the landslide pixels occur in the very high and very low susceptibility classes respectively and that 21% in the

high, moderate, and low susceptibility categories respectively. The validation set shows a total of 63% and 0% of pixels occurring in the very high and very low susceptibility classes and 47% occur in the high, moderate, and low susceptibility classes respectively. It is evident that there is a variation between results produced by the validation and training set for the very high susceptibility class, which shows a difference of 13% whereas a total of 10% represents the difference in landslide pixels in the moderate susceptibility class. 8% of the landslides in the training data belong to the low categories. These landslide events are located mainly in the outlier of the inner mountainous area of the study area which represents a small number of landslides.

In the case 6 factors LS model, the training set data indicates that 92% and 0% of the landslide pixels occur in the very high and very low susceptibility classes respectively and that 8% in the high, moderate, and low susceptibility categories respectively. The validation set shows a total of 82% and 0% of pixels occurring in the very high and very low susceptibility classes and 18% occur in the high, moderate, and low susceptibility classes respectively. It is evident that there is a variation between results produced by the validation and training set for the very high susceptibility class, which shows a difference of 7% whereas a total of 4% represents the difference in landslide pixels in the moderate susceptibility class.

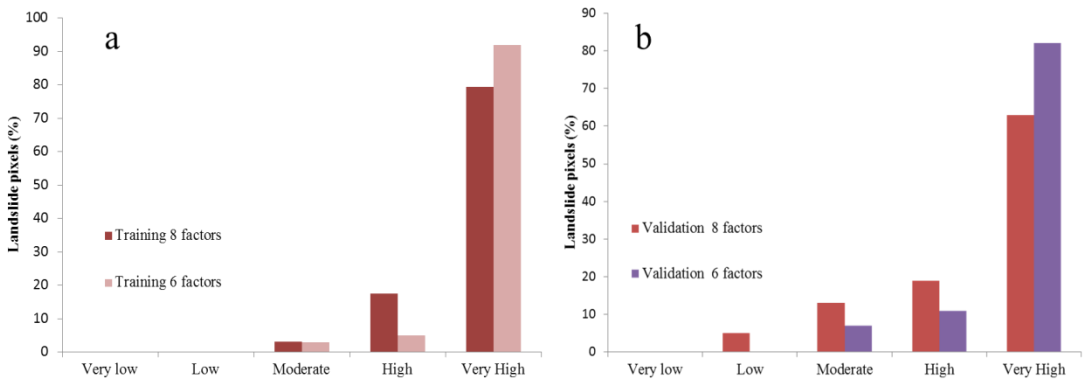

Figure 4.6 6 factors and 8 factors LS models relationship with landslide occurrences (a) training data; (b) validation data.

4.4.3 Receivers Operating Curves (ROC)

A standard validation analysis to compare prediction performance of various classifiers is the Receiver Operating Curve (ROC) and the calculation of Area Under Curve (AUC) [*Akgun et al. 2012; Tien Bui et al. 2012]*. The ROC is a useful method for representing the quality of deterministic or probabilistic landslide susceptibility model classifiers. In the ROC graph, the sensitivity of the model which is determined as the percentage of the correctly predicted landslide pixels by the model is plotted against specificity, which is the proportion of predicted landslide pixels over the total study area. The AUC represents the quality of the models to reliably predict the occurrence or the non-occurrence of landslides.

A good fit model has an AUC value from 0.5 to 1.0. The ideal model performs an AUC value close to 1.0 (perfect fit), whereas a value close to 0.5 indicate inaccuracy in the model (random fit), [*Carvalho et al*. 2014].

Fig. 4.7 show the ROC of 6 factors and 8 factors ANN models for the training and validation sets. The measurement of how well the model performs is represented in the success rate curve (training data) while the capability of the model to predict is represented in the prediction rate curve (validation data).

It is observed that all the models have good success rate with the highest one being the 6 factors ANN model (AUC: 0.770), while the 8 factors model returns AUC of 0.734. In the case of the prediction rate curve, 6 factors ANN model shows the highest value (AUC: 0.777) whereas the 8 factors model returns AUC of 0.717.

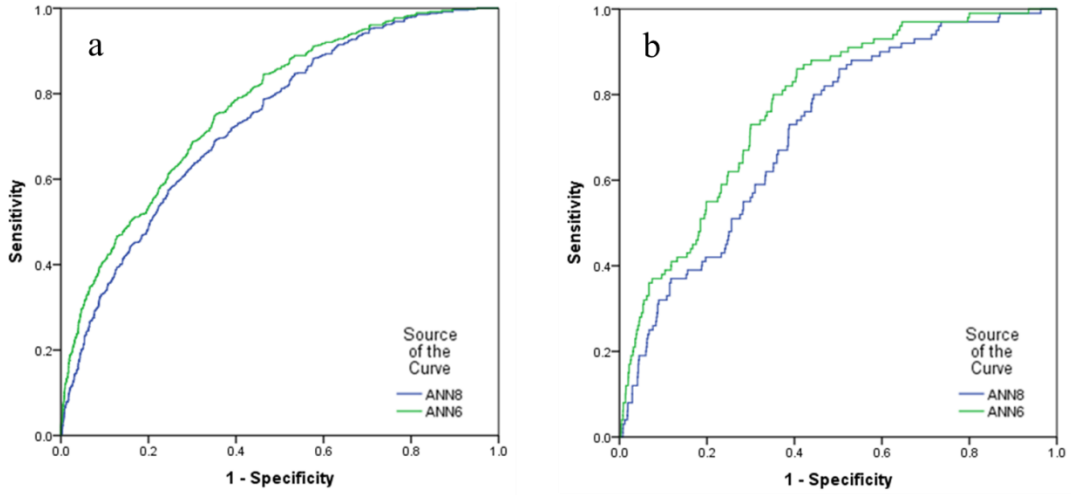

Figure 4.7 Receiver operating curves 6 factors and 8 factors artificial neural network methods. Figure 7a indicates success rate curves and Figure 7b indicates the prediction rate curve.

4.4.4 Landslide causative factors relationship with landslide occurrence

The relationship between the eight causative factors and landslide occurrences are shown in **Fig. 4.8**. The landslide frequencies are plotted in the primary axis while the landslide densities are plotted in the secondary axis.

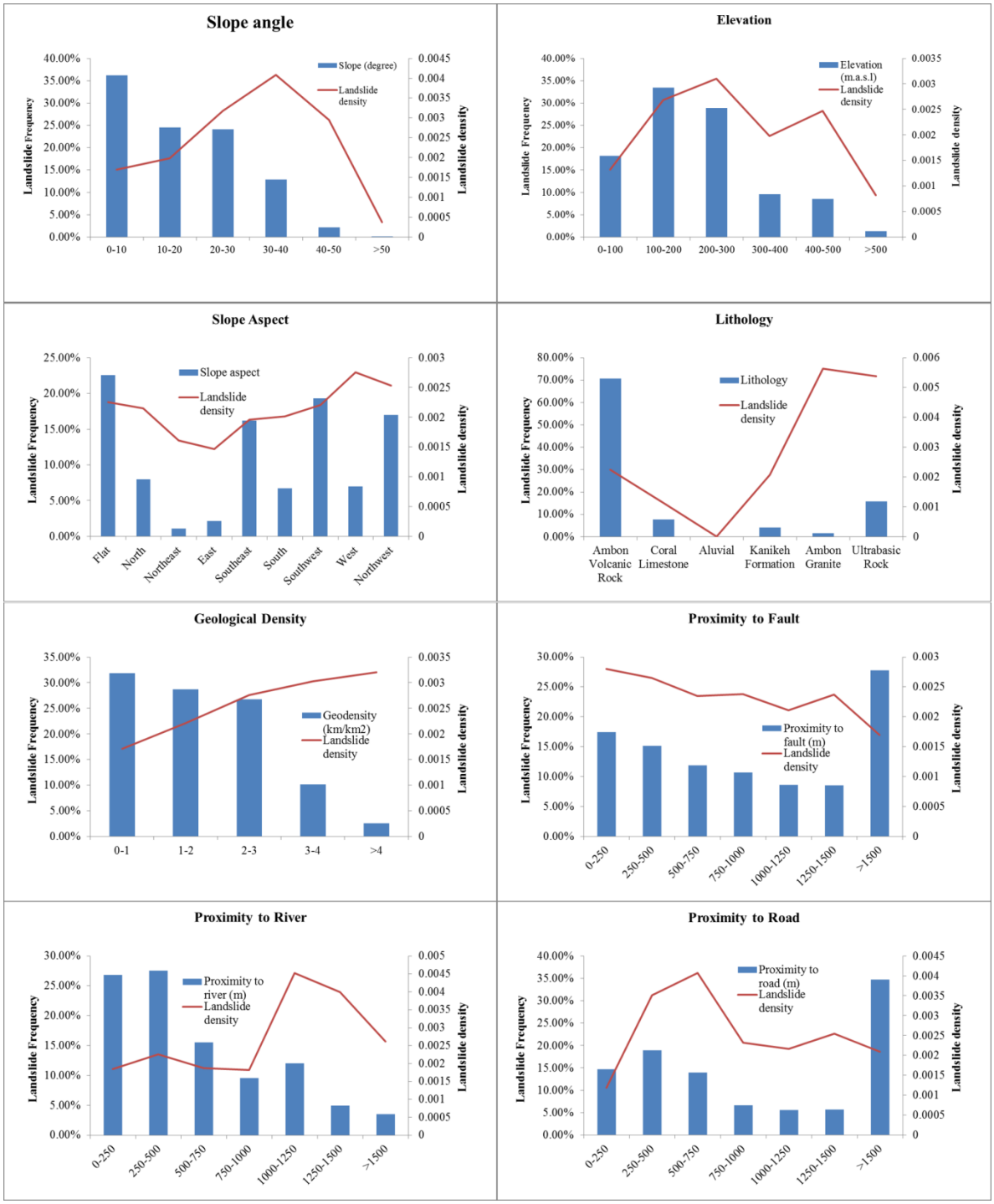

Figure 4.8 The eight causative factors relationship with landslide frequency and landslide density.

In this study, ANN method was applied to optimize the causative factors of landslide occurrences and to compare the produced LS maps. The general trends, however, dictate that

the geological factors and topography be amongst the most significant [*Sakellariou & Ferentinou* 2005]. The geomorphology and slope morphology has a definite influence on slope stability and is considered as the most important causative factors related to mass movement activity. Parameter class relationships are evident through the assessment of landslide densities with the occurrence of observed landslides **Fig. 4.8**.

Lithology varies regarding chemical and physical properties, which give rise to different levels of susceptibility to landslide occurrence. In this study area, the highest landslide occurrence is found in the Ambon granite formation which comprises of biotite granite and biotite cordierite granite. Ultrabasic formation which comprises of harzburgite, dunite, serpentinite and gabbro follows as the second highest density in the lithology parameters.

In term of geological density the parameter class >4 km/km^2 showed the highest landslide occurrence which suggests the interlayers of geological structures affects slope stability in a negative way. A consistent increase of landslide density is observed in geological density parameters suggesting that geological density showed high correlation with landslide occurrences. Based on the normalized importance value obtained from ANN (**Table 4.2**), geological density is the second most important parameter after proximity to road network (normalized importance value: 0.19). A previous study by *Kawabata and Bandibas* [2009] suggested that landslide occurrences increase as the density of geological boundaries increases due to unstable relationship between geological substrata. Higher geological density correlates with weaker slope stability which corresponds to landslide occurrences. This phenomenon is evident in the southern part of the study area which has the highest geological density where most of the identified landslides are located.

The highest landslide occurrence is associated with elevation ranging from 200–300 m

which occurs mostly along the northeastern and southwestern part of the study area. Steeper slope angles indicate larger driving forces relative to resisting forces which result in a greater potential to fail. In the studied area, most landslides are associated with slope angles ranging from 30°–40° where some municipalities are located. The western-facing slope shows the highest landslide density compared to other class in the slope aspect classes. Past study in the area showed similar findings that most of the landslide occurrence happened in the west slope due to soil resistivity contrast between adjacent rocks [*Souisa et al.* 2015].

Drainage networks impact negatively on landslide susceptibility due to their abrasion processes along the base of slopes, which also result in the saturation of associated material thereby reducing the stability of the slope [*Demir et al*. 2013]. It is thus expected that more landslides should occur within a limited distance from the stream network. However, this study findings show that the greatest landslide occurrence is associated with the class representing 1000–1250 m from the river network. This might be because of underreported landslide cases found in natural slopes. Underreported landslide cases might be due to lack of personnel to cover extensive landslide area especially in the rainy season.

The class of > 1500 m of proximity to faults shows the highest landslide occurrences. Even though realistically not associated with the occurrence of landslides, but statistically show high values of occurrence. Closer distances to faults do not show high landslide densities, which may be attributed to that fact that most observed and mapped landslides occur far from the fault lines suggesting that the statistical relationship is based solely on landslide events recorded around a single fault in the interior only.

The highest occurrence of landslides occurs within 250–500m from the road network. This pattern is expected since the excavation of road cuts reduce the lateral support of material and may trigger landslides. Moreover, this process alters the natural terrain and drainage system.

Proximity to road network is regarded as the most important parameter in this study by the ANN model (normalized importance value: 0.23)

The produced LS maps shows good accuracy of > 70%. It is evident from the obtained results that 6 factors ANN model shows higher accuracy for both success rate and prediction rate curves, AUC of 0.770 and 0.777, respectively. In the case of 8 factors ANN model shows returns 0.734 and 0.717 for the success rate and prediction rate curves, respectively. These results agree with past study by *Pradhan and Lee*, [2010] showing that the soft-computing performance of ANN could be utilized as causative factors optimization method in landslide susceptibility assessments. The relationship between training data and validation data to landslide occurrences also shows acceptable data goodness of fit demonstrated by the consistent increases of landslide pixels per susceptibility classes. Most of the landslide pixels are identified in very high and high susceptibility class in both 6 factors and 8 factors models.

4.5 Conclusion

In conclusion, the current paper provides a comparative evaluation of landslide susceptibility model using artificial neural network by employing optimization on the causative factors. The landslide locations mapped in the studied Ambon city were substantial to the spatial prediction of future landslides. Their relationship with various causative factors has proven to be that of a critical combination. The identification of areas susceptible to the occurrence of landslides is important as it could serve as a preliminary tool in future development planning and for identifying priority areas for early warning systems against potential damage.

Geological factors proved to be critical for all models where they are represented differently being lithological type, proximity to faults, and geological density. In detail,

Ambon granite and ultrabasic rocks are exposed to high degree on the susceptibility maps. Proximity to road network was found to be amongst the most influential causative factor with the center portion of the region exhibiting higher densities. In all three maps, the highest susceptibility to landslides was seen in the southwestern part of the city and on the outskirts of the eastern side. These areas are defined by subdistricts such as Nusaniwe and Leitimur Selatan. The resulting susceptibility maps were classified using Jenk's natural break into five classes (very low to very high susceptibility).

Model performance was tested using an independent validation set comprising 20% of all mapped landslides. For verification of the model performance, receiver operating curves (ROCs) were calculated and the areas under the curve (AUC) for success rate curve were 0.770, and 0.734 for optimized 6 factors and 8 factors respectively. The prediction rate curves AUC were 0.777, and 0.717 for optimized 6 factors and 8 factors respectively

The map derived from this approach is best suited to aid in land-use planning and landslide mitigation. Furthermore, this information can be employed to validate and verify any results acquired at regional and national scale. However, it must be noted that all results obtained are a function of the accuracy of the original database including input causative factors and the landslide inventory. In the study area data availability is one of the major issues in landslide susceptibility assessment. Present study employed eight landslide causative factors, future works would include more data collection to be used as inputs to improve the robustness of landslide susceptibility models in the study area.

4.6 References

Akgun, A., Kincal, C. & Pradhan, B. (2012): Application of remote sensing data and GIS for landslide risk assessment as an environmental threat to Izmir city (west Turkey). Environmental Monitoring and Assessment, Vol. 184, No. 9, pp.5453–5470.

Carvalho, L.F. et al. (2014): Digital signature of network segment for healthcare environments support. Irbm, Vol. 35, No. 6, pp.299–309.

Cilliers, P. (1998): Complexity and postmodernism: Understanding complex systems. South African Journal of Philosopy, Vol. 18, No. 2, pp.258–274.

Clerici, A. et al. (2002): A procedure for landslide susceptibility zonation by the conditional analysis method. Geomorphology, Vol. 48, No. 4, pp.349–364.

Dai, F.C., Lee, C.F. & Ngai, Y.Y. (2002): Landslide risk assessment and management: An overview. Engineering Geology, Vol. 64, No. 1, pp.65–87.

Demir, G. et al. (2013): A comparison of landslide susceptibility mapping of the eastern part of the North Anatolian Fault Zone (Turkey) by likelihood-frequency ratio and analytic hierarchy process methods. Natural Hazards, Vol. 65, No. 3, pp.1481–1506.

Guzzetti, F. et al. (2012): Landslide inventory maps: New tools for an old problem. Earth-Science Reviews, Vol. 112, No. 1-2, pp.42–66.

Jing, L. (2003): A review of techniques, advances and outstanding issues in numerical modelling for rock mechanics and rock engineering. International Journal of Rock Mechanics and Mining Sciences, Vol. 40, No. 3, pp.283–353.

Jing, L. & Hudson, J.A. (2002): Numerical methods in rock mechanics. International Journal of Rock Mechanics and Mining Sciences, Vol. 39, No. 4, pp.409–427.

Kawabata, D. & Bandibas, J. (2009): Landslide susceptibility mapping using geological data, a DEM from ASTER images and an Artificial Neural Network (ANN). Geomorphology, Vol. 113, No. 1-2, pp.97–109.

Pradhan, B. & Lee, S. (2010): Landslide susceptibility assessment and factor effect analysis: backpropagation artificial neural networks and their comparison with frequency ratio and bivariate logistic regression modelling. Environmental Modelling and Software, Vol. 25, , pp.747–759.

Sakellariou, M.G. & Ferentinou, M.D. (2005): A study of slope stability prediction using neural networks. Geotechnical and Geological Engineering, Vol. 23, No. 4, pp.419–445.

Souisa, M., Hendrajaya, L. & Handayani, G. (2015): Determination of Landslide Slip Surface Using Geoelectrical Resistivity Method at Ambon City Moluccas-Indonesia. International Journal of Emerging Technology and Advanced Engineering, Vol. 5, No. 7, pp.42–47.

Süzen, M.L. & Doyuran, V. (2004): Data driven bivariate landslide susceptibility assessment using geographical information systems: a method and application to Asarsuyu catchment, Turkey. Engineering Geology, Vol. 71, No. 3-4, pp.303–321.

Tien Bui, D. et al. (2012): Spatial prediction of landslide hazards in Hoa Binh province (Vietnam): A comparative assessment of the efficacy of evidential belief functions and fuzzy logic models. CATENA, Vol. 96, , pp.28–40.

Zhu, A.-X. et al. (2014): An expert knowledge-based approach to landslide susceptibility mapping using GIS and fuzzy logic. Geomorphology, Vol. 214, , pp.128–138.

Chapter 5 Forest Slope Stability under Heavy Rainfall Events in Volcanic Geology: A Case Study of Aso, Japan and Ambon, Indonesia

5.1 Introduction

The increasing rainfall pattern that might be induced by climate change is being observed worldwide and being studied for its influence on triggering landslides, this phenomenon is especially obvious in the northern part of Kyushu Island, Japan (Kubota, 2010). Rainfall is the major agent in triggering landslides, it is more frequent compared to earthquake and slope undercutting (Crozier, 1986). The relationship between rainfalls and slope stability is widely recognized, however drawing a distinct line of the relative roles of the antecedent rainfall (the rain that falls in the days preceding the landslide events) and the triggering rain (the rain that falls at the time of the landslide events) has proved to be difficult (Rahardjo, 2008; Sanchez et al., 2015).

In 2012, the city of Aso in western Japan experienced heavy rainfall from July 11th to July 13th counted up to 656 mm with the intensity of 493 mm/day and 106 mm/hr. This tremendous amount of rainfall translated into countless traces of debris flows and landslides. Meanwhile, during the period of May to August of 2012, the high intensity rainfall in (maximum daily rainfall: 360 mm/day) Ambon city, triggered around of 89 landslides, especially in the settlement area. The damage was particularly severe in the city and at several sites along the transportation network. The landslides resulted of 167 houses destroyed, including 32 deaths, numerous injured people and 305 people evacuated. Estimated economic losses caused by these sediment related disasters are worth of about 25

million U.S. dollars (**Fig. 5.1**). By employing numerical analysis (Finite Element Method), this paper aims to quantify the increasing rainfall in the city of Aso throughout the last decades and to quantify its effects to slope stability in forest area.

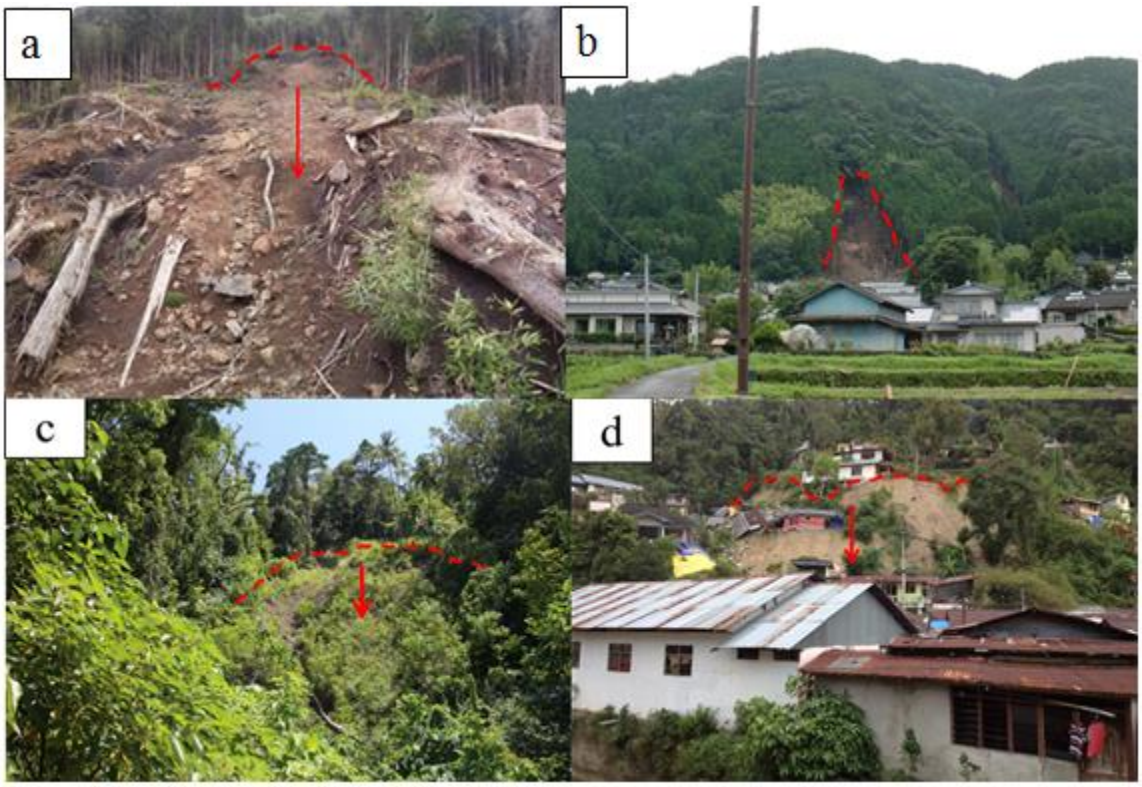

Figure 5.1 Pictures of landslide location in (a) Aso Teno; (b) Aso Nakasakanashi;, (c) Ambon Eerie; (d) Ambon Seilale.

5.2 Study area

The study areas is located in Aso, Japan and Ambon, Indonesia (**Fig. 5.2**). Two slopes from each study sites were selected as case studies:

1. Aso Teno (131^{o} 6 ’54’’E, 32 ^{o} 58’ 46’’N)
2. Aso Nakasakanashi (131^{o} 9 ’1’’E, 32 ^{o} 56’ 26’’N)
3. Ambon Eerie (128° 7'57.30"E, 3°45'15.86"S)
4. Ambon Seilale (128° 7'23.36"E, 3°45‘ 53.36“ S)

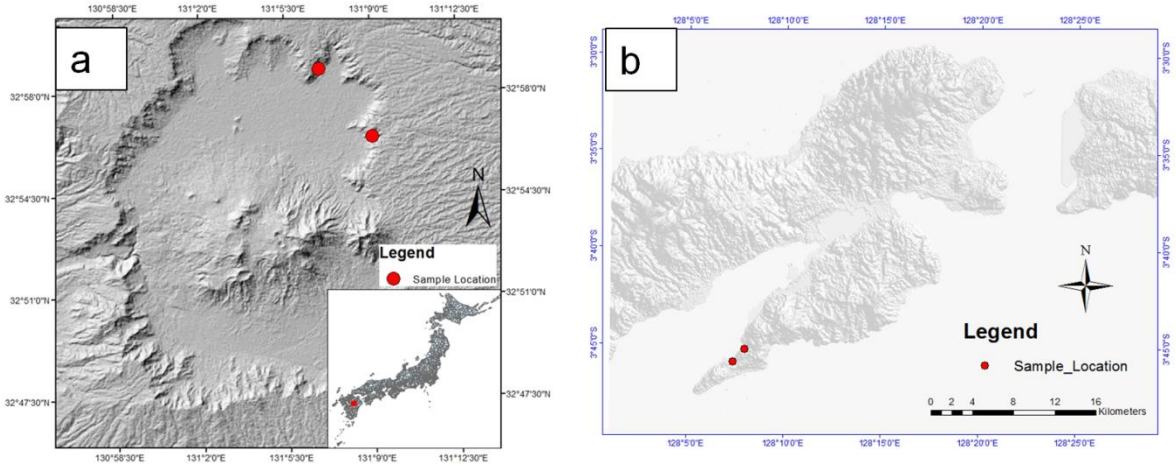

Figure 5.2 Simplified map of the study area (a) Aso slopes; (b) Ambon slopes.

The city of Aso experienced numerous landslides and debris flows during the record-breaking rainfall on July 2012. Two slopes were taken as case studies for the effect of increasing rainfall induced by climate change to the forest slope stability. The average annual rainfall of the study site is 2831 mm/year (Japan Meteorological Agency, 2013) with most rainfalls on June and July. The geological features of the study site in Aso are represented by mainly unconsolidated deposit of diluvium gravels, sands, muds, and volcanic ash. On forested slopes, broadleaved tree species, such as *Quercus crispula*, *Cornus controversa* and *Prunus jamasakura* as well as coniferous species such as *Chamaecyparis obtusa* and *Cryptomeria japonica* are common. (Paudel, 2007).

In Ambon, the parent material is weathered tuff zone is very soft rock, unstable, and muddy when mixed with water. The steep slopes implied low slope stability eventhough not being used for municipality or agricultural use. Residual soil thickness is high with varied parent materials of 2 – 5 meter.

5.3 Methodology

5.3.1 Data collection and laboratory analysis

Field investigations were conducted during the year of 2012 and 2015 to collect data from the field. Soil samples were collected from each slope for the direct shear test in the laboratory. Samples were also collected for permeability test. Collecting soil samples for slope stability analysis is a very important and crucial task. Soil sampling is difficult particularly when attempting to get representative sample from the entire area. In this study soil samples were taken from several parts of the slope (the bottom, middle, and top) above the slip surface for the direct shear test using direct shear apparatus (**Fig. 5.3**). Two samples from different depth were also collected for the permeability test. The samples were collected using sample cylinders in the undisturbed forms.

Figure 5.3 Direct shear apparatus used for soil shear test in this study.

Rainfall data were collected through the AMeDAS network of Japan meteorological agency. For the Aso region, data were obtained from Aso-otohime weather station. Data were collected from 1978 – 2012 from the Aso-otohime weather station. Ambon rainfall data were

obtained from Ambon Meteorological and Geophysical Agency from the period of 1979 – 2013.

5.3.2 Rainfall statistics

The Mann-Kendall test is applicable in cases when the data values x_i of a time series can be assumed to obey the model in **Equation. 5.1.**

$$\boldsymbol{X_i = f(t_i) + \varepsilon_i} \tag{5.1}$$

where $f(t_i)$ is a continuous monotonic increasing or decreasing function of time and the residuals ε_i can be assumed to be from the same distribution with zero mean. It is therefore assumed that the variance of the distribution is constant in time.

We want to test the null hypothesis of no trend, H_0, i.e. the observations *xi are* randomly ordered in time, against the alternative hypothesis, H_1, where there is an increasing or decreasing monotonic trend. In the computation of this statistical test we exploit both the so called S statistics given in Gilbert (1987) and the normal approximation (Z statistics). For time series with less than 10 data points the S test is used, and for time series with 10 or more data points the normal approximation is used according to **Equation. 5.2.**

$$\boldsymbol{Z} = \begin{cases} \dfrac{\boldsymbol{S}-1}{\sqrt{\boldsymbol{VAR(S)}}} & if\ S > 0 \\ 0 & if\ S = 0 \\ \dfrac{\boldsymbol{S}+1}{\sqrt{\boldsymbol{VAR(S)}}} & if\ S < 0 \end{cases} \tag{5.2}$$

The presence of a statistically significant trend is evaluated using the *Z* value. A positive (negative) value of *Z* indicates an upward (downward) trend. The statistic *Z* has a normal

distribution. To test for either an upward or downward monotone trend (a two-tailed test) at α level of significance, H_0 is rejected if the absolute value of Z is greater than Z1-α/2, where Z1-α/2 is obtained from the standard normal cumulative distribution tables.

To estimate the true slope of an existing trend (as change per year) the Sen's nonparametric method is used. The Sen's method can be used in cases where the trend can be assumed to be linear. This means that *f(t)* in **Equation. 1** is equal to

$$f(t) = Qt + B \tag{5.3}$$

where Q is the slope and B is a constant.

To get the slope estimate Q in **Equation. 5.4** we first calculate the slopes of all data value pairs

$$Q_i = \frac{X_j - X_k}{j - k} \tag{5.4}$$

Where $j>k$.

5.3.3 Finite element analysis

In this study, the slope stability analysis was performed using FEM with strength reduction technique. The soil was modelled according to Mohr-Coulomb failure criterion for its mechanical properties and Van Genuchten model for its hydraulic properties. GUSLOPE Ver 1.00 computer code was employed in this study. FEM were conducted with three different scenarios:

- No rainfall
- Under heavy rainfall of 2012

The output of the simulation is Factor of Safety. Factor of Safety of a slope is the ratio of resisting forces to driving forces. FS lower than 1.00 denotes that the slope is not stable, thus prone to landslide. FS 1.00 or more denotes that the slope is in a stable condition. The stability analyses were coupled with seepage analysis to gain comprehensive understanding on the effect of rainfall to slope stability.

5.4 Results and discussions

5.4.1 Increasing rainfall in Aso and Ambon during 1978 – 2012

Based on the obtained results, it can be inferred that the Aso area is experiencing increase in term of rainfall. Sen's slope estimator was used to estimate the slope of the increasing trend of rainfall. The Q value in the **Table 5.1** is the Sen's estimator for the true slope of a linear trend. i.e: change per unit time period (in this study a year).

The maximum hourly rainfall the Q value is 0.52 mm/hr/yr for Ambon rainfall this means that during 1978 – 2012 a total increment of 18.2 mm is happened in Aso in term of maximum hourly rainfall. While on the other hand, the maximum hourly rainfall for Ambon is increased at 0.40 mm/hr/yr this can be inferred during the year of 1979 – 2012 a total increment of 13.6 mm is happened in Ambon (**Fig. 5.4**)

Table 5.1 Rainfall trend analysis of Aso and Ambon during 1978 - 2012

Time series	**First year**	**Last Year**	**Test Z**	**Signifi c.**	**Q**	**B**
Aso Maximum Hourly Rainfall	1978	2012	1.83	+	0.052	37.88
Ambon Maximum Hourly	1979	2013	0.62	n.a	0.	86.4

Rainfall 40 4

+ if trend at α = 0.1 level of significance

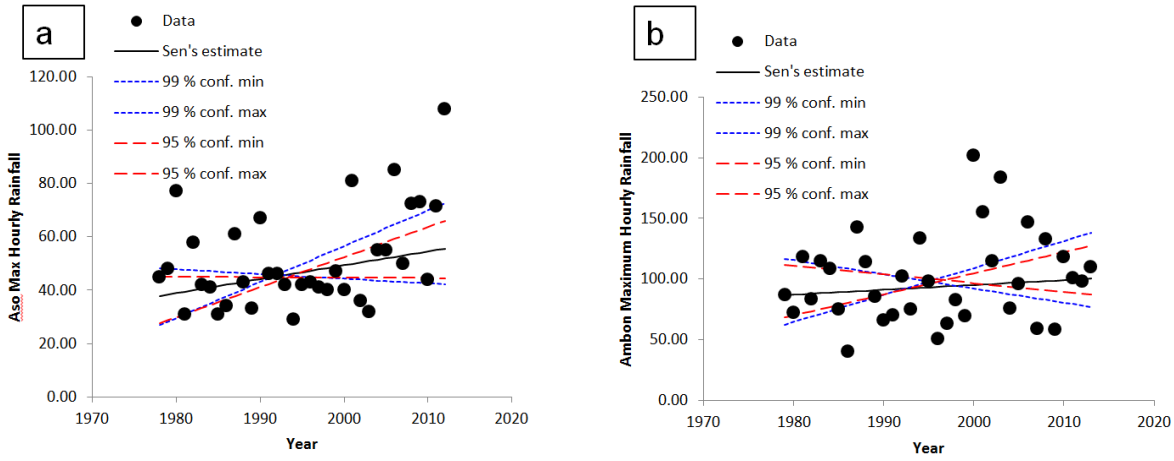

Figure 5.4 Maximum hourly rainfall trend in Aso during 1978 - 2012

5.4.2 Soil shear strength and permeability

Soil samples were analyzed in the laboratory for its geotechnical properties. The result of the soil analyses are presented in the **Table 5.2.**

Table 5.2 Soil Strength Parameter

	Sample Location			
Soil Parameter	**Aso Teno**	**Aso Nakasakanashi**	**Ambon Eerie**	**Ambon Seilale**
Unit weight (kN/m3)	24.7	15	28	26
Cohesion (kPa)	15	2	2.6	3
Angle of Internal Friction (degree)	58	26	34	26

Young Modulus (kPa)	20000	20000	20000	20000
Poisson Ratio	0.3	0.3	0.3	0.3
Permeability Rate (m/s)	$2.03x10^{-4}$	$8x10^{-6}$	$6.5x10^{-6}$	$7x10^{-6}$

From the obtained result, Aso Teno cohesion value is 15 kPa. The angles of intenal friction (φ) of is relatively high at the 58 degrees. Generally, soil with these kind of properties belong to the categories of clay which typical value is ranging between 0 – 48 kPa. The soil of Aso Nakasakanashi exhibits unit weight of 15 kN/m^3, with cohesion value of 2 kPa. The angle of internal friction (φ) is 26 degrees. These characteristics show that the soil of Aso-Nakasanishi is those of silty clay. Generally, the silty clay soil shows properties of unit weight between 16 – 20 kN/m^3, cohesion (c) ranging between 0-48 kPa, and angle of internal friction (φ) between 20-34 degrees. Clay usually generates good shear strength due to its elastic properties.

The soil in Ambon slopes exhibit similar properties with cohesion value of 2.6 kPa for Ambon Eerie soils and 3 kPa for Ambon Seilale. The angle of internal frictions are 34 degrees for the Ambon Eerie and 26 degrees for the Ambon Seilale sample.

The permeability coefficient (k) of Aso Teno is $2.03x10^{-4}$ m/s, which denotes that in this slope the rate of permeability is moderate. The soil of Aso Nakasakanashi also exhibits the same moderate permeability rate at the 6 orders of magnitude which is $8x10^{-6}$ m/s. The permeability rates in Ambon are $6.5x10^{-6}$ m/s for Ambon Eerie and $7x10^{-6}$ for Ambon Seilalo, respectively. Generally, with the permeability coefficient ranging between 4-6 orders of the magnitude, slopes of Aso, in term of permeability can be consisted of stratified clay deposits or mixtures of sand, silt, and clay.

Many factors affect soil permeability. Sometimes they are extremely localized, such as cracks and holes, and it is difficult to calculate representative values of permeability from actual measurements. A good study of soil profiles provides an essential check on such measurements. Observations on soil texture, structure, consistency, colour/mottling, layering, visible pores and depth to impermeable layers such as bedrock and claypan form the basis for deciding if permeability measurements are likely to be representative. The size of the soil pores is of great importance with regard to the rate of infiltration (movement of water into the soil) and to the rate of percolation (movement of water through the soil). Pore size and the number of pores closely relate to soil texture and structure, and also influence soil permeability.

5.4.3 Influences of increasing maximum hourly rainfall to slope stability

Slope stability analyses were conducted using GUSLOPE ver 1.00 computer code developed at Gunma University. The method of analyses was Finite Element Method (FEM) performed with strength reduction technique. The slope stability analyses were coupled with seepage analyses to compute the effect rainfall to slope stability.

Two different scenarios were employed for the slope stability analysis, the first one is without rainfall (this scenario is not considering any rainfall effects to the slope) and the second one is with the actual rainfall of July 2012. This scenario is adding the actual rainfall of July 2012.

Aso slopes showed stable condition when subjected to no rainfall scenario (**Fig. 5.5**). Aso Teno (Factor of safety = 1.10) and Aso Nakasakanashi (Factor of safety = 1.06). However all slopes experiences failure when being subjected the heavy rainfall event of July 2012: Aso Teno (Factor of safety = 0.95), and Aso Nakasakanashi (Factor of safety = 0.90). From these

results, it can be inferred that all of the studied slopes is becoming unstable after a rainfall event is introduced. Generally, rainfall affects slope stability to a negative direction.

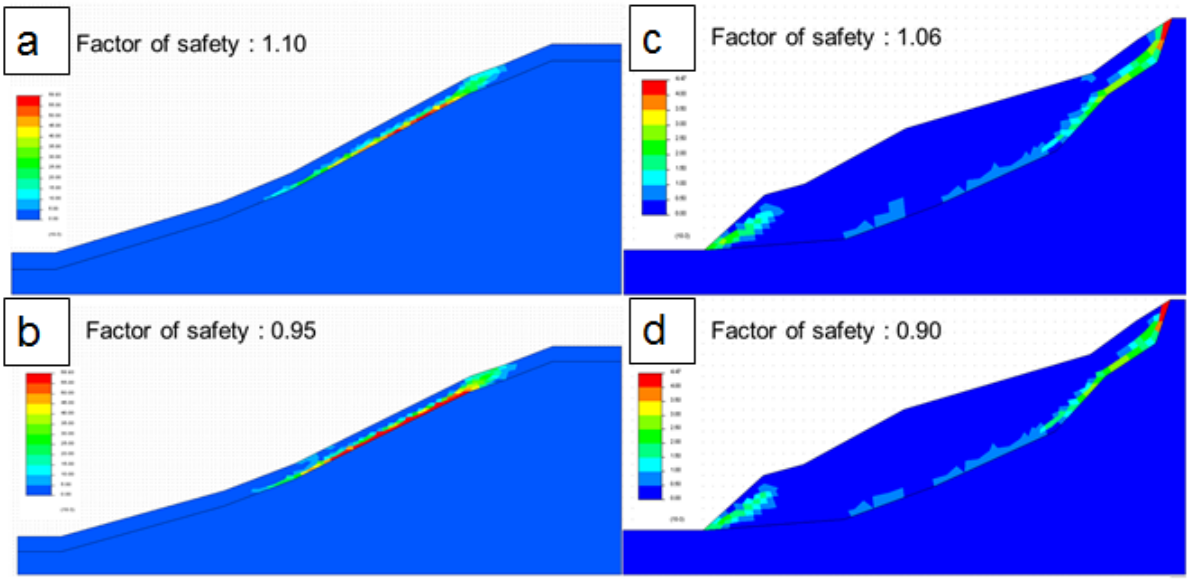

Figure 5.5 Slope stability analysis on three different scenarios. (a) Aso Teno slope with no rainfall scenario; (b) Aso Teno slope with the actual rainfall on 2012; (c) Aso Nakasakanashi slope with no rainfall scenario; (d) Aso Nakasakanashi slope with the actual rainfall on 2012.

Slope stability analysis for Ambon slopes are shown in **Fig. 5.6**. Without rainfall both slopes in Ambon show good stability without rainfall event (FS: 1.10 for Ambon Seilale and FS: 1.25 for Ambon Eerie). Under heavy rainfall scenario both rainfall experience failure (FS: 0.75 for Ambon Seilale and FS: 0.70 for Ambon Eerie).

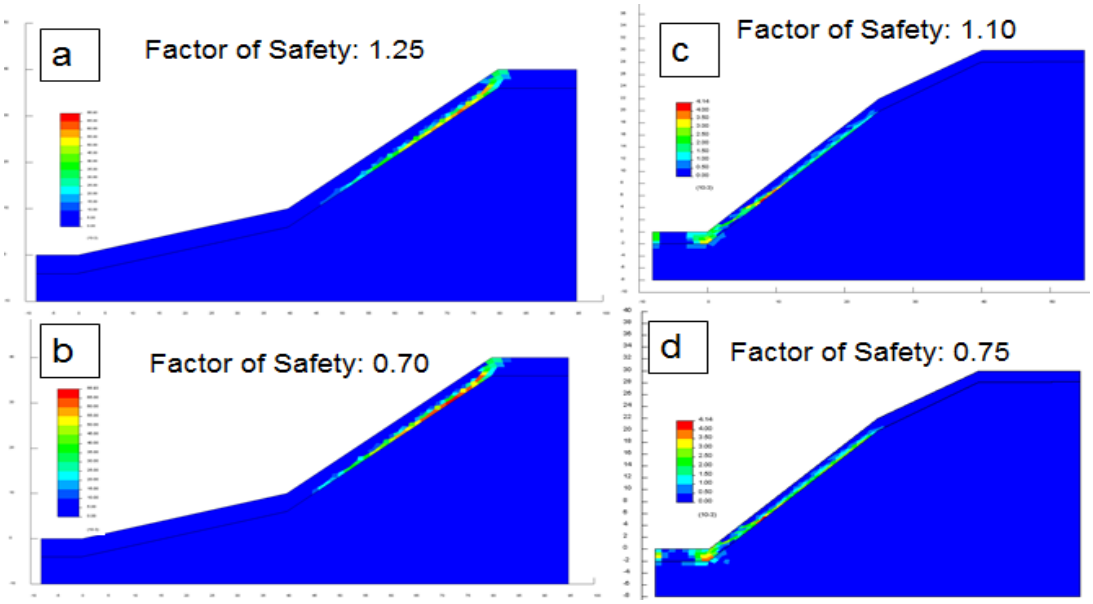

Figure 5.6 Slope stability analysis on three different scenarios. (a) Ambon Seilale slope with no rainfall scenario; (b) Ambon Seilale slope with the actual rainfall on 2012; (c) Ambon Eerie slope with no rainfall scenario; (d) Ambon Eerie slope with the actual rainfall on 2012.

This phenomenon is affecting the general slope stability in forested slopes. The apparent increase of rainfall might be due to increasing water vapor from the southern Pacific Ocean driven by the circular geostrophic wind around the pacific high pressure provoked by the increase in ocean surface temperature (Kubota, 2010).

5.5 Conclusions

Based on the presented data and subsequent discussion, the following conclusions are presented:

1. The increasing trend of maximum hourly rainfall is statistically detected in the studied slopes. The maximum hourly rainfall during 1978-2012 is increased at the rate of 0.52 mm/hr/yr and 0.42 mm/hr/yr for Ambon, respectively
2. Based on the finite element analysis, the factor of safety of Aso Teno without rainfall is 1.10, while for the factor of safety with the rainfall on 2012 is 0.95. In the case of Aso Nakasakanashi, the factor of safety without rainfall is 1.06, while the factors of

safety with the actual rainfall of 2012 0.90. In the case of Ambon, Eerie slope without rainfall is stable with factor of safety of 1.25 and with rainfall of 2012 the FS is reduced to 0.70. Similarly the slope of Seilale is safe without rainfall and becoming unstable under heavy rainfall with FS of 1.10 and 0.75, respectively.

The increase of maximum hourly rainfall is surely has negative influences in term of slope stability. Therefore, under this increasing rainfall rate, it is possible for many forest slopes to become unstable and prone to landslide disaster in the near future

5.6 References

Crozier MJ., 1986. Landslides: Causes, Consequences & Environment. Croom Helm, London, England, *Quaternary Science Reviews* **7** (1): 107-108.

Gilbert, R. O. 1987. Statistical methods for environmental pollution monitoring. Van Nostrand Reinhold, New York, New York, USA

Japan Meteorological Agency, 2013, Aso-Otohime Weather Data, *Japan Meteorological Agency Website*., accessed 7/17, 2013, http://www.data.jma.go.jp/

Kubota. T. 2010. Impact of the Increased Rain Due to Climate Change on Shallow Landslides and Sediments Runoffs in Kyushu District, Japan, *Advances in Geosciences*, Asia Oceania Geosciences Society, Vol **23**, Hydrological Science (2010), World Scientific Publishing.

Paudel, Prem P., H. Omura, T. Kubota, and B. Devkota. 2008. "Characterization of Terrain Surface and Mechanisms of Shallow Landsliding in Upper Kurokawa Watershed, Mt Aso, Western Japan." *Bulletin of Engineering Geology and the Environment* **67** (1): 87-95.

Sanchez-Castillo L, Kubota T, Cantu-Silva I, Hasnawir. 2015. Critical Rainfall for the Triggering of Sediment Related Disasters under the Urban Forest Development. J. Ecol. Dev. **30** (1) 1-10.

Rahardjo, H., Leong, E. C. and Rezaur, R. B. (2008), Effect of antecedent rainfall on pore-water pressure distribution characteristics in residual soil slopes under tropical rainfall. *Hydrol. Process*., **22**: 506–523.

Chapter 6 Conclusions and future works

6.1 Conclusions

Spatial planning based on disaster risk reduction is one of the primary issues of the Indonesia national development agenda to promote sustainable development due to the increasing frequency of disasters and continuing environmental degradation. In terms of landslide disaster risk reduction, regional development and disaster mitigation are well approached by landslide susceptibility, hazard and risk zoning.

The increasing development in Ambon region will increase pressure to the population and economic which will bring the finding of this study to the utmost relevance. The produced landslide susceptibility map is expected to be useful for government officials and urban planner in planning the development of the region. It is also worthy to be mentioned that landslide susceptibility study is still limited in the study area as a result of many unreported landslide cases.

Based on the previous chapters and the subsequent discussions the following major conclusions are presented:

1. Model performance was tested using an independent validation set comprising 20% of all mapped landslides. For verification of the model performance, receiver operating curves (ROCs) were calculated and the areas under the curve (AUC) for success rate curve were 0.688, 0.687, and 0.734 for FR, LR, and ANN respectively. The prediction rate curves AUC were 0.668, 0.667, and 0.717 for FR, LR, and ANN respectively. The results revealed that models showed promising results for shallow landslide susceptibility modeling since they all give accuracies greater

than 66%, but ANN model proved to be superior in representing landslide susceptibility throughout the study area. Since the ANN method produced more reliable results. The map derived from this approach is best suited to aid in land-use planning and landslide mitigation. Furthermore, this information can be employed to validate and verify any results acquired at regional and national scale. However, it must be noted that all results obtained are a function of the accuracy of the original database including input causative factors and the inventory.

2. The results revealed that models showed promising results for shallow landslide susceptibility modeling since they all give accuracies greater than 70%, but the 6 factors model proved to be superior in representing landslide susceptibility throughout the study area. For verification of the model performance, receiver operating curves (ROCs) were calculated and the areas under the curve (AUC) for success rate curve were 0.770, and 0.734 for optimized 6 factors and 8 factors respectively. The prediction rate curves AUC were 0.777, and 0.717 for optimized 6 factors and 8 factors respectively
3. Based on the finite element analysis, the factor of safety of Aso Teno without rainfall is 1.10, while for the factor of safety with the rainfall on 2012 is 0.95. In the case of Aso Nakasakanashi, the factor of safety without rainfall is 1.06, while the factors of safety with the actual rainfall of 2012 0.90. In the case of Ambon, Eerie slope without rainfall is stable with factor of safety of 1.25 and with rainfall of 2012 the FS is reduced to 0.70. Similarly the slope of Seilale is safe without rainfall and becoming unstable under heavy rainfall with FS of 1.10 and 0.75, respectively.

6.2 Future works

Based on the present study, further improvement could be included such as:

1. Improving the landslide inventory as the base data for landslide susceptibility assessments in the study area. Landslide inventory is one of the key input in landslide susceptibility mapping.
2. Detail weather data acquisition especially rainfall data were needed to ensure accurate slope stability analysis. The study of the effect of landuse change to landslides and the evaluation of devegetation to landslides will be great challenges for the future research. GIS techniques and remote sensing analysis should be employed to infer the landuse change and the relation between landuse change and landslide events.
3. Further studies should also employ the high accuracy of DTM, i.e. LIDAR data to obtain better accuracy of simulation and zoning.

Appendices

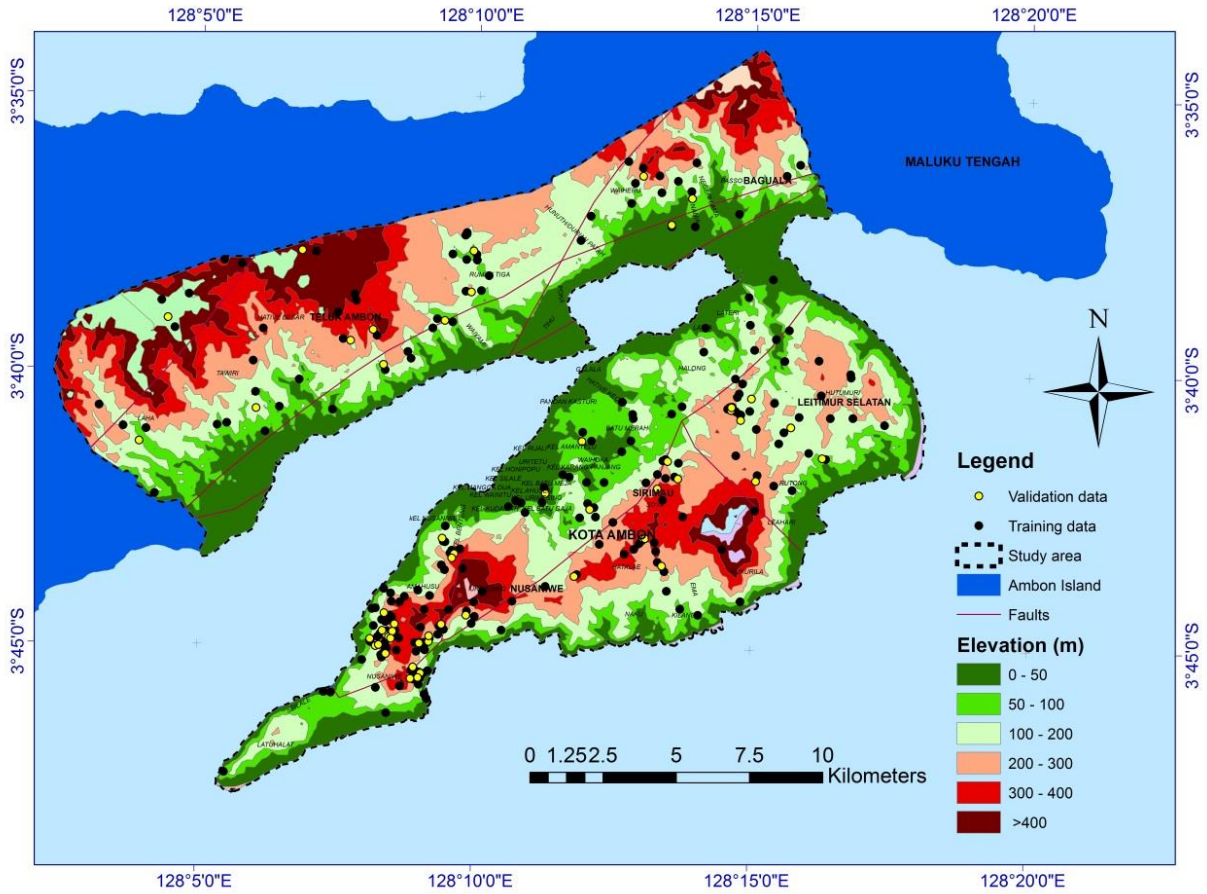

Appendix 1. Study area in Ambon, Indonesia

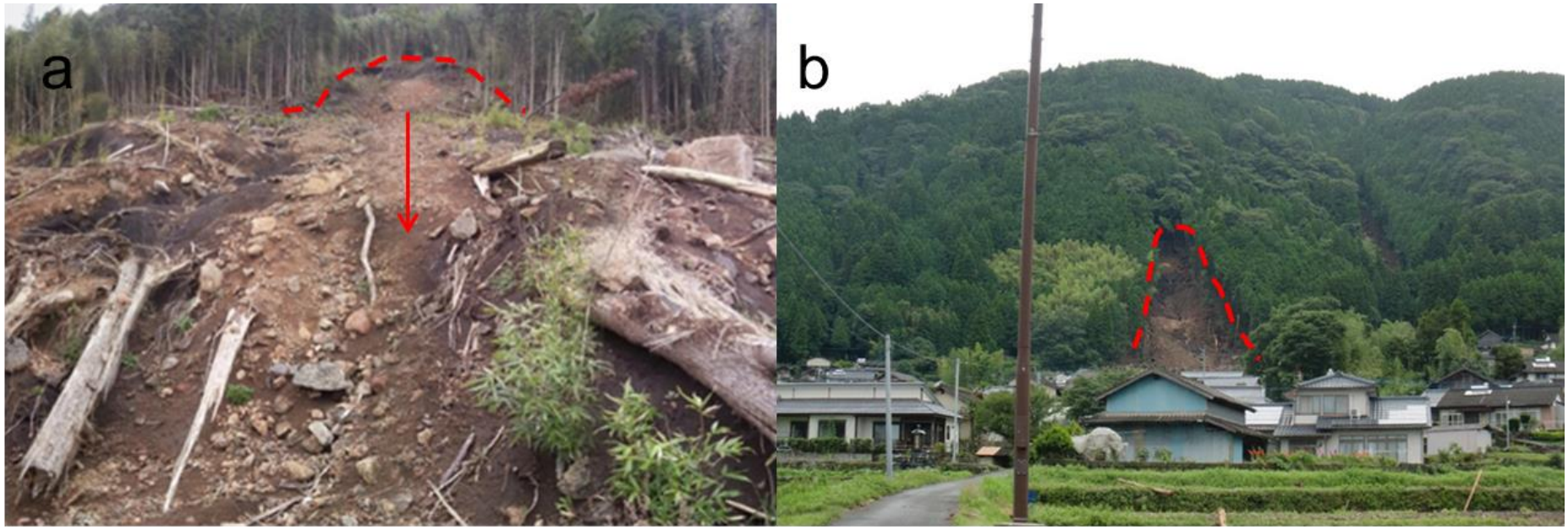

Appendix 2. Landslide slope in (a) Aso Teno and (b) Aso Nakasakanashi

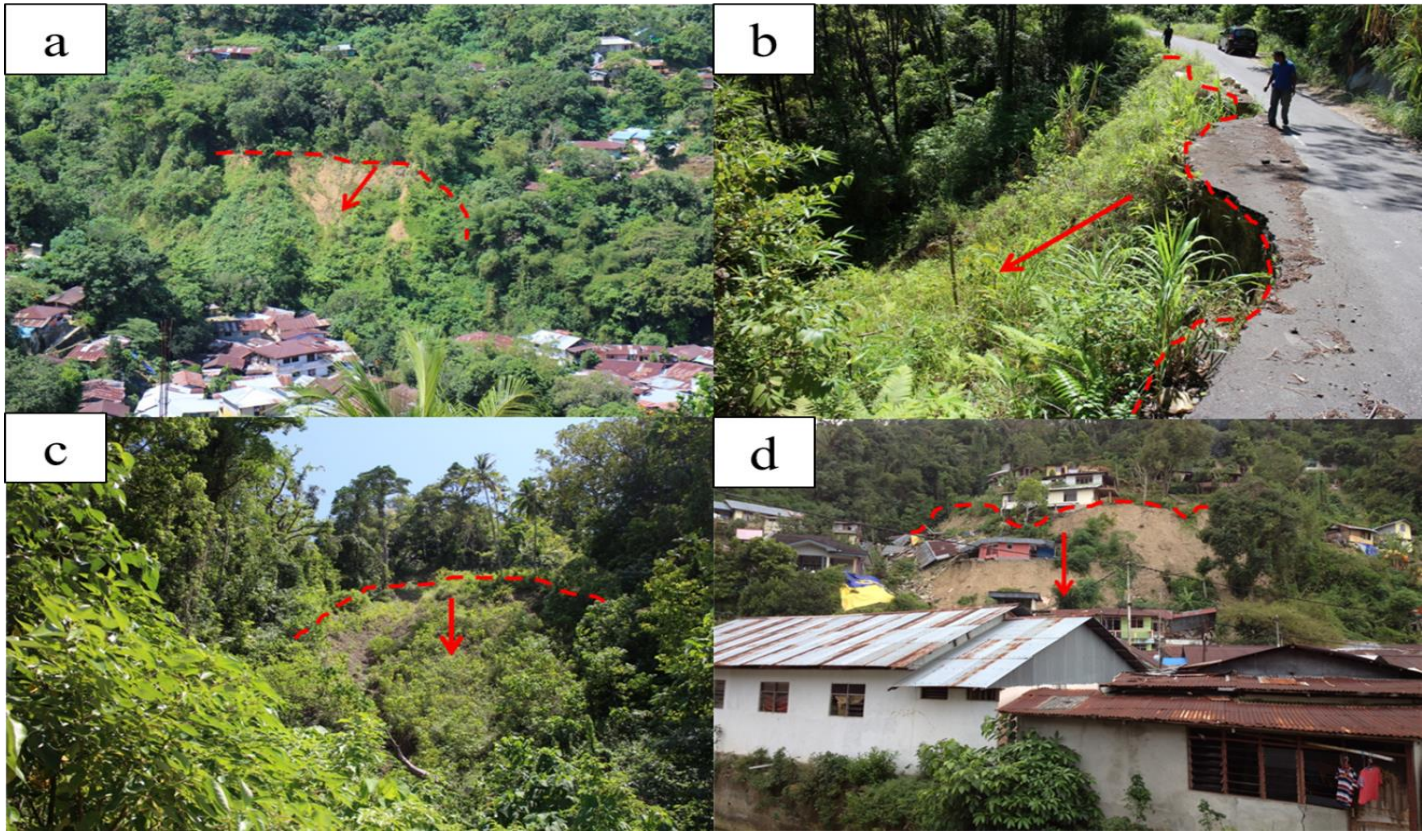

Appendix 3. a) landslides near settlement area; b) landslide along the road network; c) landslide case in the Ambon volcanic rocks geology, d) houses affected by landslides.

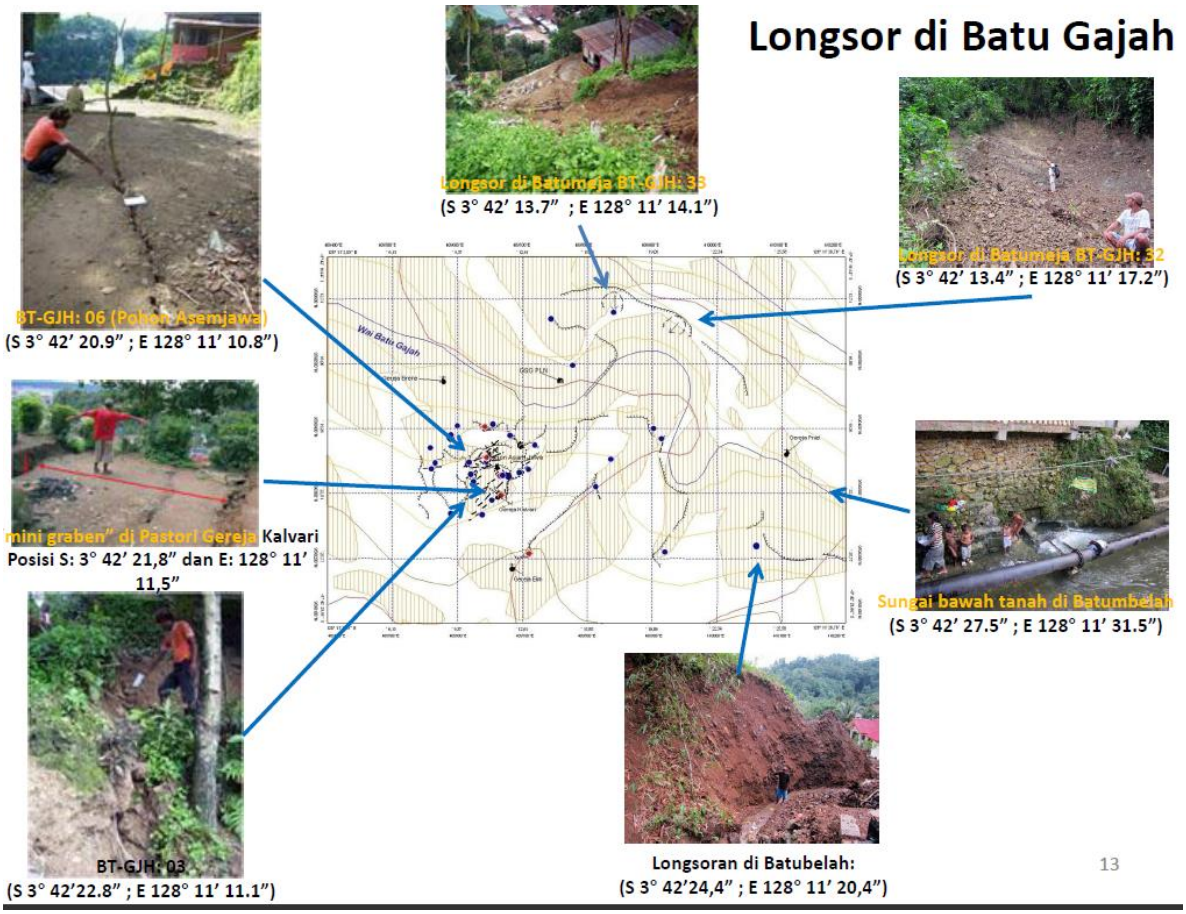

Appendix 4. Landslides investigation in Ambon conducted in January 2015

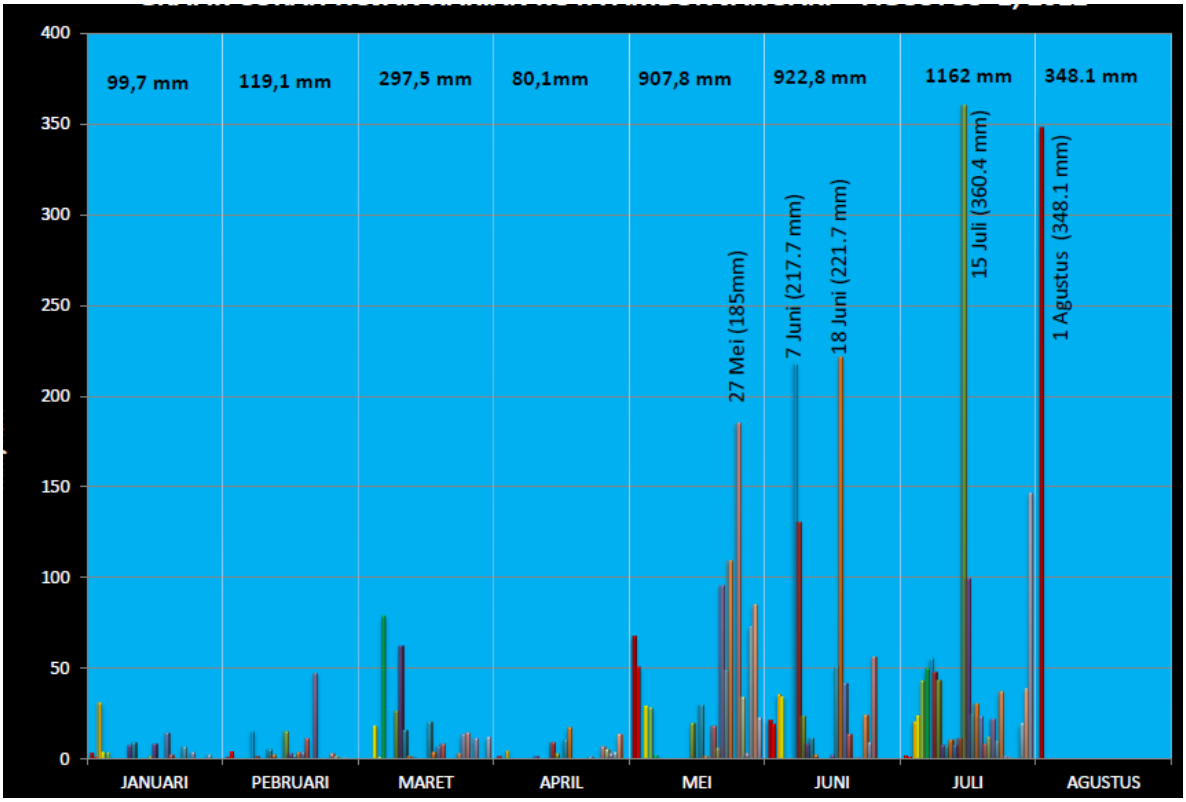

Appendix 5. Heavy rainfall events in Ambon during the year of 2012

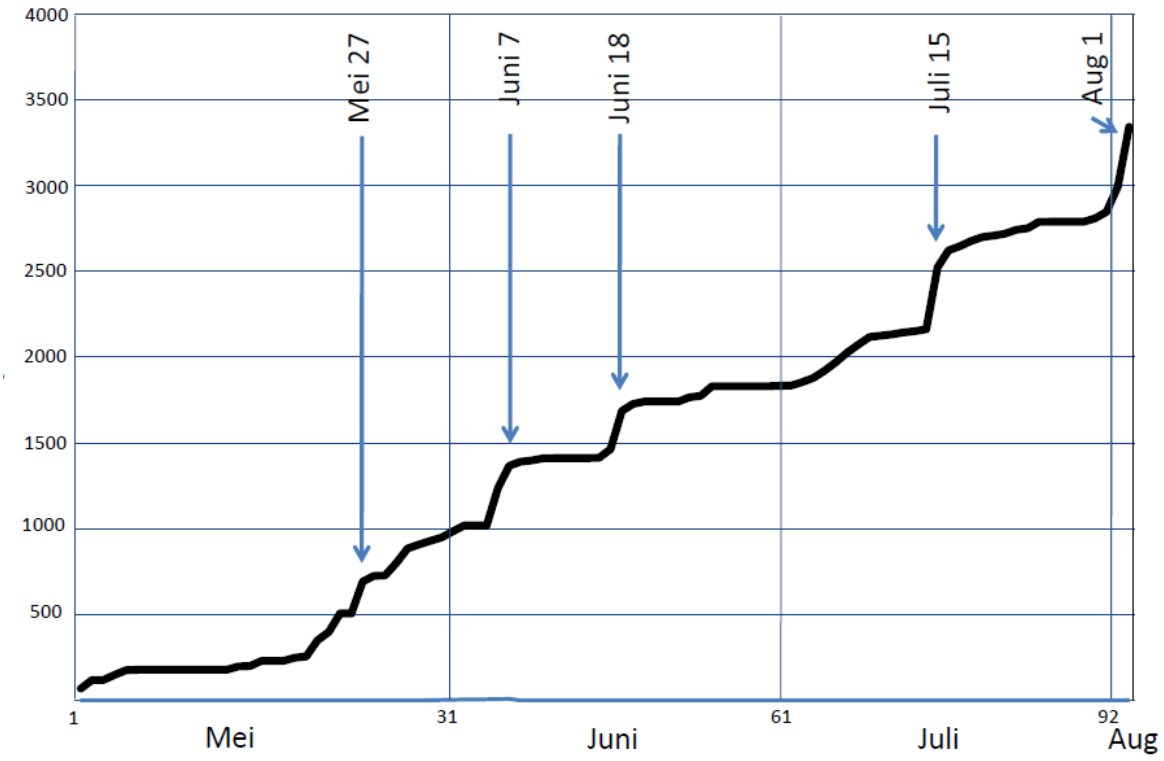

Appendix 6. Cumulative heavy rainfall events in Ambon during the year of 2012

Acknowledgements

I would like to thank my academic advisor Prof. Tetsuya Kubota for his generous advice, straight-to-the-point style of guidance, an enormous degree of research freedom, and guidance during my master and PhD course study. I would also like to thank Dr. Yoshinori Shinohara, assistant professor, for many brilliant inputs and comments that shape my thesis work to a better form.

Special thanks also dedicated to my fellow Laboratory of Forest Conservation and Erosion Control, Kyushu University. Ms. Laura Sanchez, thanks for being a great senpai. Mr. Matsui for helping me understands complex software written in Japanese, Mr. Okuyama Ryosuke for his valuable friendship throughout the master course, Mr. Andang Suryana Soma for his assistance in GIS analysis, Mrs. Putri Fatimah Nurdin for her valuable friendship, Mr. Pawan Gautam for all the craziness that happened.

I would also like to thank my mothers, whose without their support I will not be the current me of today. Thank you for Orange Band for being a stress-relieving activity in times of hardships, Thank you for Poko Funk Band (Naldy, Andri, Hiromi, Ikram, Sakti, Nizar, and Arul) for making life in Japan seems worthwhile. FOSA, FISSC, and KUFSA for making my life in Fukuoka more fun.

This study would not be possible if it is not supported by Ministry of Education, Culture, Sports, Science and Technology. I am greatly indebted to the government of Japan through the Monbukagakusho scholarship.

Special thanks for Ratu Dewi Anjani for being an inspiration when life seems so hard.